

*Development of a Wireless Borehole Extensometer for  
Monitoring Convergence in Underground Mines*

William Robert Thomas

*Thesis submitted to the faculty of the Virginia Polytechnic Institute and State  
University in partial fulfillment of the requirements for the degree of*

Master of Science  
In  
Mining & Minerals Engineering

Erik C. Westman, Chair

Mario G. Karfakis

Nino S. Ripepi

26 February 2015

Blacksburg, VA

Keywords: Extensometer, Convergence Monitoring

# *Development of a Wireless Borehole Extensometer for Monitoring Convergence in Underground Mines*

William Robert Thomas

## *Abstract*

An extensometer has been developed to continuously monitor roof extension in underground mines. The extensometer is designed to be installed in the MSHA-mandated test holes in the roof and measures the displacement between an anchorage point at the top of the borehole and the hole in the roof of the excavation. Once installed, the extensometer will report displacement through semi-wireless communications network. The extensometer is hard-wired into the permissible MIDAS datalogger, where results can be obtained wirelessly via the MIDAS user interface. Lab tests have indicated that the device produces displacement data. The device was installed in one underground coal mine to review its effectiveness in the field.

## *Acknowledgements*

I would like to thank the Department of Mining and Minerals Engineering at Virginia Tech for their hospitality over the past two years. In particular, I would like to thank my advisor, Dr. Erik Westman, and the members of my committee, Dr. Mario Karfakis and Dr. Nino Ripepi, for their time and assistance on this project. I would also like to extend a big thank you to the office members of Holden 115-A for the memories they contributed to throughout this study.

Finally, I would like to thank my family and friends for their endless support in this endeavor. Without them, this would not be possible.

This project was funded by the National Institute for Occupational Safety and Health under Contract 200-2011-40313 for “New Technologies for Identifying and Understanding Ground Stability Hazards.”

# *Table of Contents*

List of Figures.....	vi
List of Tables.....	xi
Chapter 1: Introduction.....	1
Chapter 2: Literature Review.....	3
Rock Conditions in Underground Coal Mines.....	3
Convergence.....	4
Roof Fall.....	6
Ground Control.....	8
Ground Displacement Monitoring Technologies.....	11
Wireless Communications Underground.....	14
Chapter 3: Development of a Wireless Borehole Extensometer for Monitoring	
Convergence in Underground Mines.....	17
Design Considerations.....	17
Extensometer Development.....	19
Installation and Data Collection.....	29
Calibration.....	31
Field Implementation.....	36
Results.....	39
Sources of Error.....	44
Discussion of Results and Conclusions.....	45
Chapter 4: Future Work.....	47
Works Cited.....	49
Appendix A: Extensometer Component Drawings.....	50
Appendix B: Extensometer Cost Analysis .....	54
Appendix C: Calibration Lab Results.....	55
Appendix D: Convergence Station Development and Implementation.....	58
Convergence Station Components.....	58

Installation Procedure.....	60
Installation and Data Collection.....	61
Conclusions.....	92

## *List of Figures*

Figure 3.1 - Bourns 3590S-2-102L Wirewound Potentiometer.....	19
Figure 3.2 - Constant force spring.....	20
Figure 3.3 - 3-D printed extensometer base.....	22
Figure 3.4 - 3-D printed extensometer lid.....	23
Figure 3.5 - 3-D printed borehole anchor.....	24
Figure 3.6 - Torsion spring as a borehole anchor.....	25
Figure 3.7 - MIDAS datalogger.....	26
Figure 3.8 - MIDAS user interface.....	26
Figure 3.9 - Grommets around the potentiometer arm.....	27
Figure 3.10 - Potentiometer securely placed inside the extensometer casing.....	28
Figure 3.11 - Completed wireless borehole extensometer.....	29
Figure 3.12 - Six 1" segments made from 1.25" PVC pipe.....	32
Figure 3.13 - Raw data records of calibration test.....	33
Figure 3.14 - Adjusted raw data records of calibration adjusted.....	34
Figure 3.15 - Calibration curves – 2 <sup>nd</sup> polynomial best fit line.....	35
Figure 3.16 - Extensometer location in mine, longwall panel.....	38
Figure 3.17 - Extensometer location in mine, headgate.....	39
Figure 3.18 - Raw data records of field installation.....	40
Figure 3.19 - Adjusted raw data of field test installation.....	41
Figure 3.20 - Roof extension readings of field test installation.....	42
Figure 3.21 - Examination of data from December 7 <sup>th</sup> and December 8 <sup>th</sup> .....	43
Figure 3.22 - Roof extension adjusted raw data after removing outliers.....	43
Figure 3.23 - Roof extension readings after removing outliers.....	44
Figure D.1 – JX-PA String Extensometer.....	58
Figure D.2 – MIDAS datalogger.....	59
Figure D.3 – MIDAS user interface.....	60
Figure D.4 – Map of convergence station #053's extensometer locations.....	62

Figure D.5 – Chart of convergence station #053 channel 1 extension monitoring, 20-inch scale.....	63
Figure D.6 – Chart of convergence station #053 channel 1 extension monitoring, concentrated scale.....	63
Figure D.7 – Chart of convergence station #053 channel 3 extension monitoring, 20-inch scale.....	64
Figure D.8 – Chart of convergence station #053 channel 3 extension monitoring, concentrated scale.....	64
Figure D.9 – Chart of convergence station #053 channel 5 extension monitoring, 20-inch scale.....	65
Figure D.10 – Chart of convergence station #053 channel 5 extension monitoring, concentrated scale.....	65
Figure D.11 – Chart of convergence station #053 channel 7 extension monitoring, 20-inch scale.....	66
Figure D.12 – Chart of convergence station #053 channel 7 extension monitoring, concentrated scale.....	66
Figure D.13 – Map of convergence station #040's extensometer locations.....	67
Figure D.14 – Chart of convergence station #040 channel 1 extension monitoring, 20-inch scale.....	68
Figure D.15 – Chart of convergence station #040 channel 1 extension monitoring, concentrated scale.....	68
Figure D.16 – Chart of convergence station #040 channel 3 extension monitoring, 20-inch scale.....	69
Figure D.17 – Chart of convergence station #040 channel 3 extension monitoring, concentrated scale.....	69
Figure D.18 – Chart of convergence station #040 channel 5 extension monitoring, 20-inch scale.....	70
Figure D.19 – Chart of convergence station #040 channel 5 extension monitoring, concentrated scale.....	70
Figure D.20 – Chart of convergence station #040 channel 7 extension monitoring,	

20-inch scale.....	71
Figure D.21 – Chart of convergence station #040 channel 7 extension monitoring, concentrated scale.....	71
Figure D.22 – Map of convergence station #077’s extensometer locations.....	72
Figure D.23 – Chart of convergence station #077 channel 1 extension monitoring, 20-inch scale.....	73
Figure D.24 – Chart of convergence station #077 channel 1 extension monitoring, concentrated scale.....	73
Figure D.25 – Chart of convergence station #077 channel 3 extension monitoring, 20-inch scale.....	74
Figure D.26 – Chart of convergence station #077 channel 3 extension monitoring, concentrated scale.....	74
Figure D.27 – Chart of convergence station #077 channel 5 extension monitoring, 20-inch scale.....	75
Figure D.28 – Chart of convergence station #077 channel 5 extension monitoring, concentrated scale.....	75
Figure D.29 – Chart of convergence station #077 channel 7 extension monitoring, 20-inch scale.....	76
Figure D.30 – Chart of convergence station #077 channel 7 extension monitoring, concentrated scale.....	76
Figure D.31 – Map of convergence station #078’s extensometer locations.....	77
Figure D.32 – Chart of convergence station #078 channel 1 extension monitoring, 20-inch scale.....	78
Figure D.33 – Chart of convergence station #078 channel 1 extension monitoring, concentrated scale.....	78
Figure D.34 – Chart of convergence station #078 channel 3 extension monitoring, 20-inch scale.....	79
Figure D.35 – Chart of convergence station #078 channel 3 extension monitoring, concentrated scale.....	79
Figure D.36 – Chart of convergence station #078 channel 5 extension monitoring,	

20-inch scale.....	80
Figure D.37 – Chart of convergence station #078 channel 5 extension monitoring, concentrated scale.....	80
Figure D.38 – Chart of convergence station #078 channel 7 extension monitoring, 20-inch scale.....	81
Figure D.39 – Chart of convergence station #078 channel 7 extension monitoring, concentrated scale (high).....	81
Figure D.40 – Chart of convergence station #078 channel 7 extension monitoring, concentrated scale (low).....	82
Figure D.41 – Map of convergence station #080’s extensometer locations.....	83
Figure D.42 – Chart of convergence station #080 channel 1 extension monitoring, 20-inch scale.....	84
Figure D.43 – Chart of convergence station #080 channel 1 extension monitoring, concentrated scale.....	84
Figure D.44 – Chart of convergence station #080 channel 3 extension monitoring, 20-inch scale.....	85
Figure D.45 – Chart of convergence station #080 channel 3 extension monitoring, concentrated scale.....	85
Figure D.46 – Chart of convergence station #080 channel 5 extension monitoring, 20-inch scale.....	86
Figure D.47 – Chart of convergence station #080 channel 5 extension monitoring, concentrated scale.....	86
Figure D.48 – Chart of convergence station #080 channel 7 extension monitoring, 20-inch scale.....	87
Figure D.49 – Chart of convergence station #080 channel 7 extension monitoring, concentrated scale.....	87
Figure D.50 – Map of convergence station #074’s extensometer locations.....	88
Figure D.51 – Chart of convergence station #074 channel 1 extension monitoring, 20-inch scale.....	89
Figure D.52 – Chart of convergence station #074 channel 1 extension monitoring,	

concentrated scale.....	89
Figure D.53 – Chart of convergence station #074 channel 3 extension monitoring, 20-inch scale.....	90
Figure D.54 – Chart of convergence station #074 channel 3 extension monitoring, concentrated scale.....	90
Figure D.55 – Chart of convergence station #074 channel 5 extension monitoring, 20-inch scale.....	91
Figure D.56 – Chart of convergence station #074 channel 5 extension monitoring, concentrated scale.....	91
Figure D.57 – Chart of convergence station #074 channel 7 extension monitoring, 20-inch scale.....	92
Figure D.58 – Chart of convergence station #074 channel 7 extension monitoring, concentrated scale.....	92

## *List of Tables*

Table 3.1: Constant force spring characteristics.....	21
Table 3.2: Consolidated Step Point Data from Calibration Test .....	35
Table B.1: GCF-04-15 Extensometer Setup Cost Analysis.....	54
Table B.2: GCF-04-20 Extensometer Setup Cost Analysis.....	54
Table C.1: GCF-04-20 Calibration Results.....	55
Table C.2: GCF-04-15 Calibration Results.....	55

## *Chapter 1: Introduction*

Convergence in mining is best described as the deformation in an entry or at the face in which the distance between the roof and floor decreases. In underground coal operations, deformation almost exclusively refers to convergence. Excessive convergence may be caused by a combination of heavy pressure from overburden and insufficient support within the excavation. This causes movement in the surrounding rock, which can lead to a multitude of problems at a mining operation. Excessive convergence will reduce the headroom in a mine, making it difficult to move machinery and carry out mining operations [1]. Movement in the rock can also increase the density of the fracture network, which can lead to a variety of roof fall hazards that could slow down operations and threaten the safety of the miner.

In order to prevent excessive convergence, a roof control plan is implemented at every underground mine with the intent of stabilizing the mine environment. The roof control plan incorporates directives for the development of a support system, from the type of support being used to the procedures that need to be implemented with every advancement in the excavation. Plans are designed specifically for the characteristics of the ribs, roof, coal, and overburden in the immediate area and will vary between mines [2].

Despite the proactive nature of implementing a roof control plan, the arranged maintenance may prove ineffective for unforeseen reasons. It remains critical that entries and faces be monitored continuously to observe any changes in the mining environment. Although common practice among the industry is to use a conventional tape measure to detect deformation, this approach does not offer the same level of sensitivity or ability to continuously monitor as a properly implemented extensometer.

The focus of the past few decades has been placed prominently on mine safety. With the passing of the MINER Act in 2006, great emphasis was been placed on the ability of the operators to wirelessly locate and communicate with miners underground [3]. Nine years later, the development of these communication systems has greatly increased the ability to transfer information immediately to the surface from underground and vice-versa.

Considering the development of other technologies in the industry, it is inexcusable that instrumentation has fallen behind the curve. Proper implementation of monitoring instruments

can reduce the likelihood of disasters through the immediate detection of hazardous conditions. With access to wireless technologies developed as a result of the MINER Act, there is currently a need to develop devices that can transfer data to operators working both underground and on the surface in real time.

The goal of this research is to design and construct a contact extensometer that measures displacement in the roof. The device will incorporate a potentiometer, a device that transfers mechanical energy into an electric pulse of proportional strength [4]. The particular type of transducer we are interested in simulating is the string transducer, which is capable of measuring a change in linear position. The string potentiometer is typically composed of a rope and a spring-loaded spool attached to a sensor that will emit a signal as the spool rotates [4].

The philosophy behind string transducer installation is quite simple. The first step requires that the transducer be mounted in a fixed position with the wire rope attached to a moveable object. As movement occurs, extension of the wire rope rotates a sensor that is capable of producing an electrical output signal proportional to the wire rope extension and velocity. The tension in the rope is controlled by an internal torsion spring that will retract the rope when there is no force extending the wire rope [5].

The particular advancement in this technology is the development of a borehole extensometer capable of continuous monitoring of the coal mine roof for extension. The extensometer setup should be durable, self-supporting in the roof, and capable of continuous data collection and wireless data communication. The extensometer should be designed for installation in the MSHA test hole, defined in 30 CFR 75.204 [6].

# *Chapter 2: Literature Review*

---

## **Rock Conditions in Underground Coal Mines**

---

Underground coal mines are designed to maximize the recovery of a coal seam while ensuring the safety of miners. The desire to increase recovery led to development of longwall mining, which incorporates new design challenges to the engineer. As the push to increase recovery continues, design engineers must also develop systems that manage potential hazards as a means of preserving the mine environment. Ground instability and the redistribution of stresses due to mining activity present the greatest challenge to the engineer. A thorough understanding of these conditions is essential to maximize the potential of mine design.

The causes of ground instability in underground coal mines can be divided into five different categories. The consequence of understanding these five areas is the information necessary to devise a proactive and preventative plan to reduce the number of hazards in the mine environment.

The first of these five categories is the geological factors associated with the mining environment and its immediate surroundings. In the roof, causes of instability include fracture density, joints, strata content, local faults, and local lineaments to name a few. In the floor, soft underclay can contribute to unstable ground and floor heave. In coal seams, rib rolls, washouts, cleats, and joints are the main causes of ground instability [7].

The second category of issues that could lead to ground instability is the geotechnical properties of the rock. These properties represent the characteristic nature of the rock, serving as the main features associated with rock mechanics. Often, the geotechnical properties of rock are determined in a laboratory setting as opposed to the underground environment. The list of geotechnical properties includes the unconfined compressive strength of the rock, the shear strength of the rock, the modulus of elasticity, and the Poisson's ratio [7].

The third group that contributes to ground instability is the hydrogeologic factors in the mining environment. Hydrogeologic factors describe both the mine's access or unavailability to water. A list of potential hydrogeologic factors include the location and size of local aquifers, thickness

of impermeable zones, the hydraulic pressure, porosity, and permeability of the rock, and the chemical composition of the water [7]. One study of eastern Kentucky coals found that out of 250 roof falls that occurred across five different room-and-pillar coal mines, water was present at 78.0% of the roof fall locations, the most common symptom of roof fall in the investigation [8].

In-situ stresses are the fourth category of causes of ground instability. In-situ stresses are the pressures associated with any rock location underground. Knowledge of the magnitude and directions of in-situ stresses is vital to mine design engineering [1]. Regional and local lateral stresses are the primary factors when determining in-situ stresses. The release of lateral stresses due to excavation or erosion can also have an impact on ground instability [7].

Mining processes are the fifth and final category associated with causing ground instability. One example of this category is a mine designed to recover material under bodies of water, which will inflict a variety of stress changes and potential flooding as mining progresses. Another example is mining that occurs in both over- and under-lying seams, where support systems and mining activity need to be considered and scheduled according to ground control issues [7]. These factors need to be identified in the design process and accounted for in the long-term plans.

---

## Convergence

---

Convergence is the reduction of an entry height due to stress redistributions resulting from various mining activities [9]. It is best described as the deformation in an entry or at the face in which the distance between the roof and floor decreases. In underground coal operations, deformation almost exclusively refers to convergence [1].

Excessive convergence is caused by a combination of heavy pressure from overburden and insufficient support within the excavation. This can lead to a multitude of problems at a mining operation. Excessive convergence will reduce the headroom in a mine, making it difficult to move machinery and carry out mining operations [1].

In order to prevent excessive convergence, it is critical that entries and faces be monitored continuously to observe any changes in the mine environment. It may seem obvious that this can

be achieved with conventional tape measures and rulers, but these devices do not offer the same level of sensitivity or constant ability to monitor as an extensometer [1].

In longwall mining, the amount of convergence in an area of the mine is directly related to its proximity to the active longwall panel. The side abutment is the area influenced by the stress on either side of the longwall panel and can be defined by the following equation:

$$W_s = 9.3\sqrt{h} \quad (1)$$

where  $W_s$  is the width of the side abutment (in feet) on either side of the active panel, and  $h$  is the overburden depth (in feet) above the panel [9]. The pressure associated with the tailgate (gob side) of the longwall panel is typically two-to-three times greater than the pressure associated with the headgate side. The lowest zone of pressure is dispersed from the middle third of the longwall panel and is projected towards the longwall face, in an area considered the front abutment [10].

With regard to location, the greatest amount of convergence on the headgate side occurs right where the panel rib is located. As the distance from the longwall panel on the headgate side increases, the amount of convergence decreases. As the longwall face approaches a particular location, the amount of convergence increases at an accelerating rate [9].

The tailgate side of the longwall panel experiences a different pattern of convergence than the headgate side. Overall, the tailgate entry has more convergence than the headgate entry. Convergence in the tailgate actually increases as the distance between the active panel and the location of interest increases. This difference in convergence distribution can be attributed to stress dispersion attributed to an area in the mine that is exhibiting its first longwall pass versus its second longwall pass. In the first instance of a longwall pass, the magnitude of stress in a particular area is only anticipated to increase by 40%-350%; on the second pass, the stress likely to increase by 160%-1000% of the original stress [9]. Stress redistribution is the greatest contributing factor to convergence in a longwall coal mine.

---

## **Roof Fall**

---

Roof fall can be defined as “the natural or spontaneous fall of rock from the mine roof and ribs” [1]. Roof falls and rock failures are inhibiting to mining operations, as they lead to downtime in production and present an immediate and dangerous threat to employees [8]. Coal mines are inherently more susceptible to roof fall than other types of underground mines because of the nature of the coal seam and the mining conditions. This susceptibility has led to identifying the characteristics of many different types of roof falls that occur in coal mines. Certain geologic conditions, such as paleochannels, pinch-outs, and slickenslides, have an immense effect on the stability of a roof in a coal mine [11].

A paleochannel rock failure features weak shale strata in the roof that is unsupported by a newer sandstone layer. When a paleochannel is mined underneath, the shale loses its primary means of support and collapses into the mine entry. Paleochannels are exceedingly dangerous because of their size. Fortunately, paleochannels can often be detected in the exploration process by inferring the border between sandstone and shale and laying that boundary over the mine map. The most difficult paleochannels to identify are the ones that are less than 10 meters in length. When a paleochannel is identified, the roof can be strapped and bolted to prevent an imminent roof fall. Any paleochannel collapses that are between 9.3 and 15.5 meters in size are called “washouts” [12].

A pinch-out occurs in the roof when there is a sudden termination in the roof strata. Pinch-outs are difficult to predict before roof fall occurs because the location where the strata terminates is rarely made available through exploration data. When a pinch-out is identified, additional bolting is required to support the weakened beam [12].

Slickenslides, also known as “slips,” are the most common of all roof failures. Slickenslides develop when there is movement in the roof strata between shale and claystone layers, forming curved edges in the roof. These edges tend to be very smooth and develop with a high variability of dip, with the median angle of dip being 30°. Roof falls in areas where slickenslides can be controlled with additional bolting and strapping, effectively reducing the area of coverage for each piece of support and increasing the number of supports to provide better hold [12].

Joints are near vertical planar failures that occur not only in the roof, but most locations underground. In horizontal coal seams, it is unlikely to see failure solely due to jointing in the roof because the rock continues to receive adequate support. However, if major faulting has occurred near the coal seam, joint is likely to contribute to local rock failures [B].

The Roof Rating Index (RRI) was developed as a means of evaluating the roof and its characteristics to increase awareness of areas susceptible to roof fall. With the RRI, characteristics attributed to causing roof falls (roof content, structures, fractures, etc.) are compared against the features of the underground location (entry/crosscut, three- or four-way intersection) to determine the likelihood, size, and type of roof fall faulting that will occur [11]. With this system, mine operators can take extra precaution in areas where roof fall is likely to occur in a proactive effort to prevent rock failure.

Despite monitoring records of geologic features, it has been ascertained that the major contributors to roof fall may not be as obvious as anticipated. A study of eastern Kentucky coal mines investigated 250 roof fall accidents across five different room-and-pillar mines. Most locations where roof fall occurred had been rated as “good” or better in earlier surveys of the roof [8].

The investigation took a variety factors into consideration. The results of the study showed that the presence of water in the roof (78.0%) was a better indicator of potential rock failure than any other factor, including the evidence of cracks from the mine entry (75.2%). The results also showed that a vast majority of roof falls took place in locations over 30 meters from the nearest active mining face (70.4%) and occurred less than 30 weeks after the excavation was made (71.3%). Over half (60.8%) of the areas that exhibited roof fall were rated as having “good” or better roof conditions in a prior examination. Oddly, rock failure in the ribs and floor were not great indicators of rock failure in the roof, as rib sloughing occurred in less than half of the roof fall locations (48.8%) and floor heaving in approximately one-out-of-eight (12.0%) locations. This study concluded that geologic factors that cannot be easily measured or evaluated from the mine entry contribute the most to roof fall in coal mines [8].

---

## **Ground Control**

---

Ground control refers to study of rock masses that undergo a change in equilibrium [1]. In mining, this definition can be applied to both underground and surface operations. Removal of large quantities of material from an area will have an effect on the equilibrium of adjacent rock masses, permitting the in-place rock to expand in the direction of the free face. It is essential to understand the mechanics of this interaction in order to safely plan and design mines.

Ground control can also define the means in which a mine chooses to support its surrounding environment during advancement. The objective of ground control in mining is to optimize the support systems in order to insure rock stability and control failure [1]. Prevention of ground control issues is critical to the health of the mine, as rock failures contribute to downtime and interrupt normal operations. Rock failures also present a hazard to the employee, as roof falls and other similar stability issues contribute injuries and, in some cases, fatalities [8].

The purpose of developing a roof control plan is to ensure the preservation of the mining environment as it was designed. Within the plan are designations for supports and procedures to be implemented, specifically selected to accommodate the properties of the ribs, roof, coal, and overburden parameters in the mine [2]. There are three primary objectives that require attention when assessing the validity of any ground control plan. These three goals are reinforcement, retaining, and holding, as each goal provides a different mode of stabilization within the rock. It is important to assess the features of the rock mass before determining which method(s) will be used [13].

Reinforcement is the ground control method that increases the strength of the rock and reduces the natural tendency of the rock to lose strength due to fracture. A reinforcing support system tightens the components of the rock mass in order to minimize the inconsistencies and potential points of failure [13]. In essence, a reinforcing system will artificially increase the cohesion of the rock, assuring that the rock mass will remain in one piece, even as the individual rock layers begin to break.

Retaining is the process of supporting broken rock in the immediate location of the rock failure [13]. In many situations, this may be required in order to improve the safety of the mine environment. However, ground control systems are able to take advantage of the broken rock by

using it to prevent future failures and provide resistance to rock bursts. At a minimum, a retaining support system will reduce the severity of a rock burst by providing an immediate shield of resistance to the energy released composed primarily of previously broken rock.

Holding is the process by which unstable rock is attached or mounted to stable ground. Ideally, this means that the rock surrounding the mine workings will behave as if it were a singular rock mass [13]. The stresses that act on the in-situ rock will determine the methodology used pertaining to the holding process.

Often times, the method of ground control selected for a particular mine is based on two sets of standards. The first, and more paramount, set of standards taken into consideration is safety [13]. Often, these standards are set forth by a governing body (MSHA, OSHA, etc.), but the leaders of the industrial sector may choose to improve upon and go beyond these guidelines to better ensure the safety of their employees. However, the rule of thumb remains that if the design is unsafe, it is not worth the investment.

The second set of standards that must be looked into is the cost to operate and maintain the support system in both active and inactive sections of the mine. The main expenses associated with ground control are affiliated with materials, personnel, and maintenance. The most profitable ground control systems are the ones that can minimize the expenditures in each of these three categories without inhibiting the production plans [13].

In underground coal mines, MSHA sets the standards of practice for roof control plans and manages the plan approval process. All roof control plans need to be approved by the MSHA District Manager. The MSHA District Manager is responsible for retaining the geological information of the area in which he/she is assigned so that appropriate assessments of submitted roof control plans can be made [2].

MPAS, the Mine Plan Approval System, is the program that monitors the status of roof control plans at the District Office. When any plans or revisions to plans are sent to out to be approved, the document is placed in MPAS. Once in place, the office has 45 days to complete its evaluation of the plan or must provide documented reasoning as to why the plan could not be complete in 45 days. During the evaluation process, the District Office may request additional information regarding the roof control plan, in which case the operator must reply or face

disapproval of the submitted plan. MPAS tracks all requests, updates, approvals, and evaluations for each mine using the mine's ID number [2].

When the evaluation is complete, the mine operator will receive a written document from the District Manager. In the case that the plan is approved, the document will verify the plan's approval and the plan can be implemented. If the plan is not approved, the operator will receive feedback from the District Manager identifying any problems or inaccuracies in the plan, possible solutions to any issues, in addition to a timeframe in which the revisions can be resubmitted [2].

The MSHA handbook *Roof Control Plan Approval and Review Procedures* identifies the requirements of the roof control plan for each component that needs to be submitted. The essential pieces of information for each portion of the document are cited, often referencing the laws established 30 CFR 75 as a justification for each item listed. The handbook also provides the operator with information regarding the submittal of mine specific requests, instructions on using software developed by NIOSH to design mine features, and information on the protection of miners from rock failures [2].

The roof support section of the handbook establishes that a record of all equipment and the parameters of each type of equipment needs to be submitted alongside drawings that demonstrates how the supports will be installed for both underground intersections and mine entries. Bolting patterns must include specific locations and types of bolts that are being installed. Tensioned roof bolts are required to be included in the bolting plan and are identified as a permanent support in the roof control plan. Additional information regarding the use of supplementary supports is also provided [2].

When using tensioned roof bolts, there is a requirement that test holes must be drilled in the same vicinity. 30 CFR 75.221 (a) (10) states “[w]hen mechanically anchored tension roof bolts are used, the roof control plan should include intervals at which test holes will be drilled,” [6]. These test holes should be placed at intervals that take into account the roof strata and the depth of the test hole [2]. Test holes are required to be “at least 12 inches above the anchorage horizon of the mechanically tensioned bolts being used,” as stated by 30 CFR 75.204 (f) (2) [6]. Information extracted from the test holes provides the information necessary to evaluate the

effect of the tension bolts on the roof strata and identify whether a different type of support is necessary [2].

Beyond the scope of the aforementioned, it is necessary to collect data reflecting the characteristics of the mining environment in order to begin constructing ideas on what ground control methods may be applicable for the mining environment. This data is often relayed to the engineering staff by way of underground instrumentation: technology designed to reveal the stress, strain, or load on a particular location. Common practice suggests testing various points within the mine to gain a grasp of the larger picture and better interpret the data. This fundamental practice is likely to yield mixed results, requiring that the person analyzing the data to be an expert on the topic. A good sample of data points will permit proper interpolation of the data, providing speculative data for the remaining portions of the mine [13].

Mining engineers will often rely on results yielded by underground instrumentation in order to design appropriate ground control plans for the given conditions. Inaccurate assessment of the in-situ rock may lead to improper or inadequate support, so the need for proper instrumentation to identify the surrounding stresses is critical [13]. The consequences of misguided designs can be disastrous and, in some cases, fatal. The proper evaluation of instrumentation data should be at the forefront of any design.

---

## **Ground Displacement Monitoring Technologies**

---

An extensometer is a device that measures displacement. In underground mining, there are extensometers that monitor convergence and borehole deformation; the focus of this project is on the former [14]. There are two general categories in which all extensometers will fall under: contact and non-contact.

A contact extensometer measures displacement by monitoring the physical changes in the environment by contacting the extents of the area of interest from a fixed location. The most common contact extensometers are typically mounted at two locations, identifying any displacement between the two locations.

One type of contact extensometer used in the mining industry is the tube extensometer. The tube extensometer provides two applications in the mining industry. The first function of a tube extensometer is to measure the convergence of roof and floor in a mine as a function of time.

This process indicates the stability (or instability) of the development and indicates if any additional support will be needed. The second application of a tube extensometer is to measure the separation in roof layers by placing levels at several horizons at on the roof, resulting in another measure of roof stability [14].

The tube extensometer features a telescoping tube design with a dial indicator and two contact seats, anchored to the roof and the floor to measure the change distance. The tube extensometer also features the master bar, which is made of same material as the tube of the extensometer. The master bar acts as a reference standard and can be used to gauge any error that may exist. The tube extensometer also has a thermometer to regularly assess any errors that need to be corrected based on a change in temperature [14].

Another contact extensometer is the tape extensometer. The tape extensometer is a portable device that uses hand-held measurements. One of the advantages of the tape extensometer is that it can measure distances in both the horizontal and vertical direction. Measurements are taken from preexisting base points with precision and speed. The stability of the mine can be assessed by evaluating the system's ability to repeat results between two reference points for consecutive rounds of measurements [14].

The tape extensometer is constructed of steel engineering tape with punched holes and a compression spring that controls the tension of the tape. The alignments of the anchor points are not critical because the hook fittings at either end of the device are not affected by the orientation of the anchor points. The tape extensometer often has a resolution of 0.001 in. (0.025 mm) [14]. Current designs often have digital reading capabilities and can endure harsh environments. The tape extensometer is easy to use but requires the skill of an experienced employee during operation [15].

A third type of contact extensometer used is the magnet extensometer. The magnet extensometer is used to measure heave and settlement in excavations. The magnet extensometer indicates the depth at which settlement has occurred as well as the total amount of settlement [14]. This instrument is easy to handle and is very accurate, being able to repeat measurements with an error of +/- 3 mm (0.1 in.) [15].

Implementation of the magnet extensometer is simple. Magnets line the exterior walls of an access pipe in the roof of an underground excavation. As the ground shifts, the magnets shift as well. A magnetic probe attached to a graduated cable is then placed in the access pipe to identify the present location and orientation of each magnet as a means of monitoring any shift that has occurred between readings. If the magnets do not move over an extended period of time, it can be assumed the ground is settled. In cases where the heave is expected to exceed 3%, telescoping sections can be installed to provide more fortitude to the access pipe [15].

Non-contact extensometers often use surveying equipment or lasers to indicate the location of two or more points from a fixed location. Lasers can be used if placed in a secure, fixed location with the intent of measuring displacement as it happens, yielding a rate of displacement.

Surveying equipment can be used to regularly monitor the location of multiple points of interest to determine if any displacement has occurred based on a fixed-point. Surface mounted extensometers are often used to measure the absolute displacement between various locations by using surveying equipment. Surveying systems are often viewed as large-scale extensometers [14]. The surveying equipment in a surface mounted extensometer can be part of an automated system or can be operated by a technician. Data collected will be used in triangulation analysis to evaluate the relative locations of each point of interest and detect any displacement that may have occurred since the previous set of measurements. In the surface setting, most evidence of extension and slope instability is a result of the development of tension cracks. A regular survey of preexisting points of interest will can be used to monitor the effects of these fractures over time [14].

Although this application of surveying equipment is typically used in surface monitoring, it is not unrealistic to apply this technique to monitor convergence in underground operations. Similar to the tape extensometer, the surveying equipment can monitor the distance between two reference points, with one located on both the roof and the floor. Consecutive measurements will indicate is any displacement has occurred with very good accuracy (often +/- 0.005 feet).

Another type of non-contact extensometer is the laser extensometer that uses laser interferometry to record information. A laser extensometer operates by examining the surface of the specimen, generating a virtual image of the specimen. Consecutive tests from the same fixed point will

generate several models of the surface over a specific period of time. When these virtual images of the specimen are arranged chronologically, any deformation that occurs can be detected [16].

When monitoring for convergence, a laser extensometer can be used to analyze the roof and indicate the current position of all points of interest. Analysis of consecutive virtual models over a known period of time would provide information to where (if any) deformation is occurring as well as provide a rate at which deformation occurs. Laser extensometers are particularly good for very quick testing of high volume areas, making them particularly beneficial for use in convergence studies [16].

The model piece of equipment that can be associated with analyzing roof conditions via the MSHA required test hole is the Golder Associates Remote Reading Telltale System. The Telltale provides information on rock deformation above a mine entry with a multi-color rod that moves to indicate that deformation has occurred. The Telltale can be hard-wired in succession to an interrogation unit that has the capability of distributing the information collected by up to 400 Telltales to a computer on the surface. The convenience of the Telltale's operation has led to its worldwide use in the mining industry [17].

---

### **Wireless Communications Underground**

---

In 2006, the Mine Improvement and New Emergency Response Act (or MINER Act) was signed into law as an amendment to the Federal Mine Safety and Health Act of 1977. The new law required that all underground coal mines install wireless two-way communication and tracking systems by 2011. At the time, no such communication system was readily available or permissible for operation in an underground coal mine [3]. The MINER Act inspired an industry-wide rededication to wireless technology implementation in underground mines.

Wireless communication networks have been associated with the mining industry for nearly a century. There are three different mediums in which wireless communications can be distributed in an underground mine setting: through-the-earth (TTE), through-the-wire (TTW), and through-the-air (TTA) [18].

The first of these three mediums that was used was through-the-earth communications. Beginning in the 1920s, communicators were developed to pick up radio signals underground. These devices were so well-established that the U.S. Bureau of Mines commercially offered

carrier-current radios and TTE signaling by the 1940s. Due to the limitations of TTE, particularly the retrieval rate of data and the bulkiness of the equipment, it was effectively terminated in the mining industry by 1950. In recent years, a renewed interest in TTE technology has increased, almost exclusively since the MINER Act was passed in 2006. The rise in interest can be attributed to the reliability of TTE systems in the event of a mine disaster where other wireless systems would fail. Currently, TTE is one of the most commonly used methods for tracking individuals in underground coal mines [18].

Through-the-wire communication (although the name might suggest otherwise) is a wireless system that came to fruition in the 1950s. The concept of TTW technology was developed when it was discovered that conductors, such as electrical wires and metal pipes, could propagate low frequency transmissions throughout an underground mine. Although this was not completely understood by scientists at the time, this discovery led to the creation of the leaky feeder systems used today. TTW systems are considered hybrid or semi-wireless systems since it is partially wired and partially wireless [18].

Through-the-air communications have been a major component in underground mine communications since the early 2000s. TTA is capable of providing numerous benefits in underground mines, including two-way communications, remote controlled equipment and sensing, and ability to track miners and equipment. WLAN networks, created through the use of off-the-shelf wireless units, are the most reliable in the underground setting. Using RFID technology in combination WLAN components has been the most effective means of tracking equipment underground [18].

There are times when a mine will choose to implement a combination of these three types of networks to increase the range of the signals. One study, performed in an underground coal mine in India, used TTE radio technologies to reach TTW leaky feeder networks underground, which propagated the signal deep into the extents of the mine. Neither system was capable of reaching that depth alone, so integration provided the means access [19].

Monitoring systems in underground coal are critical to the mine's performance, as they relay information regarding the conditions of the mine environment. Traditionally, these systems have been hard-wired, which is difficult when you consider the extent and size of an underground mine [20]. In addition, the commitment of mines to wireless communication systems through

the requirement of the MINER Act should provide the necessary infrastructure to complete the task of wireless monitoring systems.

The ideal method of data collection for the underground environment has been designed. The monitoring system would be permitted to work under one of two settings. The first setting is an “urgent event setting,” which would place the monitoring equipment in a state of high alert and produce data in real-time. The second setting described is as “long term periodic monitoring,” where regularly scheduled data collections occur [20].

The sensors, described as “nodes” in the wireless network, would have three states of operation: sleep, update, and awake. In the sleep mode, sensors run on low power and do not collect data in an effort to save energy in the unit. The update mode is activated during periodic monitoring sessions, permitting the recovery of data in a short interval, before returning to the sleep mode. The awake mode is activated when the urgent event setting is initiated, and makes the sensor begin to take readings in real-time, presenting the most current available information to the user [20].

# *Chapter 3: Development of a Wireless Borehole Extensometer for Monitoring Convergence in Underground Mines*

---

## **Design Considerations**

---

The intention of this exercise is to create an extensometer that will be able to detect convergence in a coal mine by measuring the extension in the roof. In order to develop the design, it is important to be able to quantify the aspects of the environment in which the device will be installed.

The first component that needs to be quantified is the MSHA-required test holes that are introduced in the roof. These holes have a one-inch diameter and must extend at least 12 inches beyond the permanent support. In most cases, the permanent support being referred to are torque-tension bolts, which are typically six feet long. This establishes that the tests holes are required to be seven feet in depth by law. Mines can also choose to evaluate secondary supports (cable bolts) via the test holes. In cases where this occurs, the same 12-inch addition will apply to the depth of the hole. Assuming the average cable bolt is 10 feet in length, it can be anticipated that average depth of test holes in these mines are 11 feet.

Asserting that the average depth of a test hole will be 7-11 feet provides insight on what kind of measurement tool can be used. Reasonably, it would be difficult to imagine more than 10% of the measurable roof strata to experience extension before breaking with respect to the original anchorage depth. Although this is a severely rough estimate, it provides some insight to the anticipated amount of movement that the device needs to be capable of identifying. On the short end, the maximum amount of extension that should be able to be measured is 8.4 inches; on the long end, maximum anticipated extension 13.2 inches. These figures will be identified as the approximate range of extensometer being developed. In addition, an anchor capable of withstanding movement within the roof strata and a method of installation that sets the anchor at the top of the test hole needs to be designed for the extensometer.

The mine environment must also be considered when developing the extensometer. Underground mines tend to be one of the most hazardous environments on the planet, with large

equipment, personnel, and raw materials constantly moving in constrained areas. In addition, the ground structures that surround the mine are continuously experience changes in equilibrium as mining activity advances, causing minor shifts in the ground due to the change in stress.

When considering the mine environment in the design process, a few things become evident. The most exterior portion of the extensometer needs to be exceedingly durable such that it can protect the measurement equipment from the everyday hazards of the mine environment. Secondly, the extensometer apparatus should be relatively small to avoid interference with regular mining operations. Another trait the extensometer should have is the capability of supporting itself in the roof.

Data collection and wireless transmission are two design components that are closely related. Data should be collected continuously and at a predetermined rate. This feature is desired because it would provide a timeframe of geotechnical events monitored by the extensometer, allowing mine operators to attribute the deformation to a particular event (blasting on the surface, nearby longwall activity, etc.) or is the result of natural equilibrium restoration, which would provide the opportunity to evaluate the roof independent of outside activity. It is also desired that the equipment used to collect data has the ability to transmit the information wirelessly. This would reduce the amount of electrical components added to the device and ensure that there is nothing lost in the transmission from data collection to wireless communication.

The cost of producing the extensometer is also critical to the design process. Ideally, the extensometer would be inexpensive to produce on economic principles alone. However, given the area of the mine roof the extensometer is capable of evaluating, the ideal design would have a low cost of production so that more extensometers can be inserted in relatively close proximity to give a more comprehensive evaluation of the roof. The ability to produce an inexpensive device is essential to creating the best representation of the convergence in the mine.

For summary, the objectives of the design can be broken down into five components:

- 1) The extensometer must give a proper evaluation of roof strata extension for convergence measurements.
- 2) The extensometer must retain the ability to continuous monitor the immediate environment for convergence.

- 3) The extensometer must be able to transmit information wirelessly throughout the mine.
- 4) The extensometer should have a casing and anchorage system suitable for the mine environment and capable of supporting itself to the roof.
- 5) The extensometer must be inexpensive to fabricate and install.

---

## **Extensometer Development**

---

The tasks involved in the development of the extensometer were numerous and consisted of many failed trials before a final design was established. In this section, a review of the device components and the information that led to final design will be reviewed.

### ***Measuring Device: Potentiometer***

To create an electrical signal capable of wireless transmission, a measurement tool must be used that can create an electrical signal when triggered by the data-logging component. To meet this requirement, a potentiometer has been incorporated into the extensometer design. A potentiometer is a device that transfers mechanical energy into an electric pulse of proportional strength [4]. The potentiometer that has been designated for this design is the Bourns 3590S-2-102L Wirewound Potentiometer, as seen in Figure 3.1 below. The potentiometer chosen has 10-turn rotating arm and a 1,000 ohm ( $1\text{ k}\Omega$ ) resistance. This potentiometer was chosen because it features the same resistance and number of turns as the JX-PA extensometer discussed in Chapter 3.



**Figure 3.1 - Bourns 3590S-2-102L Wirewound Potentiometer**

For this extensometer, the goal is to create a motion that is normally attributed to string transducers. String transducers are typically composed of a rope and a spring-loaded spool

attached to a sensor that will change resistance as the spool rotates, which causes a change in the signal emitted [4]. In order to induce tension in the extensometer and allow the potentiometer to recoil, a constant force spring will be attached to the arm. The constant force spring is wrapped around the arm of the potentiometer via a set of rubber grommets, ensuring the spring will not slip as it is pulled. On the outer edge of the constant force spring is a hole that can be attached to a string that will provide a connection to the anchor at the top of the test hole. An example of a constant force spring can be seen in Figure 3.2.



**Figure 3.2 - Constant force spring**

Four different styles of constant force springs were chosen to be analyzed based on their inner diameter, extended length, and price. After careful inspection, two of the springs, the Gardner GCF-04-15 and the Gardner GCF-04-20, were deemed acceptable for use in the extensometer design. The Gardner 04-10 was considered unreliable as it would twist and turn before recoiling. The Gardner 04-25 was determined to be too wide and too difficult to manipulate by hand to give any further consideration in design process.

Table 3.1 displays the characteristics of both the Gardner 04-15 and Gardner 04-20 for comparison [22]. From the initial inspection, it is evident that the Gardner 04-15 spring is the more sensitive of the two springs, meaning that it could provide more accurate data than a larger spring such as the Gardner 4-20. On the other hand, the Gardner 4-20 is longer, thicker, and wider than its counterpart, indicating it would be more durable and dependable addition to the design that would also increase the range of the extensometer.

**Table 3.1: Constant force spring characteristics**

Spring	GCF-04-15	GCF-04-20
Thickness (in.)	0.006	0.007
Length (in.)	22.000	26.000
Load Capacity (lbs.)	1.12	1.62
Width (in.)	0.3700	0.5000
Inside Diameter (in.)	0.51	0.59

### ***Casing: 3-D-Printed Extensometer Housing***

In order to design the casing, a 3-D printer was employed to create a custom design. The MakerBot 3000 was employed for the task. The design should be able to withstand the mine environment, provide a mechanism of supporting itself to the roof, and incorporate the designated potentiometer and a data-logging system.

The 3-D printed extensometer housing has been developed with the prior objectives in mind. The cartridge can be broken up into two pieces: the base and the lid. These two pieces of the cartridge are connected with four screws that are in the corners of the open side of the base.

The base was developed through two generations of design. The first generation of the base was designed with walls that were too thin to hold an appropriately-sized screw and a compartment that did not hold the potentiometer firmly in place. The second and final generation of the base was designed to resolve these problems. The walls were increased to 0.20" in width, permitting an adequate environment for an attachment screw in each of the four corners. The compartment for the potentiometer was redesigned to the exact dimensions of the potentiometer to ensure that the potentiometer would be secure once it is placed inside the base. There is also a small, 0.25" diameter hole in the side of the base to allow electrical wiring to pass though the wall to attach the terminals of the potentiometer to a data-logging device. The final iteration of the base can be found in Figure 3.3. The base portion of the casing takes approximately four-and-a half hours to print using the MakerBot 3000. A specifications drawing of the base has been provided in Appendix A.

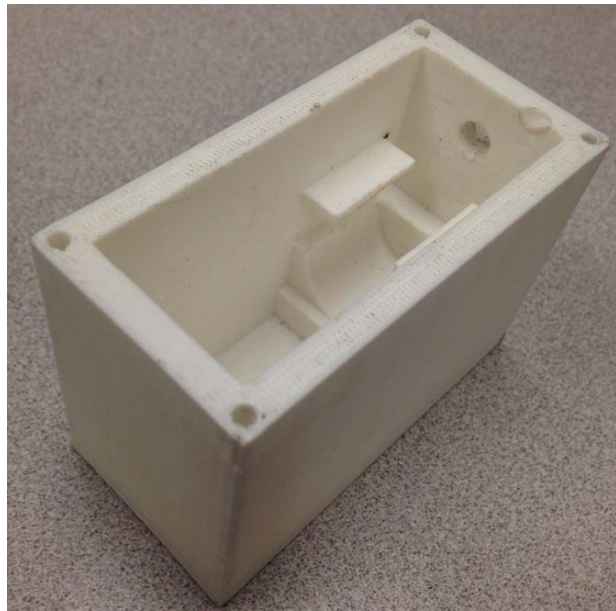


**Figure 3.3 - 3-D printed extensometer base**

The lid portion of the extensometer casing went through three generation of design. The crucial element that would determine the success of design was the mechanism designed to hold the extensometer in place. The original design features two thick-walled semi-cylinders, each with a radius of 0.5", with a path for a bolt to securely enter and push the two semi-cylinders apart and create a wedge. Between the two semi-cylinders is a slot that went through the bottom of the lid that would permit the constant force spring to emerge and extend up and into the test hole. In each of the four corners is a hole designed to permit an attachment screw to go through to attach to the base of the extensometer casing. Unfortunately, the thick-walled semi-cylinders proved too stiff to be moved and would not grip the inside the borehole.

The second generation of the lid then featured two thin-walled semi-cylinders, each with an outer diameter of 1.15" and an inner diameter of 1", erected 1" above the surface. This design was chosen because of the limited, but available, flexibility of the plastic in mind. This design permitted the plastic to bend inwards to be inserted into the test hole. When released, the semi-cylinders would try to retain their original position, providing a means of support the entire extensometer casing. The drawback to this design was when the constant force spring was introduced. As the spring emerged through the slot that was placed between the thin-walled cylinders, it would begin to twist and go off-center, creating a movement susceptible to error

when attempting to record data. This could have many implications in the field, the most detrimental of which being the creation of inaccurate data.

To resolve this issue, the final generation of the lid was designed with an additional component maintain the direction of the constant force spring. The gripping mechanism features two 3"-long thin-walled semi-cylinders, each with an outer diameter of 1.15" and an inner diameter of 1.00". The gripping mechanism was extended to provide ease of use as the longer walls provided more flexibility at the top while retaining its stiffness at the bottom. The width of each semi-circle was limited to 0.95" to ensure that it would fit inside of the test hole during installation. Inside of the gripping mechanism is a 4.5"-long slot designed to restrict the constant force spring from twisting in any other direction as it extends from and recoils into the extensometer casing. The extended slot proved to resist any twisting in the spring for several inches. The final iteration of the lid can be found in Figure 3.4. The lid takes approximately three hours to print with the MakerBot 3000. A specifications drawing of the lid has been provided in Appendix A.



**Figure 3.4 - 3-D printed extensometer lid**

#### **Anchorage: 3-D-Printed Stopper/Torsion Spring (GT6334309-MR)**

The anchor component of the extensometer design went through two phases. The first phase involved a 3-D printed anchor. The anchor consisted of a small cylinder with two arms that expanded to an overall diameter of 1.08". Inside of the two arms were two holes that extend through the length of the cylinder. These holes were designed to act as an access route for a high performance string that is to be knotted around the anchor at one end and the constant force

spring at the other. The string is precut to the depth dimension of the hole to ensure that the greatest amount of roof length is represented by the extensometer. The design's intention was to have the arms that would bend inward slightly to enter the test hole and then prohibit further movement as the arms attempted to retain their original form, thus anchoring the string. The final iteration of the 3-D printed anchor can be seen in Figure 3.5. The anchor takes approximately 45 minutes to print with the MakerBot 3000. A specifications drawing of the anchor has been provided in Appendix A.



**Figure 3.5 - 3-D printed borehole anchor**

This first design successfully passed all lab testing. However, the 3-D printed anchor did not fair as well in the field. Although occasionally successful (~20%), this design proved unreliable in the field. Test holes in the field had more inconsistencies than lab samples, particularly with shifting and discontinuities. As the 3-D printed anchor was being placed, the arms regularly snapped off and the entire anchor fell out of the test hole. After a second attempted field study, it was clear that the anchor needed to be improved.

The second phase of anchor design was to incorporate a torsion spring, which can be seen in Figure 3.6. By inserting the torsion spring into the test hole with the prongs facing downward, the spring acts as a grappling hook at the top of the test hole. Although this design was not incorporated in the field, it proved exceeding well in lab studies and is considered better than the 3-D printed anchor. The loop available on the torsion spring provides easy access for the string to be knotted around.



**Figure 3.6 - Torsion spring as a borehole anchor**

#### ***Data-Logging and Wireless Communication Equipment: MIDAS***

For data logging and wireless communications, an outside instrument was used to complete the project. The Golder Associates Miniature Data Acquisition System (MIDAS) both collects data and transmits it wireless, thus fulfilling the remaining requirements of the design objectives.

The MIDAS was developed by NIOSH as a way to collect data in underground coal mines and is capable of using wired or wireless data transmission. Serving as a self-powered, intrinsically safe (electrically self-contained) data-collector, the MIDAS datalogger, as seen in Figure 3.7, was designed with the intention of updating older equipment being used in U.S. coal mines. The datalogger is capable of monitoring up to eight instruments at a single time. Wireless data collection is feasible through the MIDAS user interface, as seen in Figure 3.8, and stored in a MicroSD card, located in the back panel of the user interface [21].

For this study, the borehole extensometer was hard-wired into the MIDAS datalogger. Data was logged at varying rates that were highly dependent on the experiment being performed. Data was collected via the MIDAS user interface and transferred to a computer spreadsheet through the MicroSD card.



**Figure 3.7 - MIDAS datalogger**



**Figure 3.8 - MIDAS user interface**

### ***Extensometer Assembly***

The procedure for assembly the extensometer requires a few simple steps. The first step is to attach the potentiometer to electrical wiring. Provide enough wiring for the extensometer can be attached to the wireless component of the design; this could be anywhere from a few inches to a few hundred feet. Slide the wire though the hole in the base portion of the casing before

soldering the wires to the proper terminal on the potentiometer. Solder the wires outside of the extensometer casing such that you do not melt the plastic of the casing.

The next step is to attach the spring to the potentiometer. Depending on the spring chosen will determine this setup. For the GCF-04-15, the connection to the rotating arm of the potentiometer uses two grommets that have an inner diameter of 0.25" and an outer diameter of 0.5625". This set of grommets attached firmly to the potentiometer arm and the GCF-04-15 wraps tightly around the outside of the grommets, as seen in Figure 3.9, so there is no need for additional adhesive.



**Figure 3.9 - Grommets around the potentiometer arm**

To set up an extensometer with the GCF-04-20, an extra step must be taken. The grommets that can be used for this constant force spring are larger, with an inner diameter of 0.375" and an outer diameter of 0.625". Since the inner diameter of these grommets is too large to independently wrap around the arm of the potentiometer, electric tape is wrapped around the arm of the potentiometer until it is suitable for the grommet to be wrapped tightly around it.

When the grommets are secure in either case, test the setup by placing the constant force spring around the grommets so it will unwind in a clockwise direction. Turn the potentiometer arm as far counterclockwise as possible. Look to ensure that the grommets do not slip and that the potentiometer arm turns at a consistent rate as the spring is being pulled. If there is slippage, additional tape may become necessary to connect the constant force spring and potentiometer. If the setup can be verified as competent, the potentiometer may be placed in the designated area of

the extensometer base where it can be securely fastened to the base of the casing, as seen in Figure 3.10.



**Figure 3.10 - Potentiometer securely placed inside the extensometer casing**

The next step is probably the most difficult of the portion of the assembly procedure. Before the extensometer can be screwed tightly shut, the constant force spring must be run through the extended slot of the lid. In order to do this, the loose end of the constant force spring must be bent backwards, creasing where the hole is located. After creasing the spring, pull out approximately eight inches of the spring while keeping the base restricted/in place. Place the creased edge of the spring inside the bottom opening of the lid and slide the spring through the slot. When the spring emerges on the other side, it should catch itself with the creased edge. Slowly, repel the lid back towards the base so the holes for the attachment screws align. Screw the lid into the base.

The final step is the addition of the anchor. Cut a piece of string that is approximately the length of a roof test hole at the location where equipment is going to be installed. At one end of the string, create a secure extension with the hole of the constant force spring, which should be readily available after the prior step. At the other end of the string, connect the torsion spring anchor. It is important in this step to not cut the string that has a greater length than the test hole. This could cause slack in the rope and interfere with data collection. A photo of the completed extensometer can be seen in Figure 3.11.

A complete evaluation of the financial requirements of the borehole extensometer design are available in Appendix B.

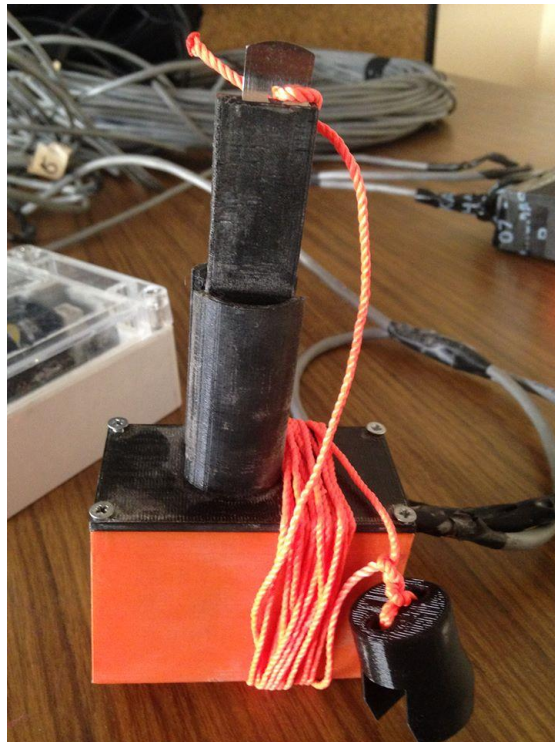


**Figure 3.11 - Completed wireless borehole extensometer**

---

## Installation and Data Collection

---

In order to install the extensometer, some required and auxiliary equipment will be necessary. The required equipment includes 0.5" PVC piping, cut to an appropriate length, and electrical wiring. PVC was selected because of its durability and relatively light weight. The length of the PVC piping will be dependent on the test hole depth. The reason 0.5" PVC pipe is used is to ensure that the pipe will not get lodged into test holes if there is bending in the test hole. The PVC may be cut into more than one piece to ease the burden of moving this equipment around the mine and reconnected as it is inserted into the borehole. The electrical wiring will be used to connect the potentiometer inside of the extensometer to the MIDAS datalogger.

In the event that the test hole in the roof is beyond reach, a ladder will be necessary for the installation process. In addition to the extensometer, it is recommended that the MIDAS datalogger is also attached to the roof in an effort to remove the datalogger from moving equipment and other types of intervention. The MIDAS can be effectively attached to the roof mesh via rope or hooks. Wire mesh cutters may be appropriate if roof mesh is present to cut a

hole big enough to install the extensometer as far into the test hole as possible. A hammer can be used to hit the bottom of the PVC pipe when the anchor is being installed.

The installation procedure begins outside of the mine where the extensometers are connected to the MIDAS datalogger. Up to four extensometers can be connected to the MIDAS datalogger simultaneously. In order to attach the two components, an electrical wire must be soldered at each end to the following corresponding parts: ground (1, black), output (2, red), and input (3, white). When the electrical wiring is set up for all devices, reattach the lid of the MIDAS datalogger to ensure that the device retains its permissible standards. When the lid is replaced, it is important to activate the datalogger using the MIDAS user interface. At this time, the user can name the datalogger, set the time on the datalogger, set the rate of data collection, and turn data collection on, ensuring that the device is operating correctly by checking to see if a green light is blinking. The string should be cut to the anticipated test hole length and attached to the constant force spring at one end and torsion spring anchor at the other. The wiring for each set of dataloggers and extensometers should be neatly wound and bound before travel underground to ensure no intertwining of wire occurs.

Once underground, the first part of the installation process is to examine test holes in the area with the PVC pipe. In the best-case scenario, these test holes would be examined shortly after the test hole is drilled to ensure that little-to-no manipulation has occurred. A desired test hole will retain the same depth as indicated in the mines roof control plan for anchor installation. If there is any mesh wiring present, it may be necessary to cut a hole in the mesh to provide enough access for the extensometer during installation.

If the test hole is found suitable, the test hole installation can begin. Placing the torsion spring coil-side up into the test hole, use the PVC pipe to push the spring up to the top of the test hole. As the constant force spring emerges from the extensometer, hold the extensometer against the roof; this will ensure that the constant force spring will coil back inside extensometer during installation. When the anchor has reach the top of the test hole, slowly insert the extensometer into the hole, paying attention to the constant force spring reentering the device. When the two half-cylinders reach the roof, squeeze the top portion of each half-cylinder together until it can be inserted. Put pressure on the bottom of the extensometer until it has been properly secured in the roof. Check the immediate area to ensure there are no threats to the extensometer or the

electrical wiring. When all applicable extensometers are installed, secure the MIDAS datalogger to a safe location in the immediate area, preferably to roof or rib mesh.

To collect data, the miner must have the MIDAS user interface and be in line-of-sight and within 200 feet of the MIDAS datalogger of interest. When using the interface, the data collection process is activated from the user interface and stored on a MicroSD flash memory card that is installed within the user interface. Data collected will reflect all the information that has been stored since the datalogger was activated or since the last time the datalogger had been reset. If data has been collected, the datalogger will be placed in a “paused” mode and the blinking light will turn red. If the user would like to continue collecting data, it is necessary to place the datalogger back into “run” mode. Information stored on the MicroSD card can be easily uploaded to a user-friendly spreadsheet developed specifically for the MIDAS.

---

## Calibration

---

The purpose of calibrating the extensometer is to understand the rate at which each respective spring will change the output of the potentiometer. When dealing with raw data, it is important to understand this rate of change since the null reading at the beginning of tests can vary based on how the extensometer is set up. Both setups will undergo the same controlled evaluation, and each set of data produced will be given a quadratic equation of best fit using least-squares regression. The quadratic equation was picked to represent the line of best fit because the ever-changing outer diameter of the constant force spring ensures that the rate of change in the potentiometer outputs will not be linear. The y-intercept of the equation of best fit for each extensometer setting will be set to zero to represent that no change in displacement has occurred.

To calibrate the extensometer, an experiment was run to simulate a test hole and the possible extension that may occur in a mine setting. To perform this experiment, a replica test hole had to be constructed. For the length of the original test hole, two pieces of 5' long, 1.25" PVC pipe were employed. This size pipe was selected because it features a 1" inner diameter, the same diameter as the MSHA-required test holes and did not require any change to the original extensometer design.

To simulate extension in the roof, a portion of 1.25" PVC pipe was cut into six segments, each segment cut to approximately 1" in length. Each segment had a slit cut into the side to provide a means of permitting the string attached to the anchor to slide through. A picture of the six segments is available in Figure 3.12.



**Figure 3.12 - Six 1" segments made from 1.25" PVC pipe**

In order to run the experiment, both 5' segments of the PVC pipe were lined up end-to-end on the floor. Two extensometers, one with each type of spring setup, were installed to a MIDAS datalogger and with anchors attached. One at a time, an extensometer was installed, with the anchor crossing the intersection between the two pipes and continuing into the second pipe. The data logger was turned on to collect data once every five seconds.

After about 30 seconds, the pipes were pulled apart and a 1" segment was installed in-between the two long pieces of PVC. After another 30 seconds, the pipes were pulled apart and another segment was added. This process was repeated until all the segments were used. When the first extensometer had completed the experiment, the string was cut and both the extensometer and the anchor were removed from the PVC pipes.

This same process was repeated with the second extensometer. In both cases, the segments were used in the exact same order and orientation to ensure that both extensometer setups experienced that same simulated extension. Every precaution was made to ensure that the experimental apparatus remained identical.

The results of the calibration data can be seen in Figure 3.13. This chart illustrates the raw data of the experiment. Since both tests were recorded in the same session, there is an offset between the two sets of results. In order to get the data represented accurately, the data must be first adjusted to zero and isolated from the excess data; this information is represented in Figure 4-15. A complete table of the results collected for the calibration test is available in Appendix C.

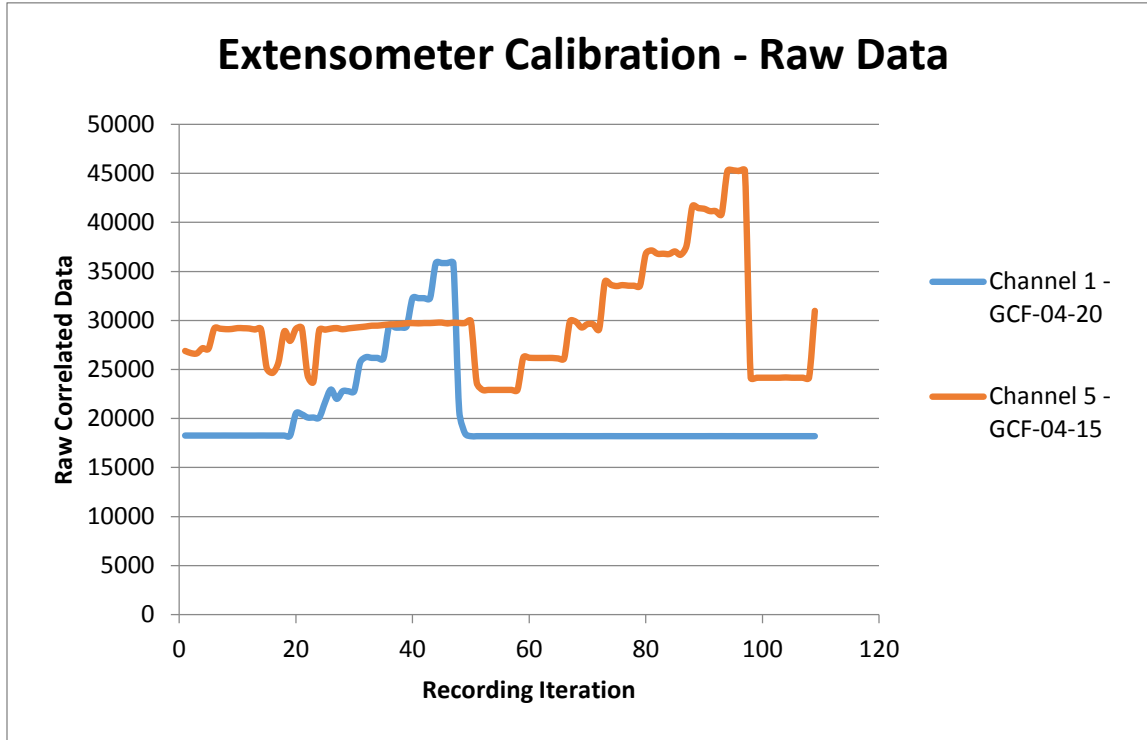


Figure 3.13 - Raw data records of calibration test

## Extensometer Calibration - Adjusted Data

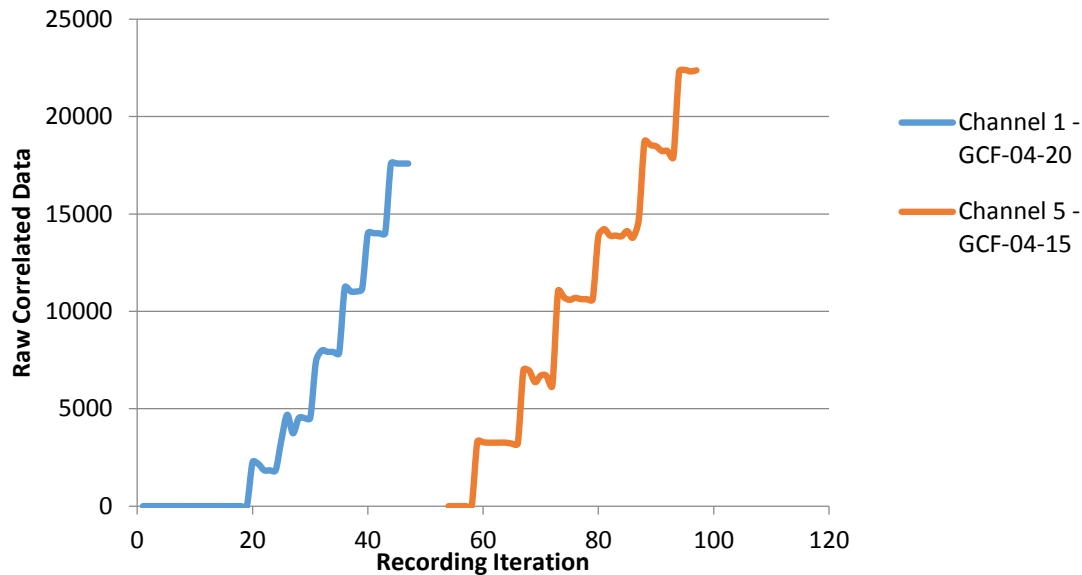


Figure 3.14 - Adjusted raw data records of calibration adjusted

The data in Figure 3.14 clearly observes the step-like increments created by the insertion of the 1" segments. To design a set of data that can determine a line of best fit, the data points representing each step is required to be isolated into a singular data point. The cluster of data points that represents each step can be averaged in order accommodate this requirement. After the initial average was taken for each step, the raw data points were examined against the average each point represented. If the raw score for a particular data point did not obviously reflect a particular step in the analysis, it was considered to be an outlier and removed. Table 3.2 reflects the results of this analysis. Further information regarding the calculation of each step's final figure Appendix C.

To determine the equation of best fit for each spring setting, the consolidated step data was plotted, as seen in Figure 3.15. Trendlines were created for each array of points. Each trendline represents the linear equation of best fit for its particular set of data with the y-intercept set to zero.

**Table 3.2: Consolidated Step Point Data from Calibration Test**

Inches Extended	Channel 1 GCF-04-20	Channel 5 GCF-04-15
0	0	0
1	1840	3263
2	4577	6648
3	7919	10645
4	11022	13858
5	14009	18354
6	17589	22349

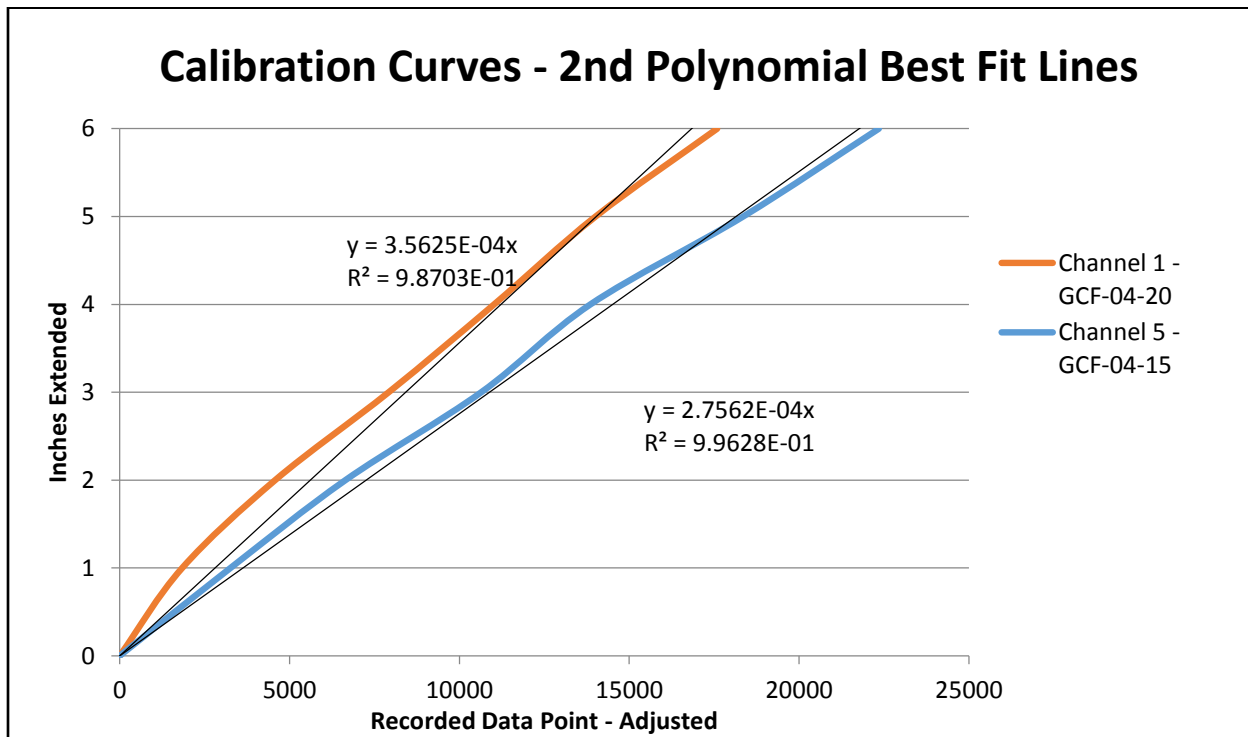


**Figure 3.15 - Calibration curves – 2<sup>nd</sup> polynomial best fit line**

As shown by this experiment, the amount of displacement correlating to extension for each setup are as follows:

For the GCF-04-15 spring:

$$\text{Inches of Extension} = (2.76 * 10^{-4})x \quad (2)$$

For the GCF-04-20 spring:

$$\text{Inches of Extension} = (3.56 * 10^{-4})x \quad (3)$$

In each equation, x represents the adjusted raw data point for each respective extensometer. The linear line of best fit was chosen because of the number of available data points. In a larger sample set, a quadratic or higher order equation would better characterize the data set.

---

## Field Implementation

---

Two attempts were made to install the borehole extensometer for roof extension measurement at an underground longwall coal mine. The mine is located in northern West Virginia where high-grade bituminous coal is mined in the Lower Kittanning seam. The average cutting height in the mine is 96" and the average depth of cover is 600 feet. The roof of the mine is considered very good in most areas. To date, the mine has completed two longwall panels and is currently mining a third panel. Measuring for roof extension is fundamentally different than measuring for roof-to-floor convergence. Roof extension is a measurement that reflects the change in length of the roof strata; convergence, however, measures the change in available headroom in the excavation. Comprehensive convergence measurements require both the displacement of the roof as well as the displacement of the floor through heaving. For the sake of completeness, roof-to-floor convergence measurements were completed and can be found in Appendix D.

The first attempt at installing the borehole extensometer took place on October 10<sup>th</sup>, 2014. Equipment was scheduled for installation in the #2 headgate between the 22<sup>nd</sup> and 19<sup>th</sup> crosscuts. This occasion was met with a variety of challenges and complications. These issues were documented and resolved by the next installation attempt.

The first major issue that occurred was the failure of the 3-D printed anchors in the mine environment. Four of the six anchors that were attempted to be installed had the restraining arms snap and break off, rendering the equipment useless. In order to resolve this issue, an alternative means of anchorage was sought out. This issue directly resulted in the use of torsion springs in later experiments.

The second problem that occurred in October 10<sup>th</sup> installation was attributed to the use of 0.75" PVC pipe as a means of pushing a stopper up the test hole. The primary issue with this approach was that the pipe would regularly get stuck in the test hole, particularly in areas where movement in the roof had already occurred and the test hole had been curved. In one instance, the PVC actually became stuck in the test hole and became irretrievable. In addition, the portion of the

installation where the PVC is removed and the extensometer replaces it in the test hole was more difficult with the larger diameter PVC pipe. The issues experienced with the 0.75" diameter PVC pipe led to the use of 0.50" diameter PVC pipe in future installations.

The last item that needs to be mentioned was the use of the GCF-04-10 constant force spring in the extensometer design. Originally, the GCF-04-10 was the most sensitive spring considered for the extensometer and was favored over other springs because it was the most likely to detect a small change in the ground environment. However, when introduced to the mining environment and the envisioned installation process, the GCF-04-10 setup did not work. In addition to twisting uncontrollably as the anchor was being installed, it was not strong enough to maintain its grip around the potentiometer arm, ejecting from the extensometer to a fair distance up the test hole. The complications involved in the installation of the extensometer with the GCF-04-10 spring eliminated it from future design consideration.

The second attempt to install equipment at the aforementioned mine took place on November 20<sup>th</sup>, 2014. At this time, two borehole extensometers were successfully installed in the #2 headgate and the 10<sup>th</sup> crosscut. At the time of the installation, the longwall was currently running at a location between the 15<sup>th</sup> and 14<sup>th</sup> crosscut.

The intention of installing equipment at this location was to gauge the amount of deformation that could be attributed to the side abutment stresses. Permission was not granted to install equipment in the entry immediately adjacent to the longwall panel, where the highest amount of deformation would typically occur on the headgate side of the active panel. In addition, a stopping was located halfway through the 10<sup>th</sup> crosscut at the time of installation, providing a limited number of locations to install the extensometers.

One of the extensometers installed was set up with a GCF-04-15 spring. This extensometer was connected to the MIDAS datalogger in channel 5. This extensometer was installed approximately halfway between the headgate entry and the track entry in the 10<sup>th</sup> crosscut. The anchor used was a 3-D printed stopper. The only issue was that the initial failure of two 3-D printed anchors. The arms broke as they had in the previous installation attempt. The third anchor was installed with no issue.

The other extensometer installed was set up with a GCF-04-20 spring. This extensometer was connected to the MIDAS datalogger in channel 1. This extensometer was installed approximately 20' from the track entry into the 10<sup>th</sup> crosscut on the #2 headgate side. The anchor used was a 3-D printed stopper. There were no issues in the process of installing the equipment.

Mine map drawings reflecting the locations of the extensometers in the mine can be found in Figures 3.16 and 3.17.

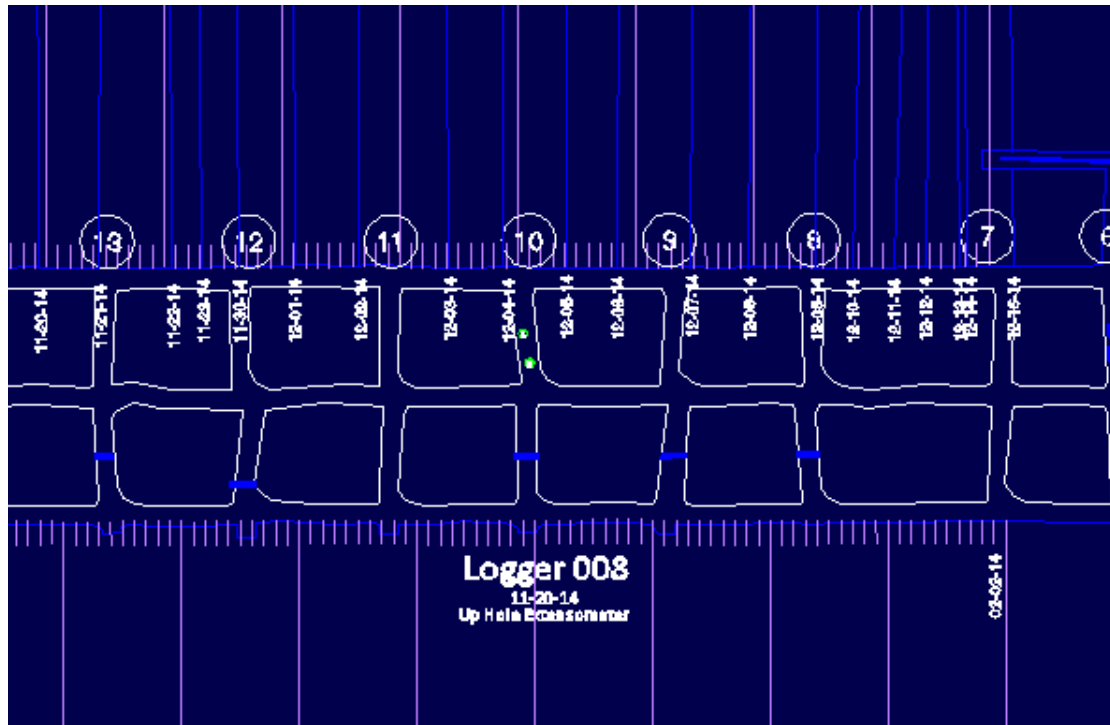


**Figure 3.16 - Extensometer location in mine, longwall panel**

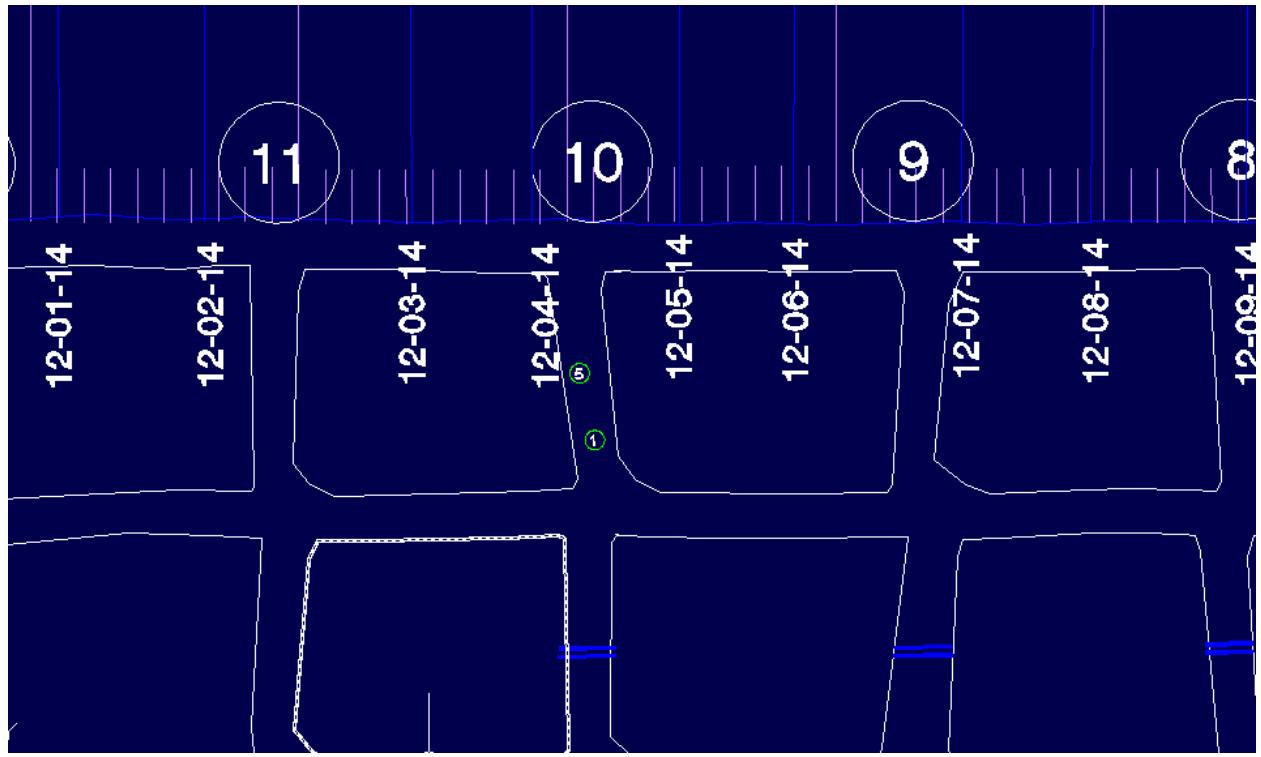


**Figure 3.17 - Extensometer location in mine, headgate**

---

## Results

---

Data was collected from the MIDAS datalogger located in the 10<sup>th</sup> crosscut of the #2 headgate on March 11<sup>th</sup>, 2015. 2672 data points were recorded for each extensometer. It was reported that the long wall passed the 10<sup>th</sup> crosscut on December 5<sup>th</sup>, 2014 during the day shift. The raw data from each extensometer is available in Figure 3.18; the adjusted raw data can be seen in Figure 3.19.

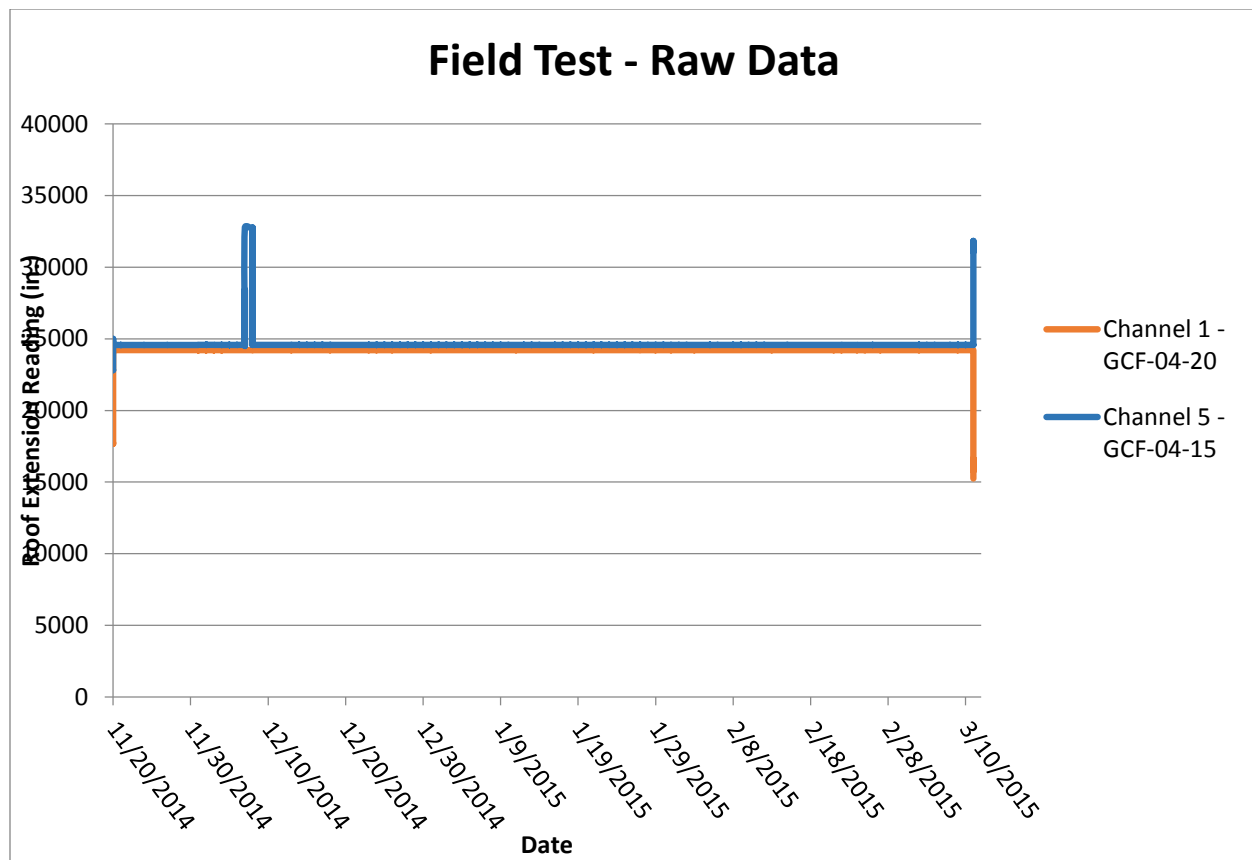
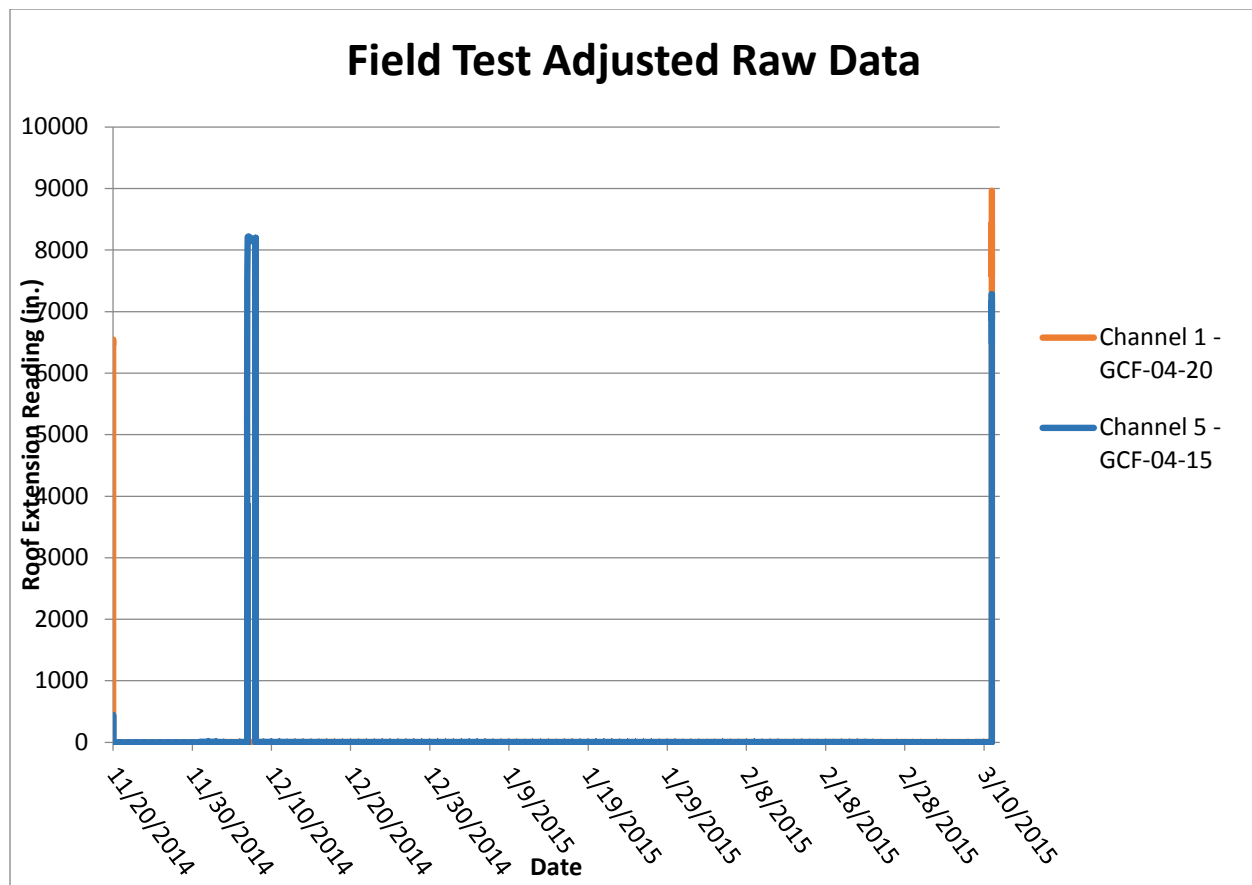
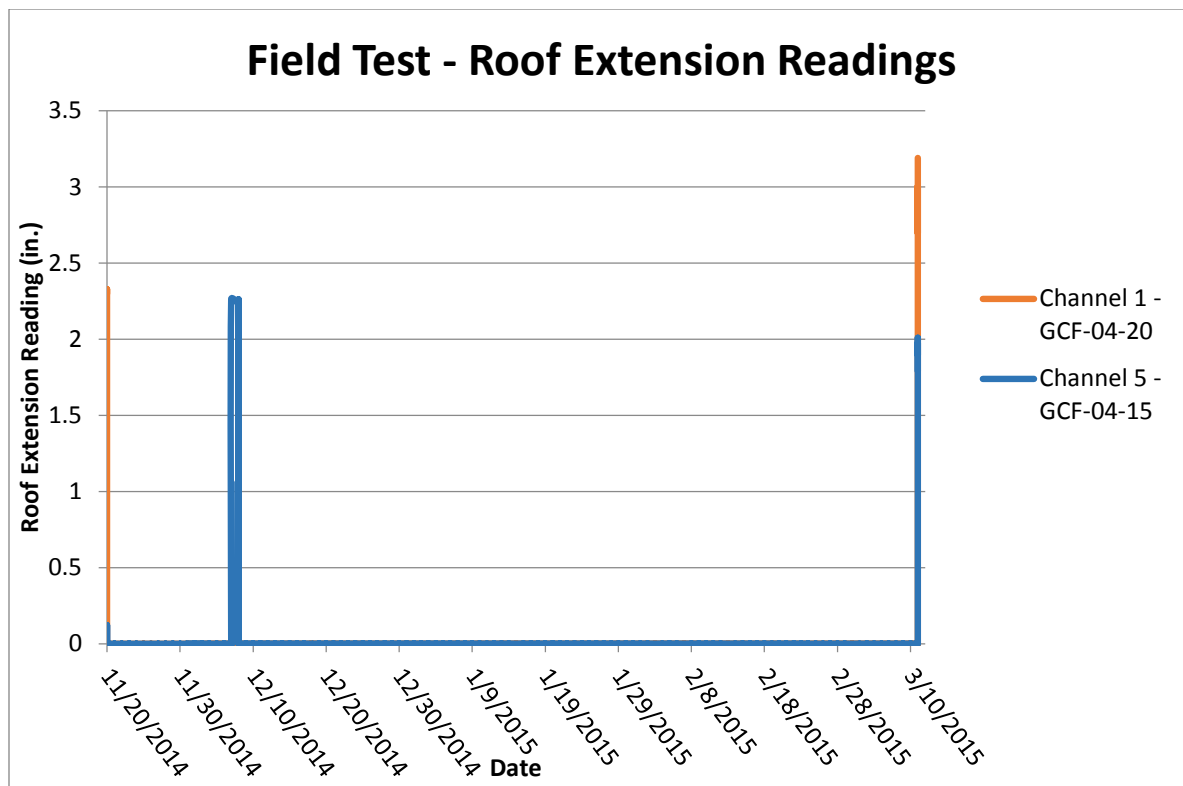


Figure 3.18 - Raw data records of field installation



**Figure 3.19 - Adjusted raw data of field test installation**

Using equations (2) and (3), the amount extension in the roof examined by each extensometer can be evaluated. Figure 3.20 represents the record of roof extension observed.



**Figure 3.20 - Roof extension readings of field test installation**

In order to properly evaluate the data set, it is important to identify the outlier. Figure 3.21 gives a clear insight as to the data obtained between December 7<sup>th</sup>, 2014 at 12:00PM and December 9<sup>th</sup>, 2014 at 12:00AM. After careful consideration, it has been determined that the spike in the data set was due to an electrical malfunction in the MIDAS datalogger. Although it was speculated, the raw data figure between the smaller magnitude spike and the larger magnitude spike is not exactly double (3852 to a range of 7821-8200), but it is close. The reason for this error is unclear, but has occurred in previous studies using the MIDAS datalogger.

The outliers were removed from the data set. Updated roof extension charts are presented with regards to raw data set and the actual length of extension are present in Figures 3.22 and 3.23.

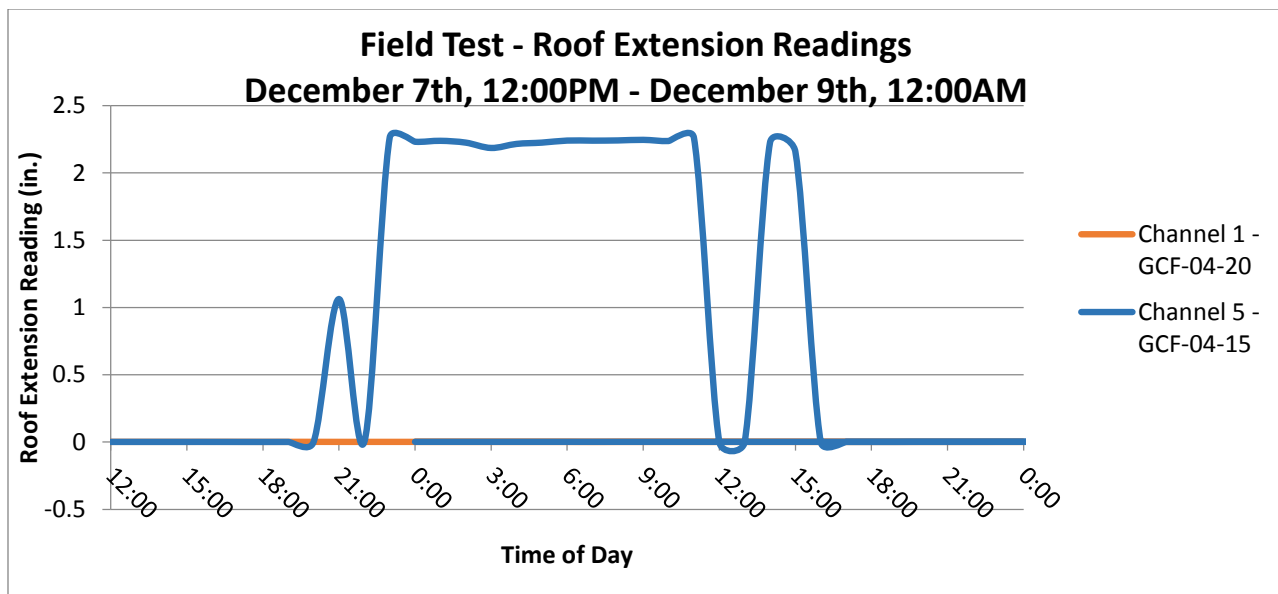


Figure 3.21 - Examination of data from December 7<sup>th</sup> and December 8<sup>th</sup>

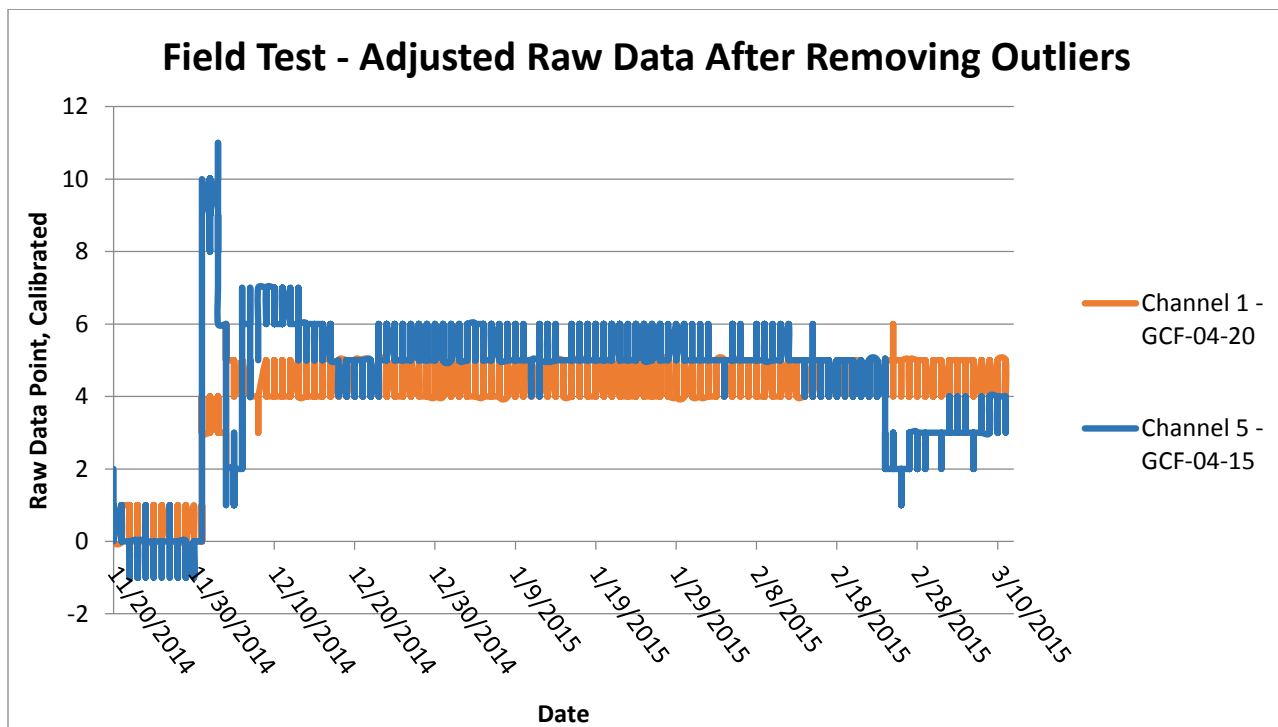
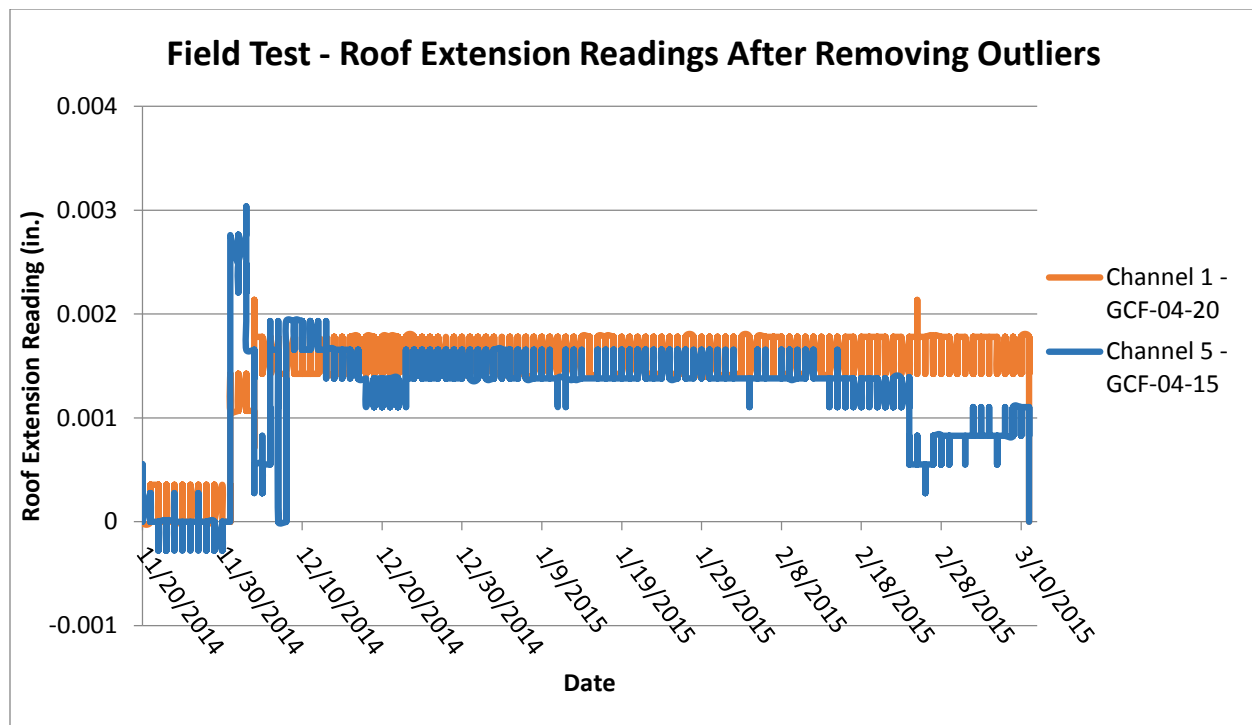


Figure 3.22 - Roof extension adjusted raw data after removing outliers



**Figure 3.23 - Roof extension readings after removing outliers**

### Sources of Error

There are various items that could have contributed to error in the results. Regarding underground installation, the viability of the equipment, particularly with the 3-D printed stopper, may not have been suitable for the mine environment. Had the opportunity presented itself, more equipment would have been installed to correct any features of the extensometer that may need improvement.

Error could have also been the result of the MIDAS. Prior investigations with the MIDAS datalogger have shown circumstances where outliers appear without reason and automatically correct themselves in a short amount of time, as seen in Appendix D. The MIDAS has also exhibited issues with picking up crosstalk between internal terminals in lab tests, where unsolicited data will appear on channels in which the extensometer was not attached.

In the calibration lab test, more precision could have been taken in collection of data. More data points could have been collected per 1" segment addition, which would have produced more data to analyze. Having more data points would have also polarized the readings that were not truly affiliated with any particular segment addition and may have been recorded during the process of

segment addition. Another potential source of error in the calibration test is the true length of each of the 1" segments. Although they were cut to the 1" specification, the edges were not truly straight and may have attributed to a small deviation in the readings.

Another potential source of error is the constant force spring. Although the spring moves fairly linearly for the first few inches it is extended outside of the extensometer, it will begin to curl if the extensometer is experiencing excessing extension. This would rarely be a contributor to extreme error, but could affect the overall accuracy of readings at great lengths. Fortunately, the borehole acts a secondary slot extension, forcing the constant force spring to remain primarily straight in the test hole.

---

## **Discussion of Results and Conclusions**

---

The results for the Channel 1 – GCF-04-20 extension data indicates that little to no extension of the roof occurred between the anchor point at the top of the test hole and the extensometer. The range of the raw data corresponds to a displacement of less than 0.003", a negligible amount. If no extension or movement occurred in the roof at this location, the extensometer data is correct.

The results of the Channel 5 – GCF-04-15 extension data indicate similar results to that of the Channel 1 – GCF-04-20. A low range of extension in the roof only correlated to a displacement reading of about 0.003".

This low range of displacement is likely due to the placement of the extensometers. Had the extensometers been located nearer to the longwall panel on the headgate side or experienced a second longwall-pass with the adjacent panel, there would be a greater chance that significant displacement would have occurred. However, the limited availability of suitable test holes and the permissions the mine allowed for testing prevented this from happening.

No information regarding the condition of the site where the installation took place has been provided since installation that could assert a conclusion as to if any equipment error occurred.

To conclude, a wireless borehole extensometer was developed and implemented in a lab setting as well as in an underground coal mine. The extensometer was designed to mimic the traits of a string transducer and was implemented with a wireless data component. The exterior casing of the extensometer is adequate for the mine environment and acts as a self-supporting system that

allows the extensometer to hold itself onto the roof at the location of a MSHA required test hole. The 3-D printer permitted several iterations of the extensometer casing to be produced in a timely fashion, where it could then be evaluated for its feasibility regarding the design objectives. A cheap, effective anchor was discovered to replace a less competent alternative. The anchor, when in place at the top of the test hole, acted as a second means of support for the extensometer to hold it in place against the roof.

The results of the lab study prove that the borehole extensometer that was developed can adequately measure extension in a borehole environment. When extension in the roof occurs, the extensometer is capable of transmitting that information through a potentiometer and to a data-logging device that relays information regarding the magnitude of displacement.

In the field, the extensometer was successfully installed, but returned data that could not verify whether the device was recording data properly. Further field testing is necessary to ensure the device is appropriate for the roof extension monitoring.

## *Chapter 4: Future Work*

If work is to be continued in this area of research, more underground installations need to occur in areas where convergence occurs at a premium. Installing the extensometer at these locations alongside a redundant and commercially available extensometer will increase the likelihood that measurements will be taken and can be verified with other equipment. The great uncertainty in this study is the actual impact the extensometer can have in the mine environment. Components of the extensometer design can only be improved on once they are met with failure, so having more opportunities to install would inevitably develop the extensometer further.

Another point of emphasis that needs to be improved is the wireless communication system. Currently, information can only be recorded using the MIDAS user interface when in line of sight of the datalogger. The objective of future work should be to provide the extensometer the ability to communicate data in real-time to the surface. Improving this wireless feature in the extensometer would place this equipment on the cutting edge of mining technology. The likely course of action to pursue this goal is to install a WLAN wireless device and set it up to the extensometer; readings will be taken and can be communicated to a leaky feeder system, and provide information to the surface.

A design feature that can be improved is the feature of tension for the potentiometer. While the constant force spring performs adequately, the goal for this objective would be to improve upon the ease of use in the system. A spring-loaded potentiometer could serve as the source of tension, although a manufactured one is typically ten times the cost of a potentiometer that is not spring-loaded.

If the constant force spring is chosen to continue in future iterations of the design, the grommets should be replaced with a part that is specifically fabricated to connect the spring and the potentiometer arm. This will reduce the likelihood of error due to the component parts of the device and ensure no slippage occurs between the two parts.

The permissibility of the device also needs to be evaluated. The parts of the device should be secure to one another and permit no airway with access to the outside environment. This may

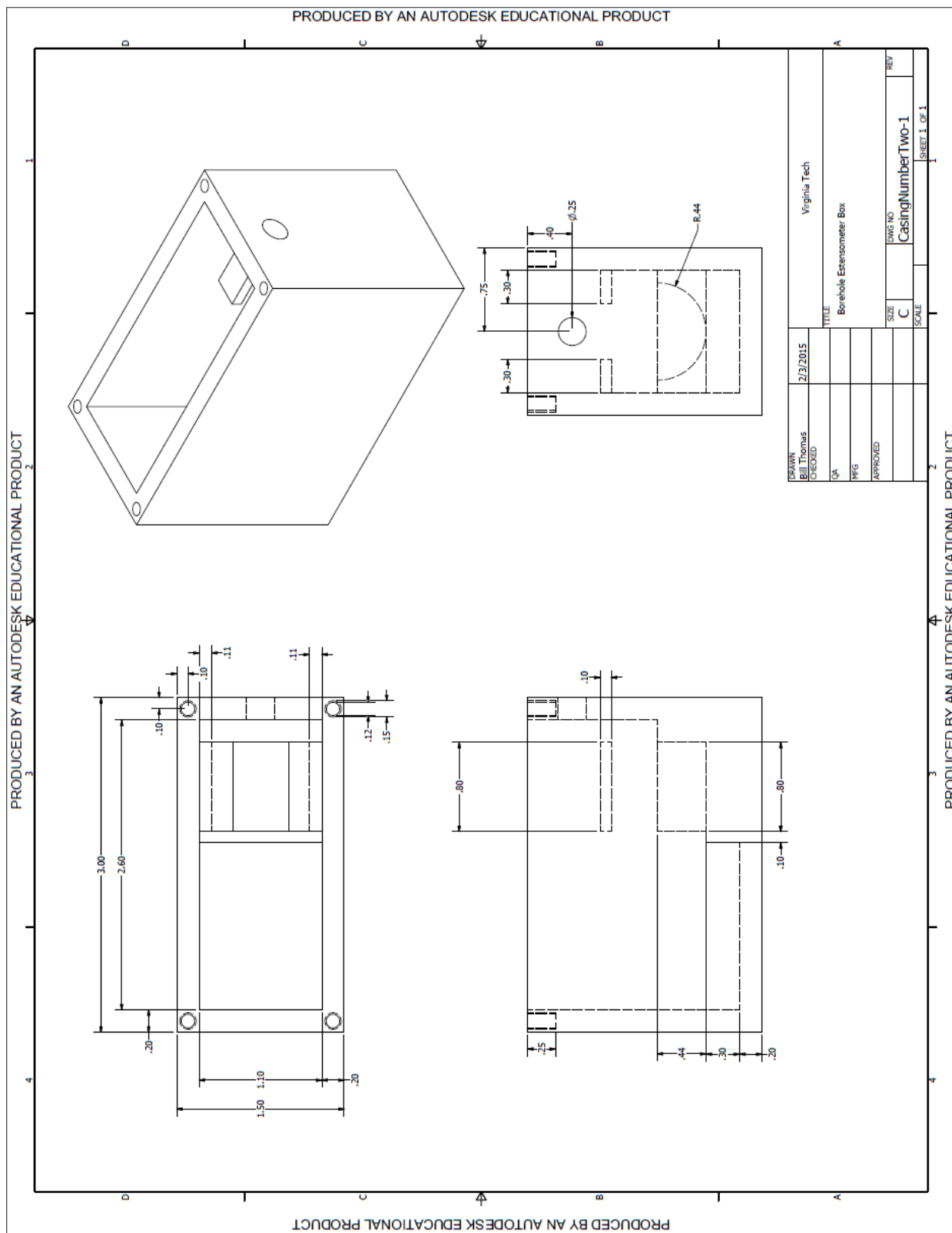
require the addition of plugs or rubber stoppings that restrict access during the fabrication of the device. Additional attention should be paid to the electrical wire that is connected to the potentiometer inside the extensometer such the possibility any sparks that may occur during the communication process are minimized.

## Works Cited

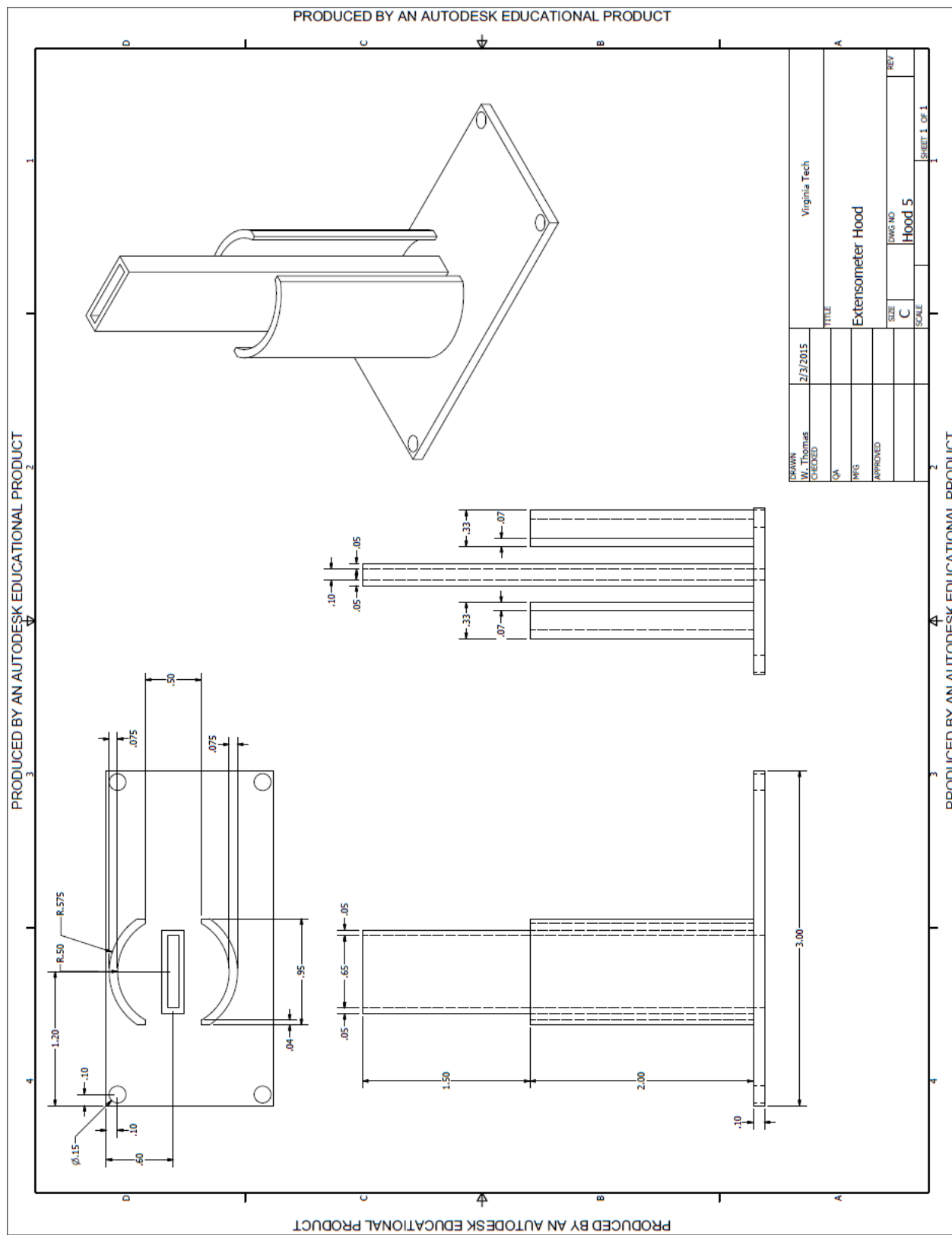
- [1] Peng, S. (1986). *Coal Mine Ground Control* (2nd ed.). New York: Wiley.
- [2] Stricklin, K. (Ed.). (2013, December 1). Roof Control Plan Approval and Review Procedures. MSHA. [Online]
- [3] MINER Act, 2006. MSHA. [Online]
- [4] Boyes, W. (Ed.). (2010). *Instrumentation Reference Book* (4th ed.). Amsterdam: Butterworth-Heinemann/Elsevier.
- [5] UniMeasure: Linear Position Transducers. (2013, June 17). [Online]
- [6] 30 CFR 75
- [7] Chugh, Y., & Silverman, M. (1982). Premining Investigations for Ground Control State-of-the-Art. *Ground Control in Room and Pillar Mining*, 9-15.
- [8] Smith, A. (1984). Relationships of Assumed Condition of Mine Roof and the Occurrence of Roof Falls in Eastern Kentucky Coal Fields. *Second International Conference on Stability in Underground Mining*, 2.
- [9] Peng, S., & Chiang, H. (1984). *Longwall Mining*. New York: Wiley.
- [10] Lu, P. (1984). Rock Mechanics Studies in a Mechanical Longwall Coal Mine. *Second International Conference on Stability in Underground Mining*, 2.
- [11] Karmis, M., & Kane, W. (1984). An Analysis of the Geomechanical Factors Influencing Coal Mine Roof Stability in Appalachia. *Second International Conference on Stability in Underground Mining*, 2.
- [12] Moebs, N., & Ellenberger, J. (1982). Hazardous Roof Structures in Appalachian Coal Mines. *Ground Control in Room and Pillar Mining*.
- [13] Bawden, W., Tod, J., Lausch, P., & Davison, G. (2002). The Use of Geomechanical Instrumentation in Cost Control in Underground Mining. *International Seminar on Deep and High Stress Mining Instrumentation*. [Online]
- [14] Hartman, H. (Ed.). (1992). *SME Mining Engineering Handbook* (2nd ed.). Littleton, Colo.: Society for Mining, Metallurgy, and Exploration.
- [15] Extensometers. (2012). [Online]
- [16] Dripke, M. (2008, October 17). Choosing the Right Extensometer for Every Materials Testing Application. *Quality Magazine*.
- [17] *Remote Reading Telltale System*. Golder Associates (2013).
- [18] Forooshani, A., Bashir, S., Michelson, D., & Noghanian, S. (2013). A Survey of Wireless Communications and Propagation Modeling in Underground Mines. *IEEE Communications Surveys & Tutorials*, Vol. 15 (4), 1524-1545.
- [19] Bandyopadhyay, L., Mishra, P., Kumar, S., & Narayan, A. (n.d.). Radio Frequency Communication Systems in Underground Mines.
- [20] Yang, Wei & Huang, Ying. (2007). Wireless Sensor Network Based Coal Mine Wireless and Integrated Security Monitoring Information System. *Proceedings of the Sixth International Conference on Networking*.
- [21] *MIDAS (Miniature Data Acquisition System) USER MANUAL*, (Issue 1). (2012).
- [22] Constant Force Springs. (2015). MSC Direct. [Online]

## *Appendix A: Extensometer Design Drawings*

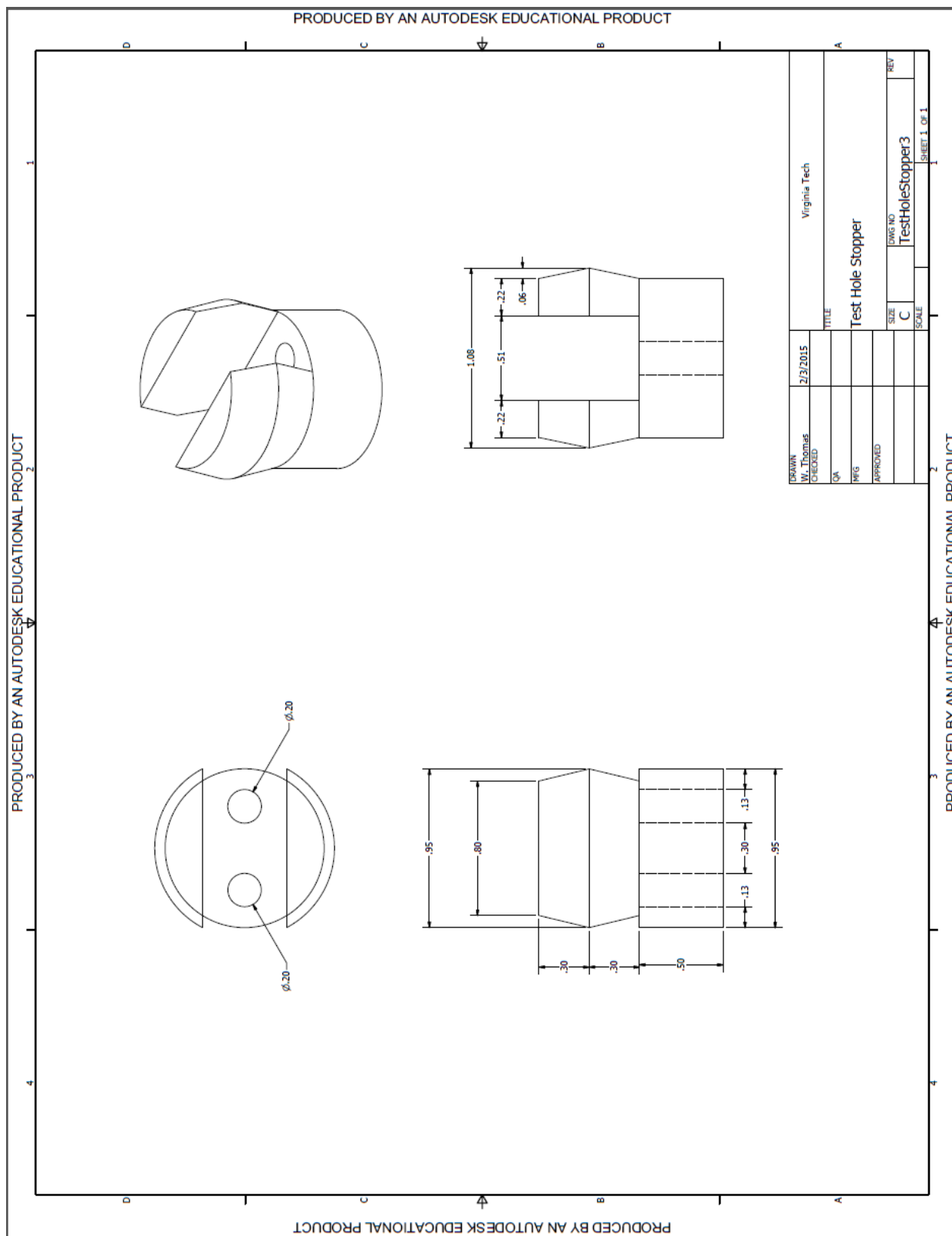
# 1) Extensometer Case Drawing



## 2) Extensometer Lid Drawing



### 3) 3-D Printed Anchor Drawing



## *Appendix B: Extensometer Cost Analysis*

The raw cost of the materials for either setup can be calculated. The setup for an extensometer with the GCF-04-15 spring costs \$25.47 to produce; the extensometer with the GCF-04-20 spring costs \$26.73. A complete tabulation of the product costs for the GCF-04-15 and GCF-04-20 springs can be found in Table 3-2 and Table 3-3, respectfully.

**Table B.1: GCF-04-15 Extensometer Setup Cost Analysis**

	GCF-04-15 Setup			
	Type	Quantity (#,lb)	\$/unit	Cost
Potentiometer	3590P-2-102L	1	\$10.58	\$10.58
Spring	GCF-04-15	1	\$8.25	\$8.25
Base	3D Print	0.0954	\$37.50	\$3.58
Lid	3D Print	0.0448	\$37.50	\$1.68
Grommets	Small	2	\$0.35	\$0.70
Tape	N/A	None	-	\$0.00
Electrical Wire	LL7874	Varies	-	\$0.00
Screw	M3x8, .50 Pitch	4	\$0.17	\$0.68
Total Production Cost				<b>\$25.47</b>

**Table B.2: GCF-04-20 Extensometer Setup Cost Analysis**

	GCF-04-20 Setup			
	Type	Quantity (#,lb)	\$/unit	Cost
Potentiometer	3590P-2-102L	1	\$10.58	\$10.58
Spring	GCF-04-20	1	\$9.51	\$9.51
Base	3D Print	0.0954	\$37.50	\$3.58
Lid	3D Print	0.0448	\$37.50	\$1.68
Grommets	Large	2	\$0.35	\$0.70
Tape	Electrical	Negligible	-	\$0.00
Electrical Wire	LL7874	Varies	-	\$0.00
Screw	M3x8, .50 Pitch	4	\$0.17	\$0.68
Total Production Cost				<b>\$26.73</b>

## Appendix C: Calibration Lab Results

Below are the tables associated with the data used during the calibration exercise. “RAW” indicates the datum that was relayed via the MIDAS datalogger; “Calibrated” is the RAW minus the null value (the value associated with zero extension); “Pertinent” are the values from the “Calibrated” column associated with that spring’s respective test (absent figures are considered not “Pertinent”); “Steps” are the values associated with the values used in the calibration curve, with the colors highlighting the “Pertinent” values used to ascertain that value through averaging.

**Table C.1: GCF-04-20 Calibration Results**

GCF-04-20			
RAW	Calibrated	Pertinent	Steps
18264	0	0	0.052632
18264	0	0	1840.333
18264	0	0	4562.75
18264	0	0	7918.75
18264	0	0	11022
18264	0	0	14009.25
18264	0	0	17588.5
18265	1	1	
18263	-1	-1	
18264	0	0	
18264	0	0	
18264	0	0	
18264	0	0	
18265	1	1	
18264	0	0	
18264	0	0	
18264	0	0	
18264	0	0	
18264	0	0	
18264	0	0	
18264	0	0	
20524	2260	2260	
20428	2164	2164	
20106	1842	1842	
20104	1840	1840	
20103	1839	1839	
21660	3396	3396	
22954	4690	4690	
22004	3740	3740	
22784	4520	4520	

**Table C.2: GCF-04-15 Calibration Results**

GCF-04-15			
RAW	Calibrated	Pertinent	Steps
26893	3975		0
26671	3753		3262.6
26643	3725		6647.833
27175	4257		10644.83
27116	4198		13858.4
29184	6266		18354.17
29163	6245		22349
29111	6193		
29131	6213		
29223	6305		
29209	6291		
29181	6263		
29075	6157		
29118	6200		
25137	2219		
24653	1735		
25718	2800		
28871	5953		
27915	4997		
29149	6231		
29234	6316		
24417	1499		
23752	834		
29022	6104		
29057	6139		
29172	6254		
29224	6306		
29106	6188		

22785	4521	4521	
22784	4520	4520	
25701	7437	7437	
26252	7988	7988	
26184	7920	7920	
26183	7919	7919	
26112	7848	7848	
29493	11229	11229	
29286	11022	11022	
29286	11022	11022	
29417	11153	11153	
32273	14009	14009	
32274	14010	14010	
32273	14009	14009	
32273	14009	14009	
35852	17588	17588	
35852	17588	17588	
35853	17589	17589	
35853	17589	17589	
20801	2537		
18484	220		
18199	-65		
18200	-64		
18200	-64		
18200	-64		
18200	-64		
18201	-63		
18201	-63		
18201	-63		
18201	-63		
18201	-63		
18201	-63		
18201	-63		
18202	-62		
18201	-63		
18201	-63		
18201	-63		
18201	-63		
18201	-63		
18202	-62		
18201	-63		
18201	-63		
18201	-63		
18201	-63		
18201	-63		
18201	-63		
18201	-63		
18201	-63		

29192	6274		
29257	6339		
29320	6402		
29383	6465		
29467	6549		
29474	6556		
29534	6616		
29594	6676		
29613	6695		
29644	6726		
29715	6797		
29732	6814		
29703	6785		
29734	6816		
29734	6816		
29771	6853		
29789	6871		
29693	6775		
29778	6860		
29741	6823		
29729	6811		
29930	7012		
23674	756		
22923	5		
22919	1		
22918	0	0	
22918	0	0	
22918	0	0	
22918	0	0	
22918	0	0	
26230	3312	3312	
26194	3276	3276	
26177	3259	3259	
26177	3259	3259	
26178	3260	3260	
26177	3259	3259	
26126	3208	3208	
26126	3208	3208	
29913	6995	6995	
29870	6952	6952	
29284	6366	6366	
29624	6706	6706	
29607	6689	6689	

18201	-63		
18202	-62		
18202	-62		
18201	-63		
18201	-63		
18201	-63		
18201	-63		
18201	-63		
18201	-63		
18201	-63		
18201	-63		
18201	-63		
18201	-63		
18201	-63		
18201	-63		
18201	-63		
18201	-63		
18201	-63		
18201	-63		
18202	-62		
18201	-63		
18202	-62		
18201	-63		
18201	-63		
18201	-63		
18201	-63		
18201	-63		
18200	-64		
18201	-63		
18201	-63		
18201	-63		
18200	-64		
18200	-64		

29097	6179	6179	
33963	11045	11045	
33640	10722	10722	
33509	10591	10591	
33607	10689	10689	
33546	10628	10628	
33546	10628	10628	
33529	10611	10611	
36790	13872	13872	
37140	14222	14222	
36807	13889	13889	
36807	13889	13889	
36773	13855	13855	
37038	14120	14120	
36705	13787	13787	
37639	14721	14721	
41649	18731	18731	
41458	18540	18540	
41394	18476	18476	
41153	18235	18235	
41153	18235	18235	
40826	17908	17908	
45227	22309	22309	
45311	22393	22393	
45236	22318	22318	
45294	22376	22376	
24162	1244		
24161	1243		
24161	1243		
24161	1243		
24161	1243		
24190	1272		
24161	1243		
24161	1243		
24161	1243		
24161	1243		
30979	8061		

## *Appendix D: Convergence Station Development and Implementation*

---

### **Convergence Station Components**

---

In order to evaluate roof to floor convergence in underground coal mines, a semi-wireless convergence monitoring station was developed. The monitoring system is designed to be installed in the artificial standing support common to underground coal mines. The two types of support that the monitoring system would be installed in are timbers and cement-filled standing supports.

There are two components to the monitoring system: the UniMeasure JX-PA extensometer and the Golder Associates MIDAS datalogger. The UniMeasure JX-PA extensometer is a string extensometer that contains a spring-loaded,  $1\text{ k}\Omega$  potentiometer that controls tension in the string. The JX-PA has a measurement range of 20 inches. In order to increase the distance that the JX-PA extensometer can monitor, a string can be attached to the hook at the end of the string. This, however, will not increase the range of deformation that can be detected. The JX-PA extensometer has two screw holes for anchorage purposes that can be rotated to various positions around main axis of the device. Ten feet of standard red/white/black electrical wire is attached to potentiometer inside the device and expels from the side opposite the string. An photo of the JX-PA extensometer can be found in Figure D.1.



**Figure D.1: JX-PA String Extensometer**

For data logging and wireless communications, an outside instrument was used to complete the project. The Golder Associates Miniature Data Acquisition System (MIDAS) both collects data and distributes it wireless, thus fulfilling the remaining requirements of the design objectives.

The MIDAS was developed by NIOSH as a way to collect data in underground coal mines and is capable of using wired or wireless data transmission. Serving as a self-powered, intrinsically safe data-collector, the MIDAS datalogger, as seen in Figure D.2, was designed with the intention of updating older equipment being used in U.S. coal mines. The datalogger is capable of monitoring up to eight instruments at a single time [21]. Wireless data collection is feasible through the MIDAS user interface, as seen in Figure D.3, and stored in a MicroSD card, located in the back panel of the user interface.

For this study, the borehole extensometer was hard-wired into the MIDAS datalogger. Data was logged at varying rates that were highly dependent on the experiment being performed. Data was collected via the MIDAS user interface and transferred to a computer spreadsheet through the MicroSD card.



**Figure D.2: MIDAS datalogger**



**Figure D.3: MIDAS user interface**

---

### **Installation Procedure**

---

The first portion of the installation is connecting the JX-PA to the MIDAS datalogger. Up to four extensometers can be attached to each MIDAS datalogger. It is essential to provide an adequate amount of additional wire to each extensometer to ensure the extensometers can reach the desired underground support locations.

The next step is to attach the extensometer to the standing support. Ideally, the extensometer will be placed at a location very close to the roof or the floor in a space in which it is unlikely to be tampered. For timber supports, the easiest method of attaching the extensometer is to take a screw, place it in one of the anchorage holes of the extensometer, and screw it in to the wood. For cement-filled supports, the support will need to have a hole punched in the side before the screw can be inserted; it is recommended that a handheld pick-ax or a designed hole-puncher be used to complete this task. A second screw can be attached in the opposite screw hole of the extensometer if possible to add extra anchorage (this may not be feasible in cement-filled supports).

On the opposite end of the support, a screw is installed directly above or below the extensometer, depending on which location the extensometer was installed. Attach a string that is approximately the length equal to the distance between screw and the extensometer to the hook

of the extensometer. Expelling the cord from the extensometer, wrap the string around the screw, such that the extensometer cord is fully extended to its 20-inch maximum length. Knot the string around the screw, ensuring that the string is secure while maintaining the 20-inch extension.

Repeat the previous steps with all of the extensometers. When all are installed, ensure that the electrical wires and the MIDAS datalogger secure and out of harm's way and away from areas of heavy traffic. Interference with the electrical wires or the MIDAS datalogger may cause inaccurate results or a loss of transmission from the extensometer to the datalogger.

---

## Installation and Data Collection

---

The mine where the installation of convergence stations occurred is in northern West Virginia. It is mine a high-grade bituminous coal in the Lower Kittanning seam. The average cutting height in the mine is 96" and the average depth of cover is 600 feet. The roof in the mine is considered very good in most areas. To date, the mine has completed two longwall panels and is currently mining a third panel.

Several convergence stations were installed and monitored throughout the course of one year. The location and feedback of each monitoring station has been compiled in this section. The convergence stations can be identified by the number associated with its respective datalogger. The graphs display the length of string extension of each extensometer attached to that specific extensometer. Each extensometer data set will produce two graphs: one on a 0-20 inch scale, and another concentrated on the range of the data representing any deformation that may have occurred. Any outliers due to transportation or faulty signal transmission will be available on the first chart and explained if necessary. In theory, as the extension of the extensometer decreases, the amount of convergence in the entry is increasing as the artificial support deforms.

The first convergence station installed incorporated the #053 MIDAS datalogger. This convergence station began recording information on November 19<sup>th</sup>, 2013 and was mounted in roof supports that were located in the bleeders at the beginning of the first longwall panel. A map of location of the convergence station can be found in Figure 3.4. The extensometers connected into channels 1 and 3 were installed in cement-filled supports. The extensometers connected into channels 5 and 7 were attached to Link-N-Lock timber supports. A data point

was collected at this site once every six hours. The most recent date of data collection was May 16<sup>th</sup>, 2014. Charts regarding the extension of the #053 extensometers can be found in Figures D.5 through D.12.

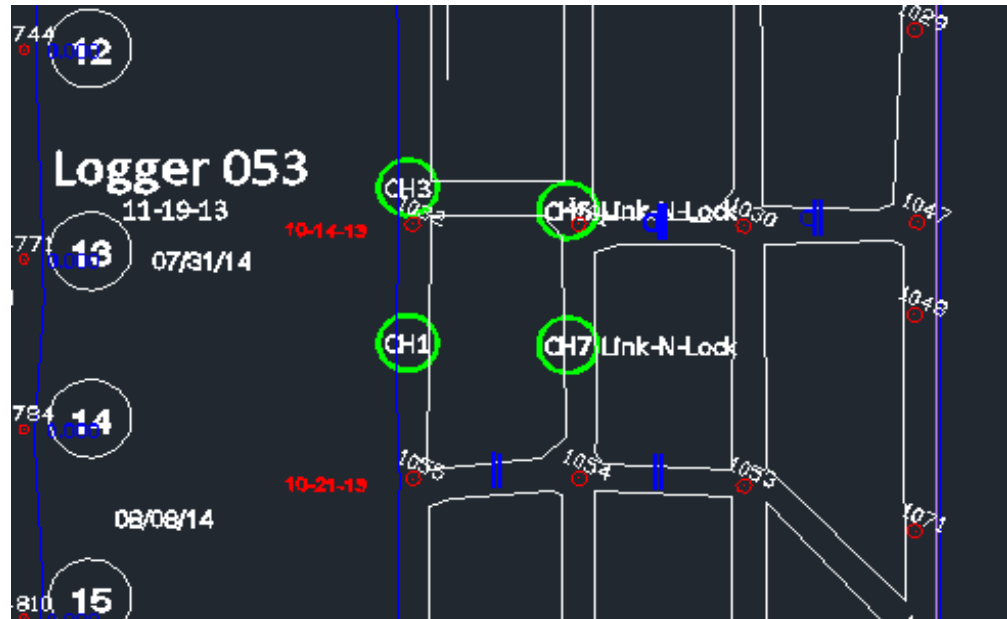


**Figure D.4 – Map of convergence station #053's extensometer locations**

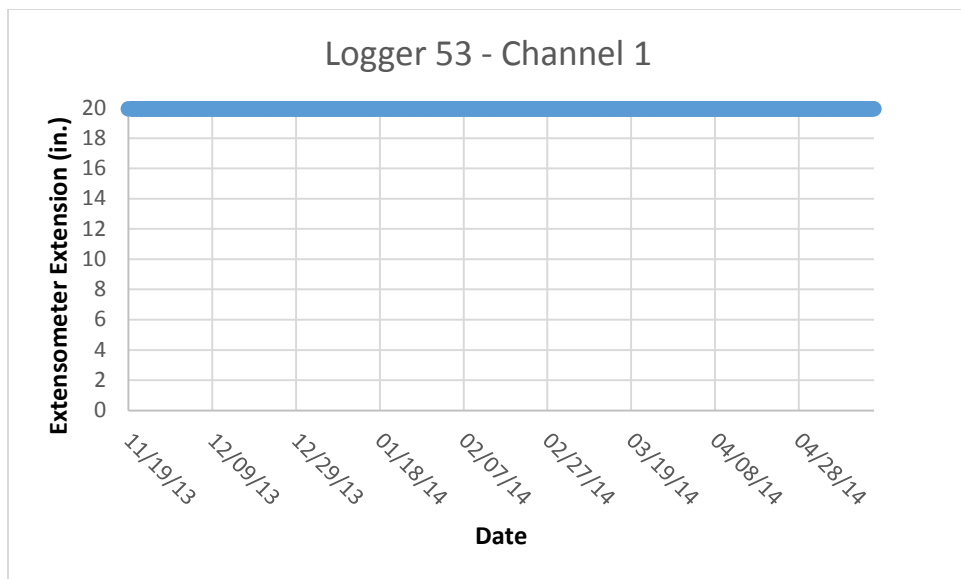


**Figure D.5 – Chart of convergence station #053 channel 1 extension monitoring, 20-inch scale**

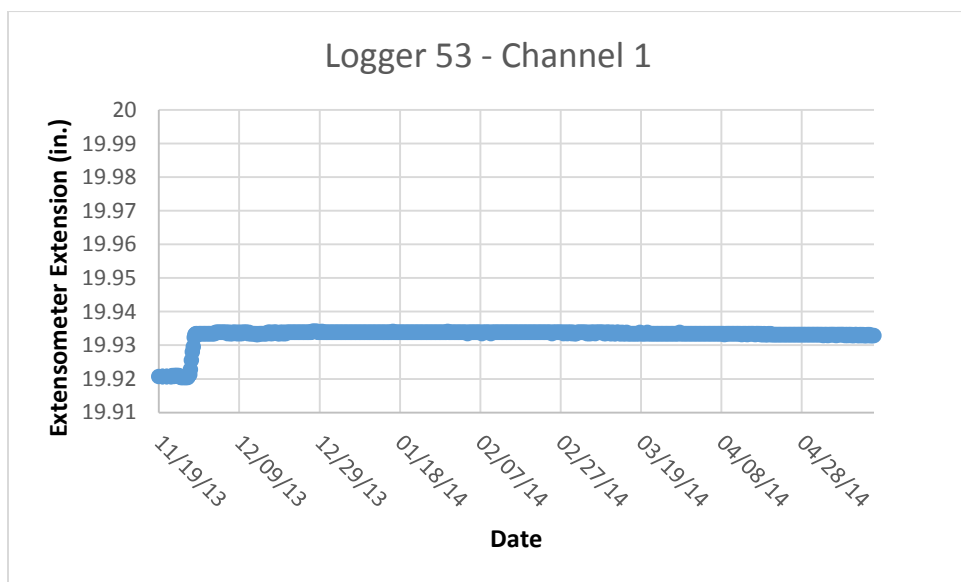


**Figure D.6 – Chart of convergence station #053 channel 1 extension monitoring, concentrated scale**

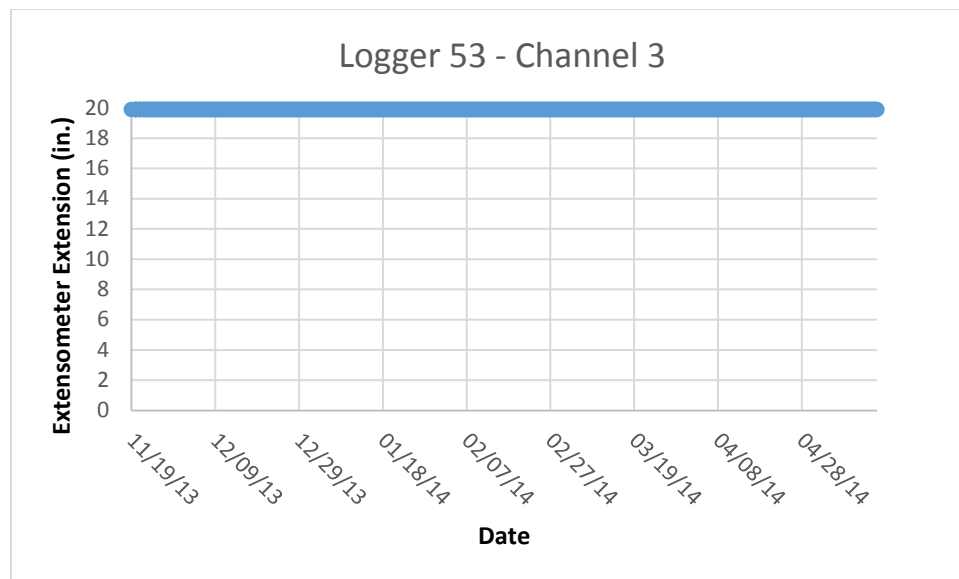


**Figure D.7 – Chart of convergence station #053 channel 3 extension monitoring, 20-inch scale**

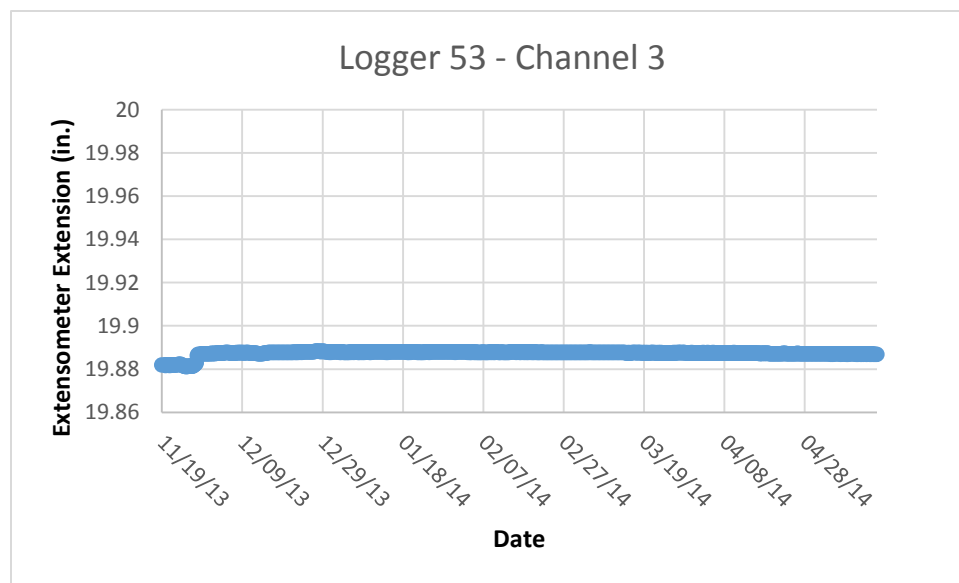


**Figure D.8 – Chart of convergence station #053 channel 3 extension monitoring, concentrated scale**

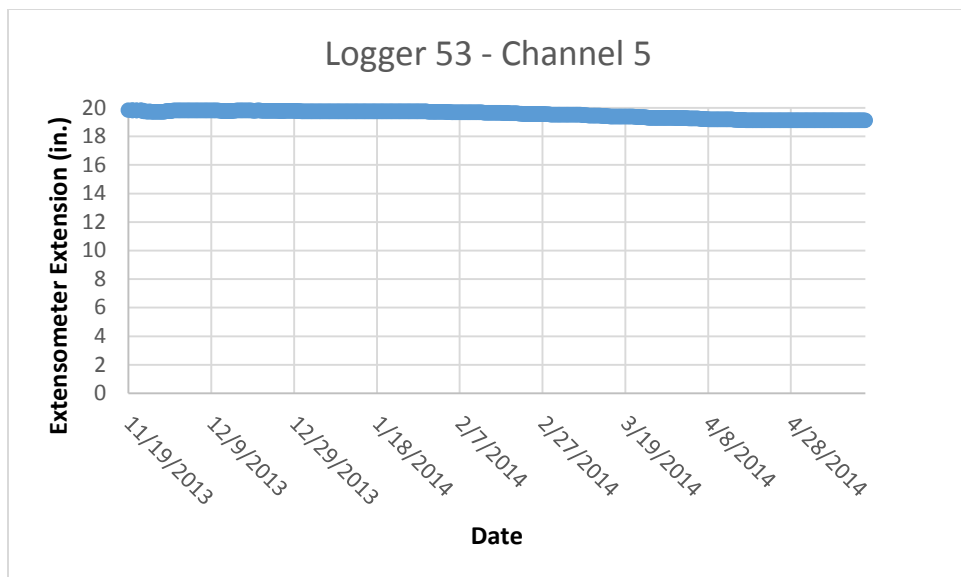


Figure D.9 – Chart of convergence station #053 channel 5 extension monitoring, 20-inch scale

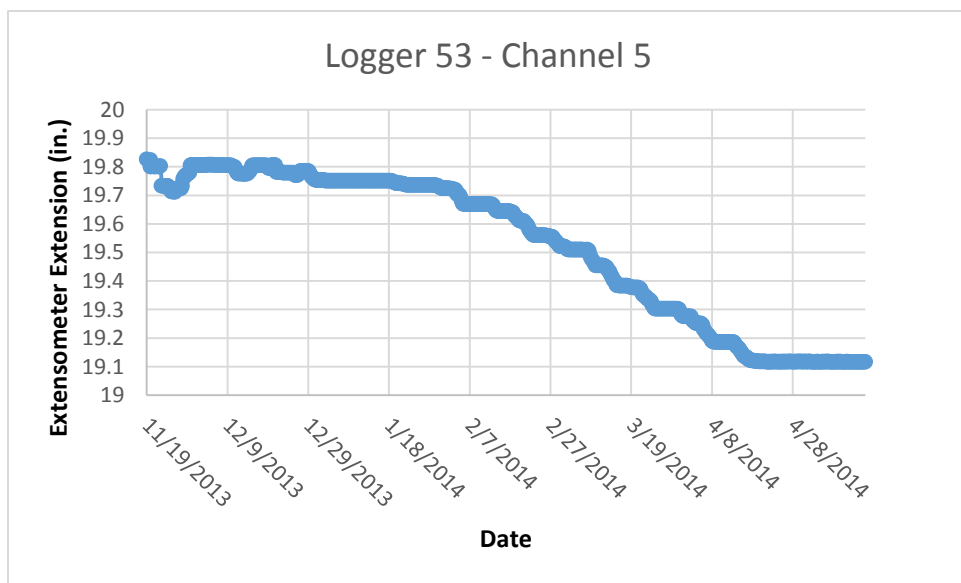
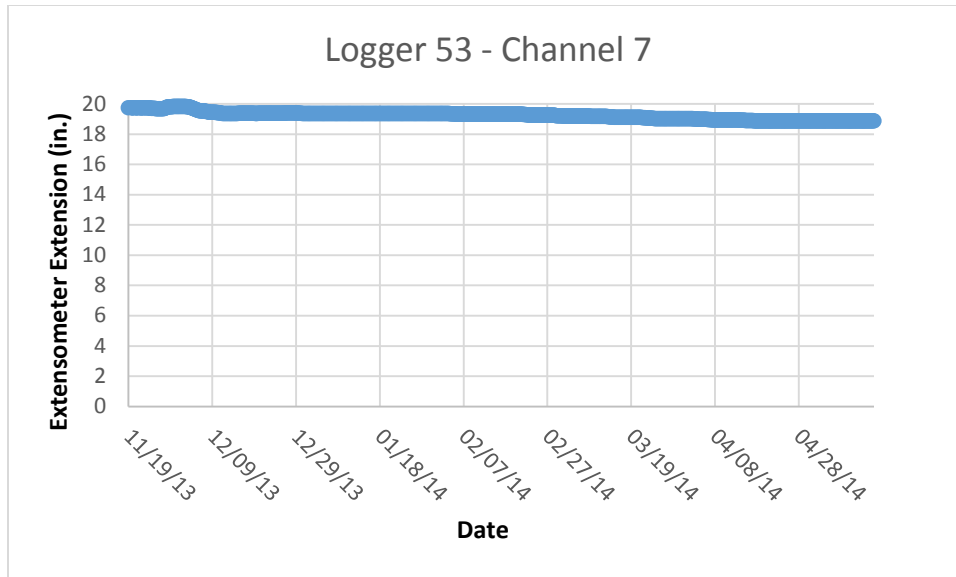
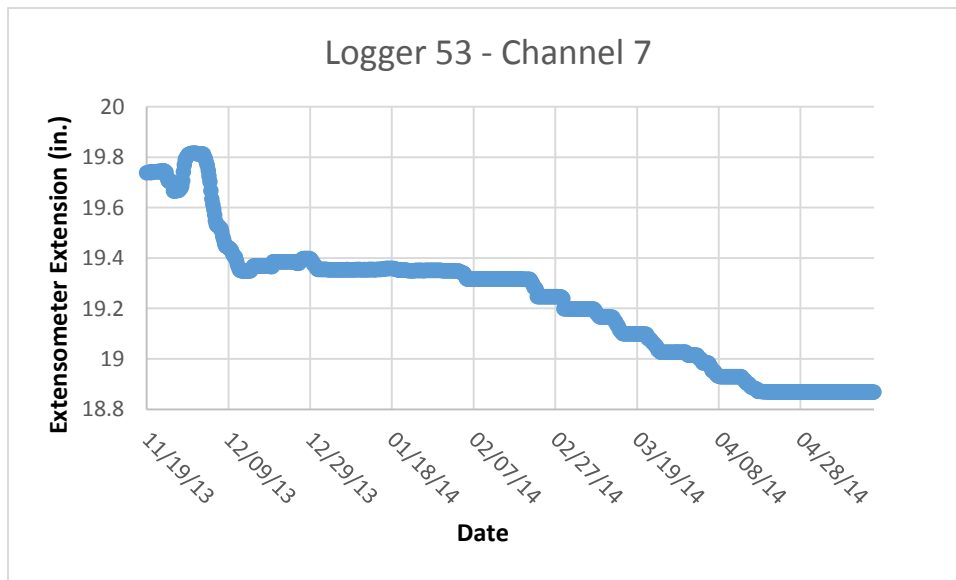


Figure D.10 – Chart of convergence station #053 channel 5 extension monitoring, concentrated scale



**Figure D.11 – Chart of convergence station #053 channel 7 extension monitoring, 20-inch scale**



**Figure D.12 – Chart of convergence station #053 channel 7 extension monitoring, concentrated scale**

The second convergence station installed incorporated the #040 MIDAS datalogger. This convergence station began recording information on December 30th, 2013 and was mounted in roof supports that were located in the headgate of the first longwall panel in the gate entry between crosscuts 39 and 38. A map of location of the convergence station can be found in Figure D.13. All the extensometers were connected into cement-filled supports. A data point was collected at this site once every two hours. The most recent date of data collection was

April 11<sup>th</sup>, 2014. Charts regarding the extension of the #040 extensometers can be found in Figures D.14 through D.21. The ring attached to the string of the extensometer that was connected to channel 7 detached during monitoring on December 31<sup>st</sup>, rendering that extensometer useless there afterwards.

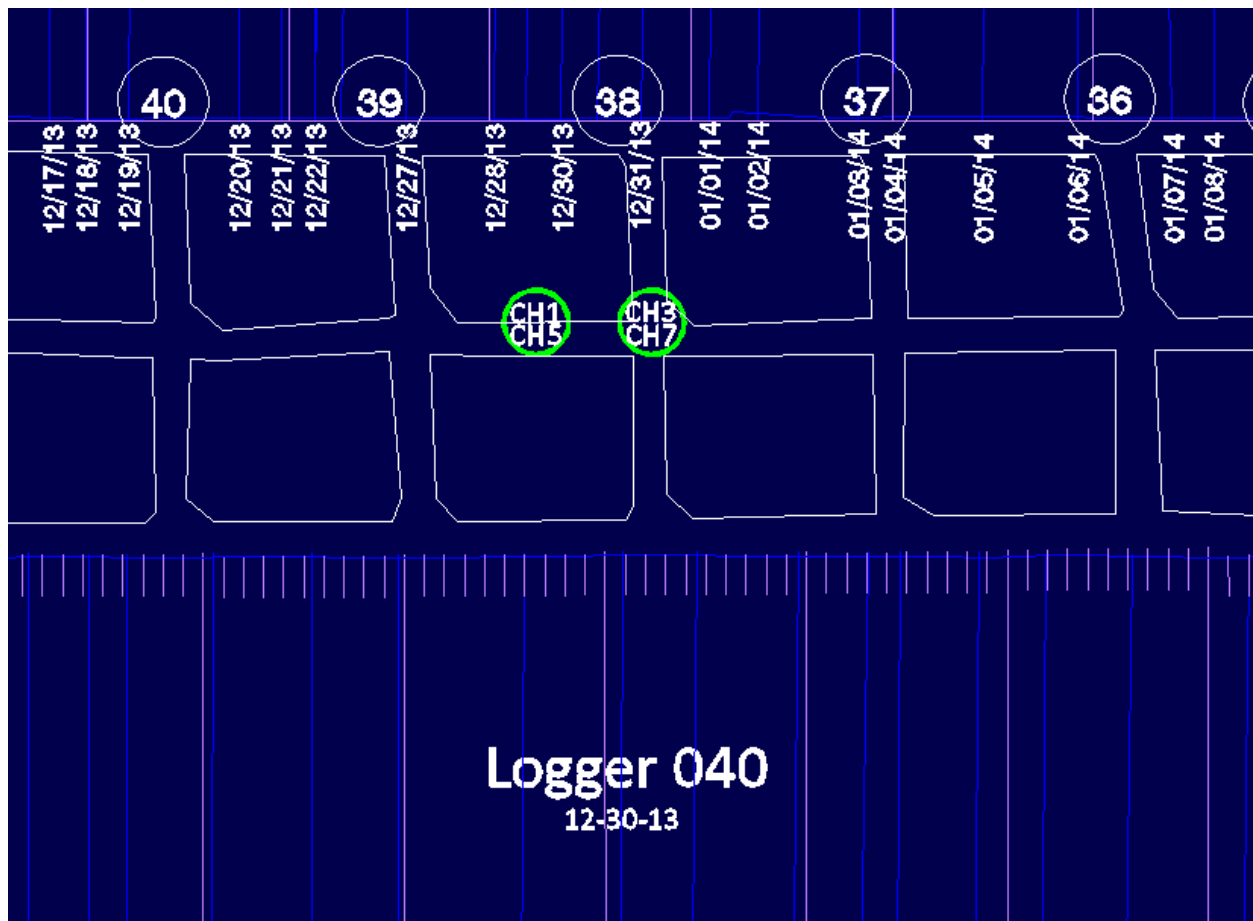


Figure D.13 – Map of convergence station #040's extensometer locations

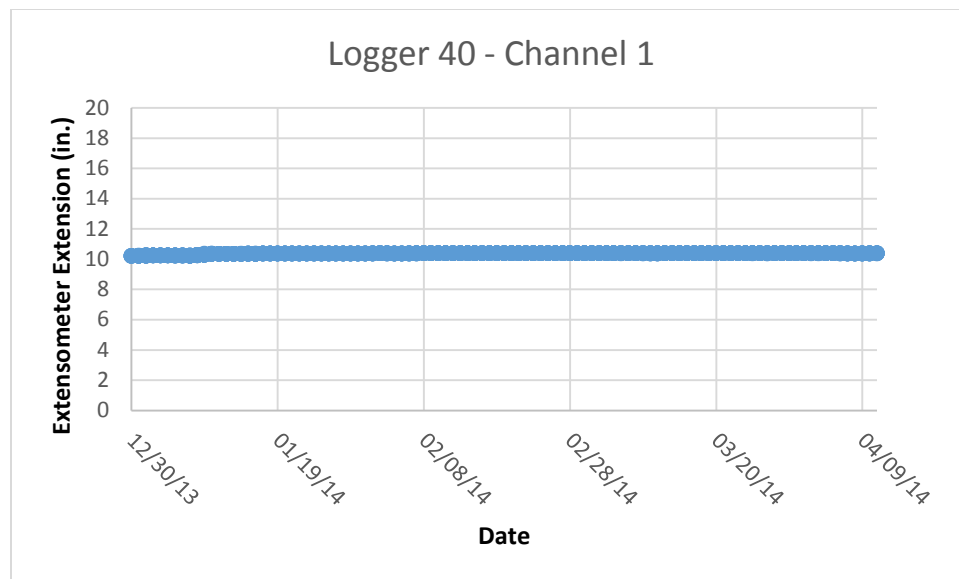


Figure D.14 – Chart of convergence station #040 channel 1 extension monitoring, 20-inch scale

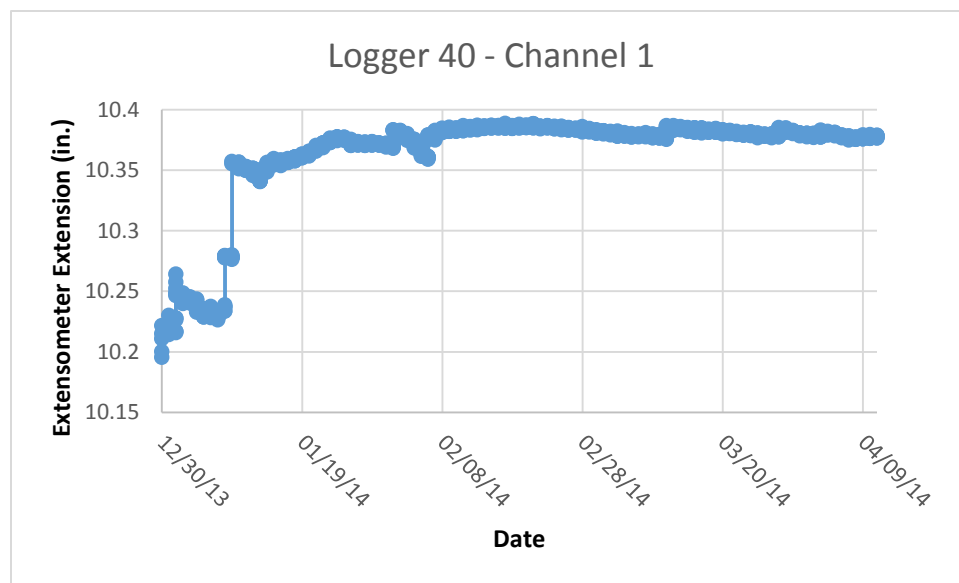


Figure D.15 – Chart of convergence station #040 channel 1 extension monitoring, concentrated scale

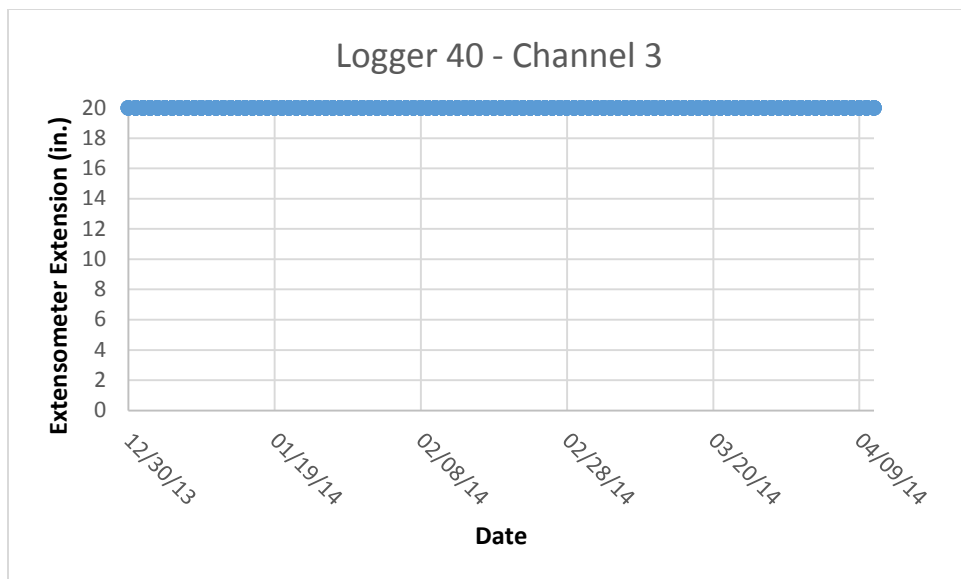


Figure D.16 – Chart of convergence station #040 channel 3 extension monitoring, 20-inch scale

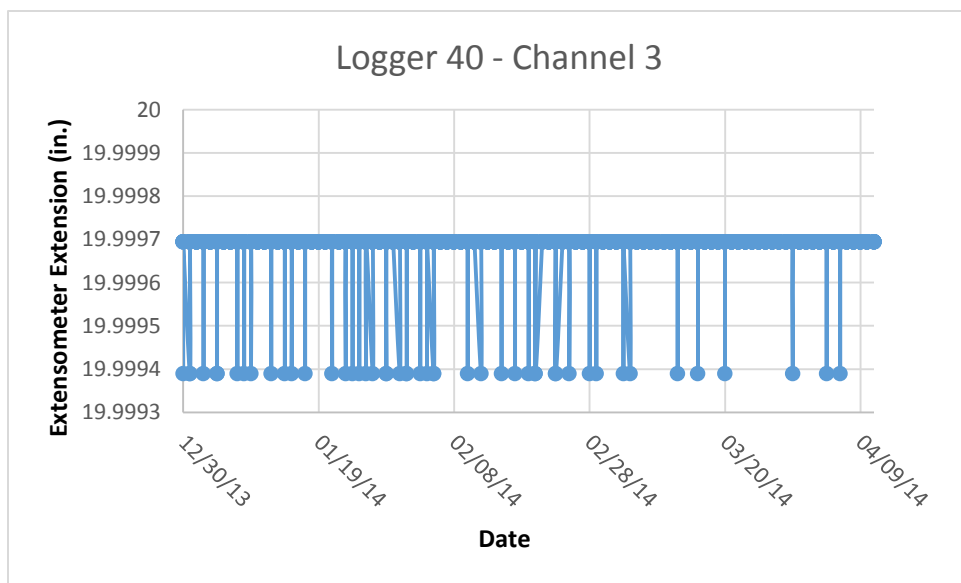
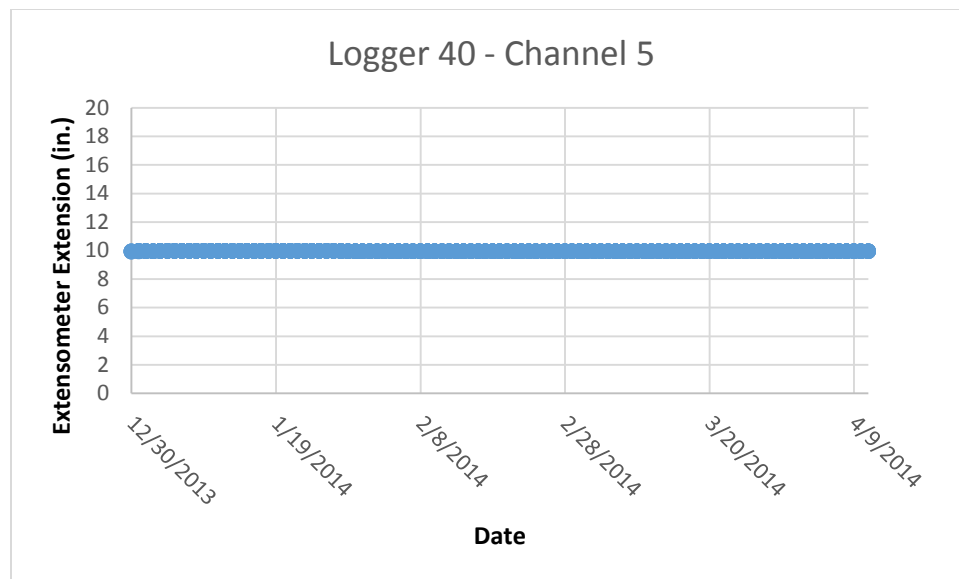
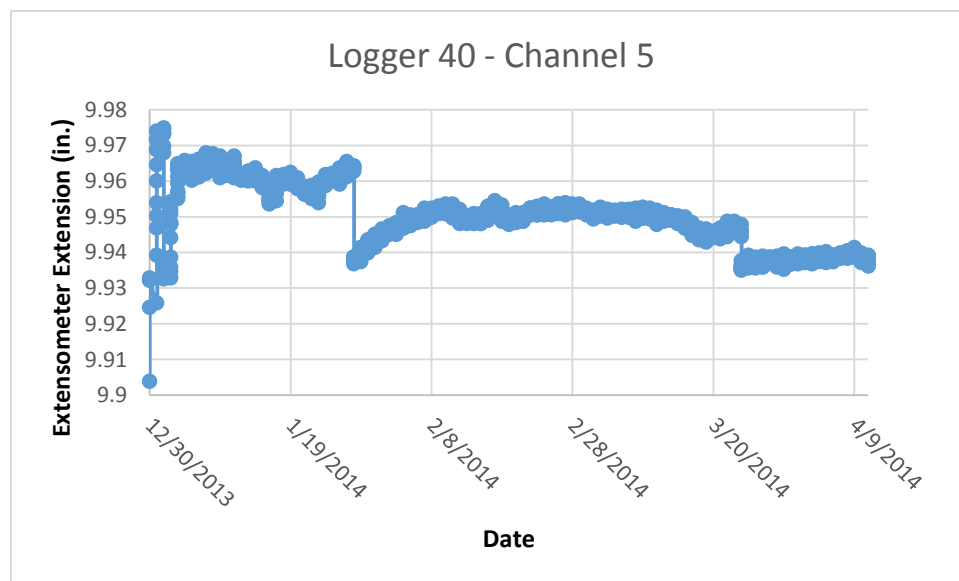


Figure D.17 – Chart of convergence station #040 channel 3 extension monitoring, concentrated scale



**Figure D.18 – Chart of convergence station #040 channel 5 extension monitoring, 20-inch scale**



**Figure D.19 – Chart of convergence station #040 channel 5 extension monitoring, concentrated scale**

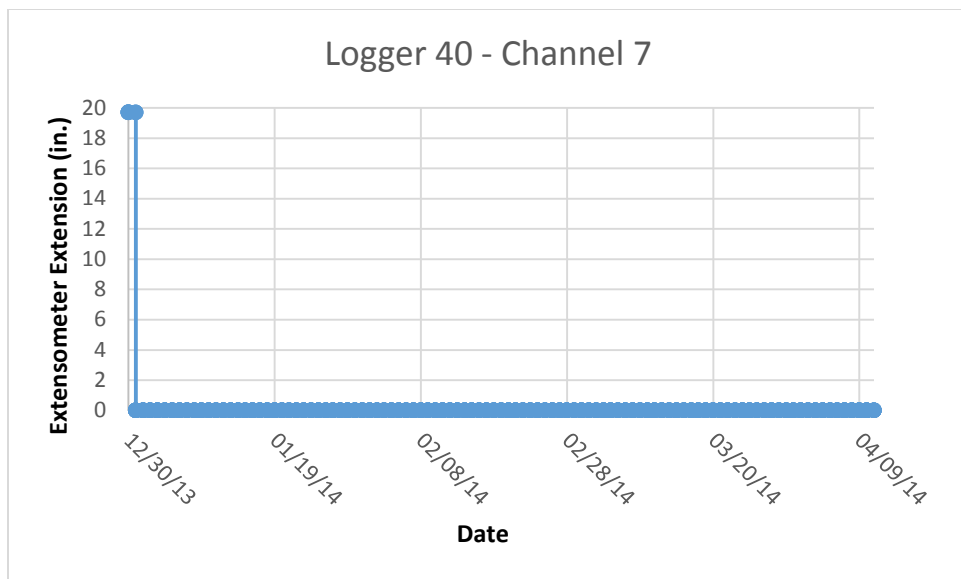


**Figure D.20 – Chart of convergence station #040 channel 7 extension monitoring, 20-inch scale**

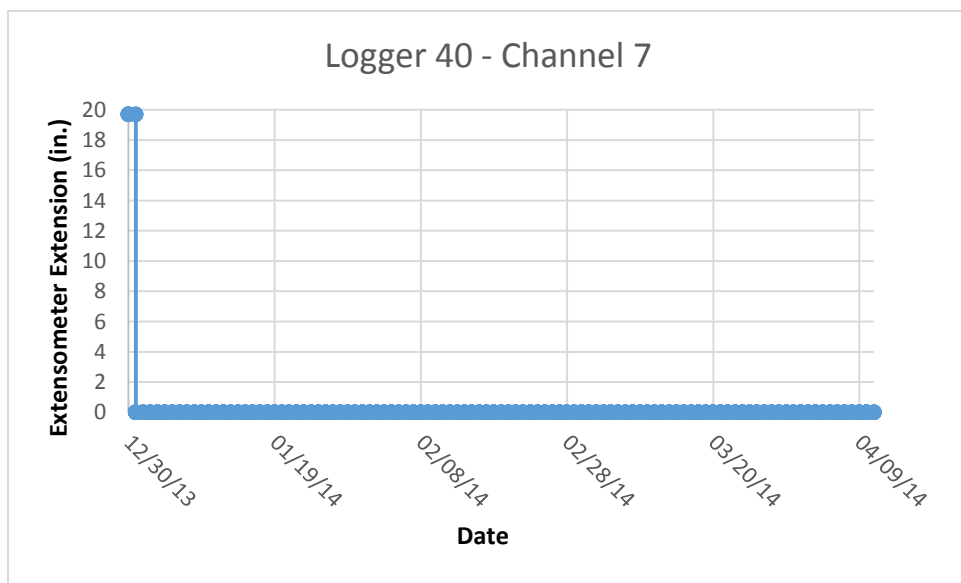


**Figure D.21 – Chart of convergence station #040 channel 7 extension monitoring, concentrated scale**

The next convergence station installed incorporated the #077 MIDAS datalogger. This convergence station began recording information on March 11th, 2014 and was mounted in roof supports that were located in the headgate of the first longwall panel in the gate entry between crosscuts 22 and 21. A map of location of the convergence station can be found in Figure D.22. All the extensometers were connected into cement-filled supports. A data point was collected at this site once every 12 hours. The most recent date of data collection was November 20<sup>th</sup>, 2014.

Charts regarding the extension of the #077 extensometers can be found in Figures D.23 through D.30. On October 10<sup>th</sup>, this convergence station was taken down and moved to another location for a different experiment. Data collected after October 10<sup>th</sup> will not be included in this study.

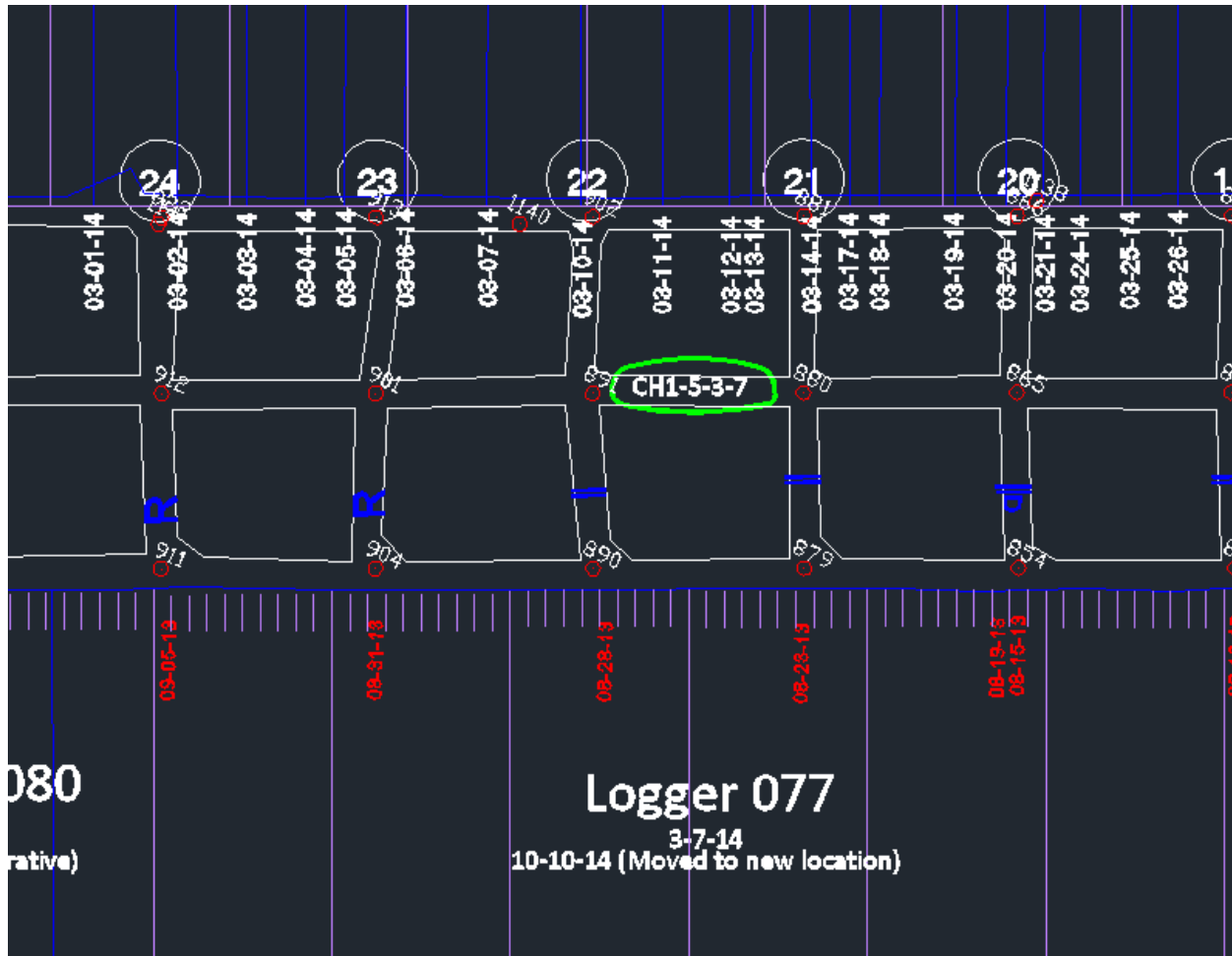


**Figure D.22 – Map of convergence station #077’s extensometer locations**

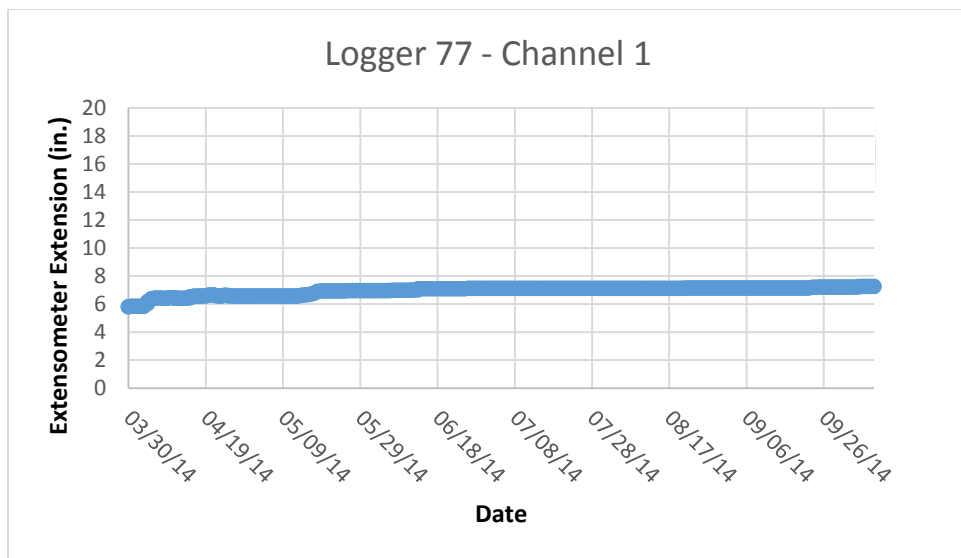


Figure D.23 – Chart of convergence station #077 channel 1 extension monitoring, 20-inch scale

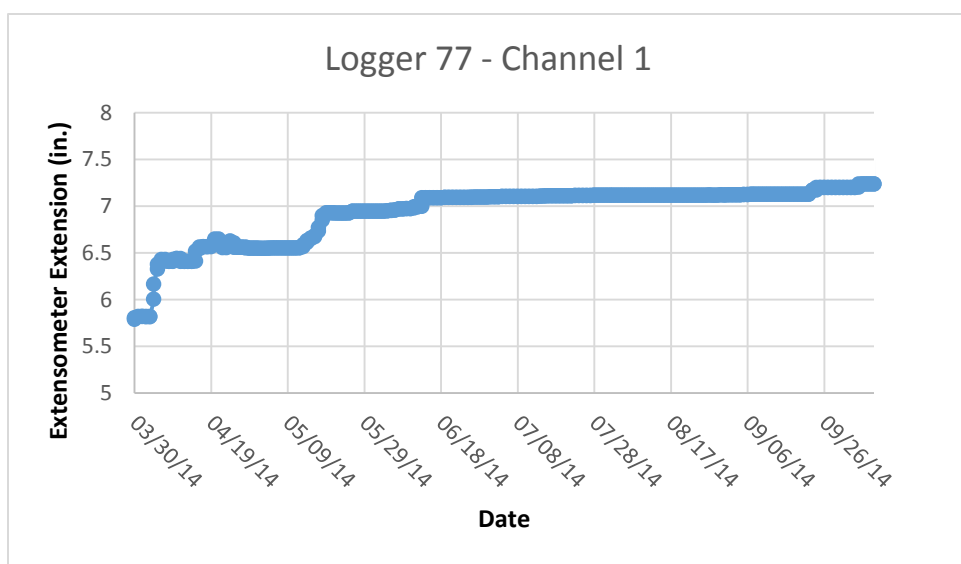


Figure D.24 – Chart of convergence station #077 channel 1 extension monitoring, concentrated scale

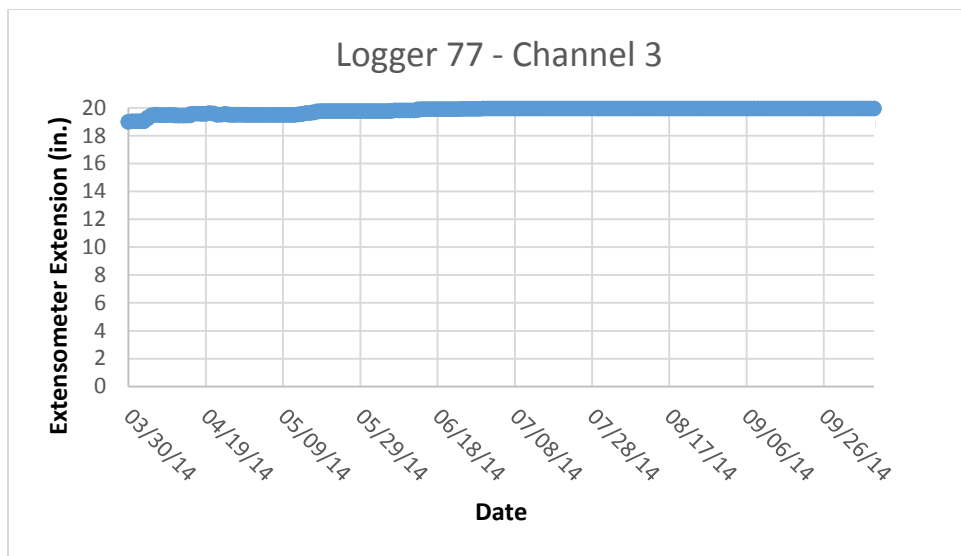


Figure D.25 – Chart of convergence station #077 channel 3 extension monitoring, 20-inch scale

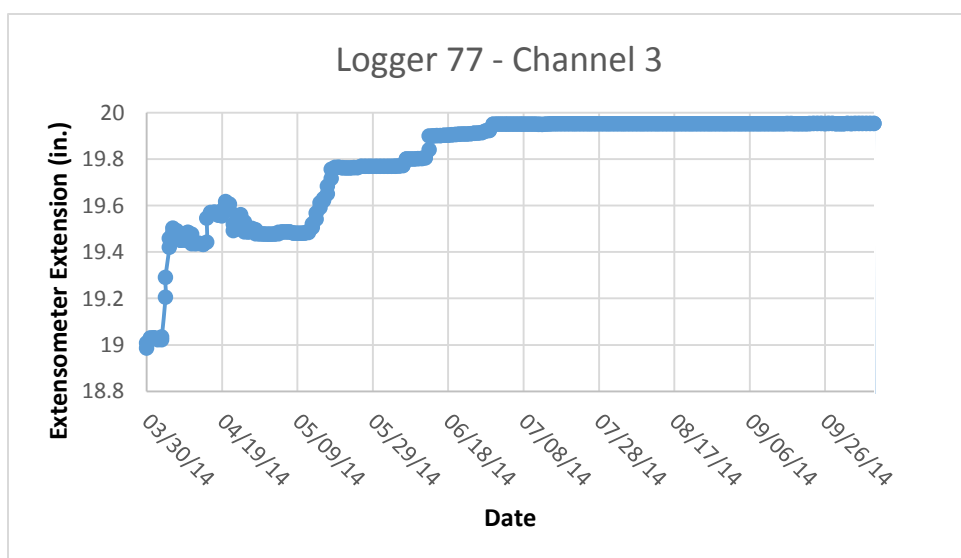


Figure D.26 – Chart of convergence station #077 channel 3 extension monitoring, concentrated scale

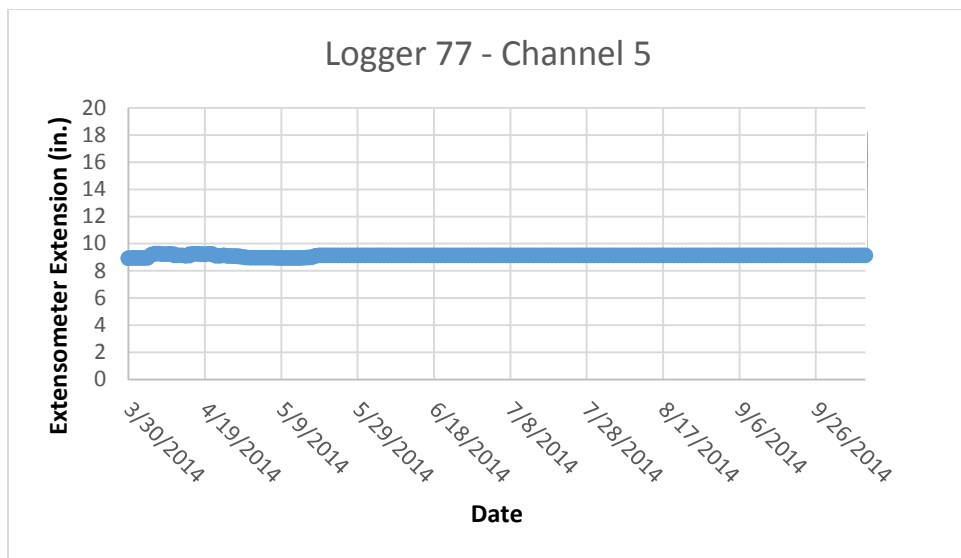


Figure D.27 – Chart of convergence station #077 channel 5 extension monitoring, 20-inch scale

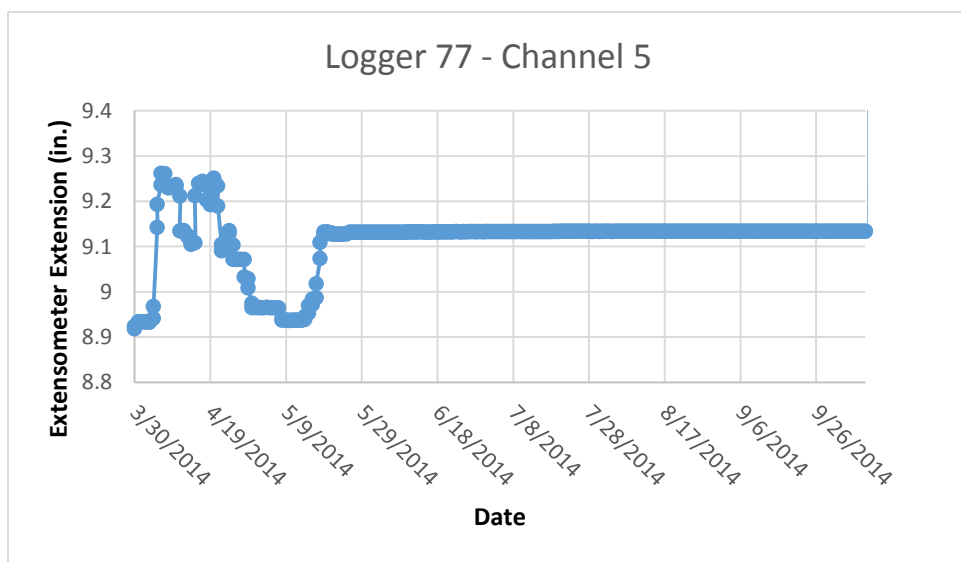
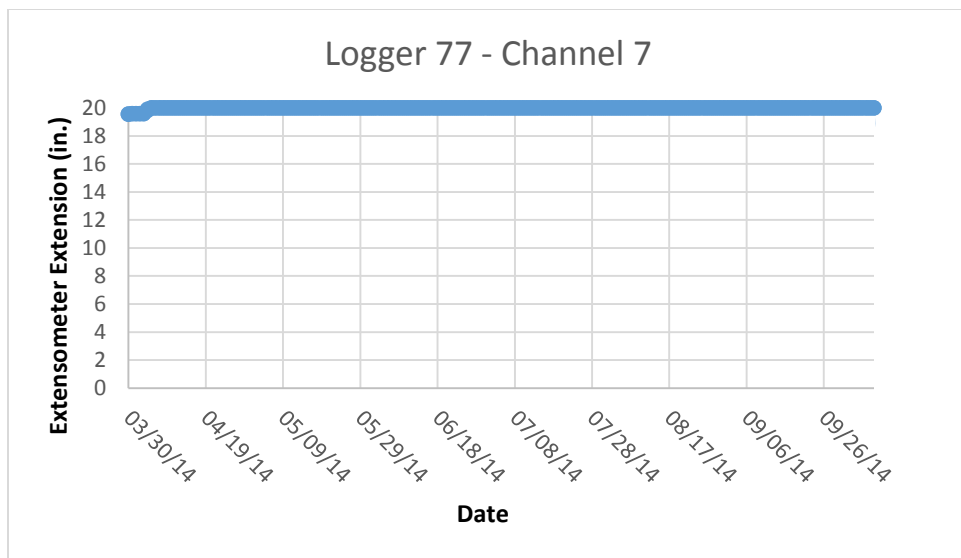
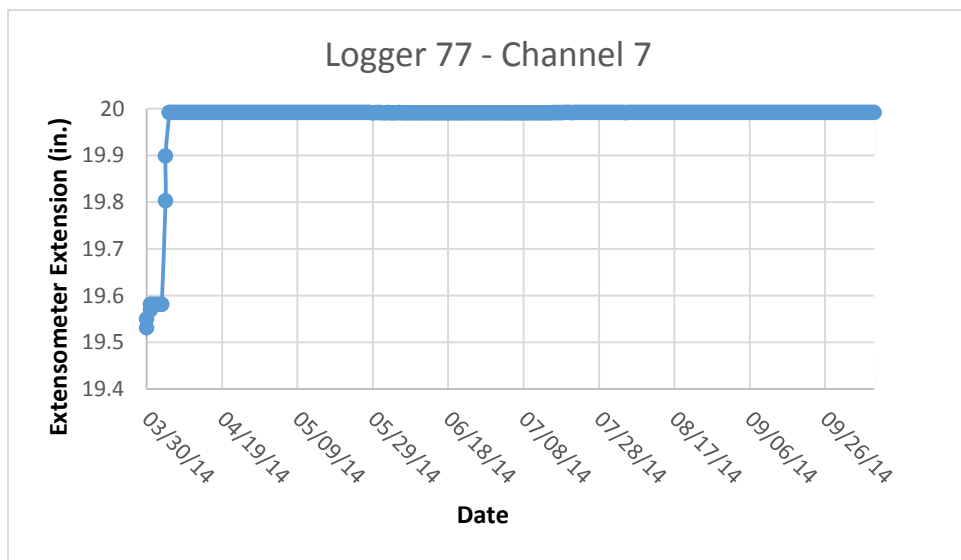


Figure D.28 – Chart of convergence station #077 channel 5 extension monitoring, concentrated scale



**Figure D.29 – Chart of convergence station #077 channel 7 extension monitoring, 20-inch scale**



**Figure D.30 – Chart of convergence station #077 channel 7 extension monitoring, concentrated scale**

Convergence station #078 was installed and began collecting data on April 11<sup>th</sup>, 2014. This convergence station was mounted in roof supports that were located in the headgate of the first longwall panel in and around crosscut 17. A map of location of the convergence station can be found in Figure D.31. All the extensometers were connected into cement-filled supports. A data point was collected at this site once every 12 hours. The most recent date of data collection was October 30th, 2014. Charts regarding the extension of the #078 extensometers can be found in Figures D.32 through D.40. The significant portion of channel 7 is shown over two graphs.

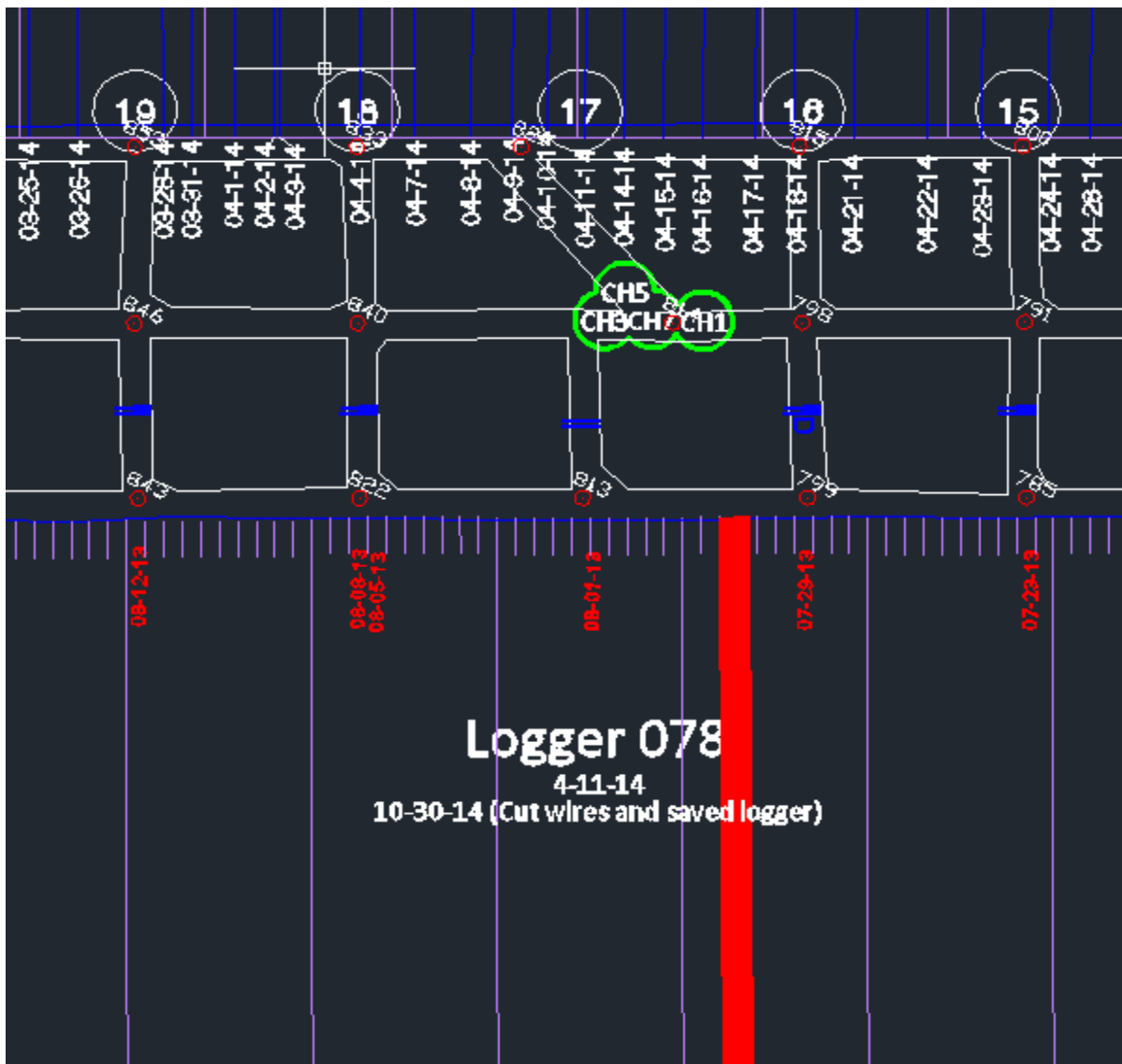


Figure D.31 – Map of convergence station #078's extensometer locations

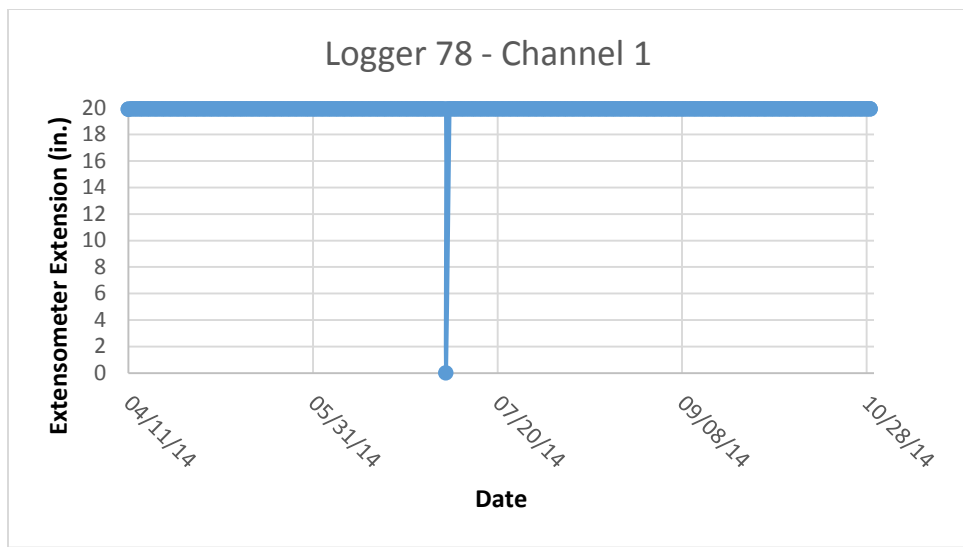


Figure D.32 – Chart of convergence station #078 channel 1 extension monitoring, 20-inch scale

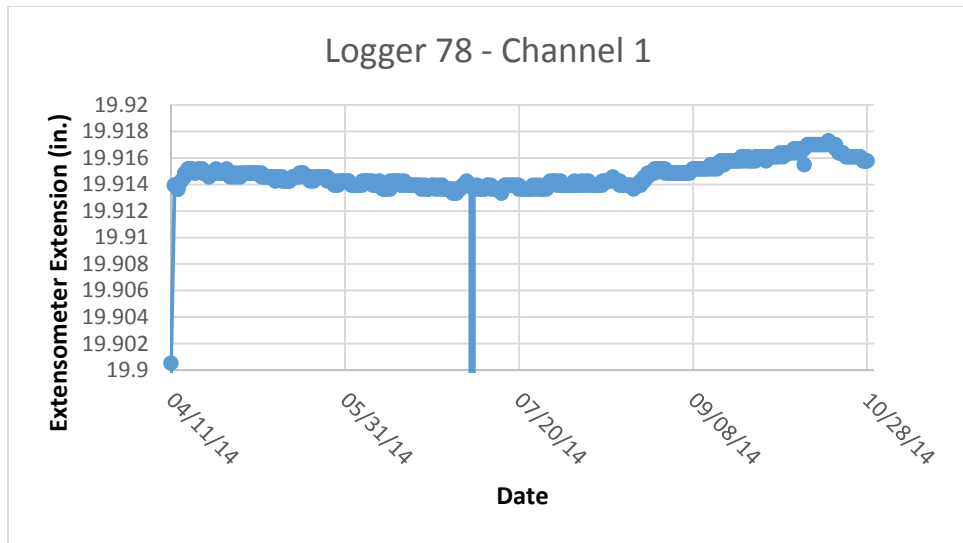


Figure D.33 – Chart of convergence station #078 channel 1 extension monitoring, concentrated scale

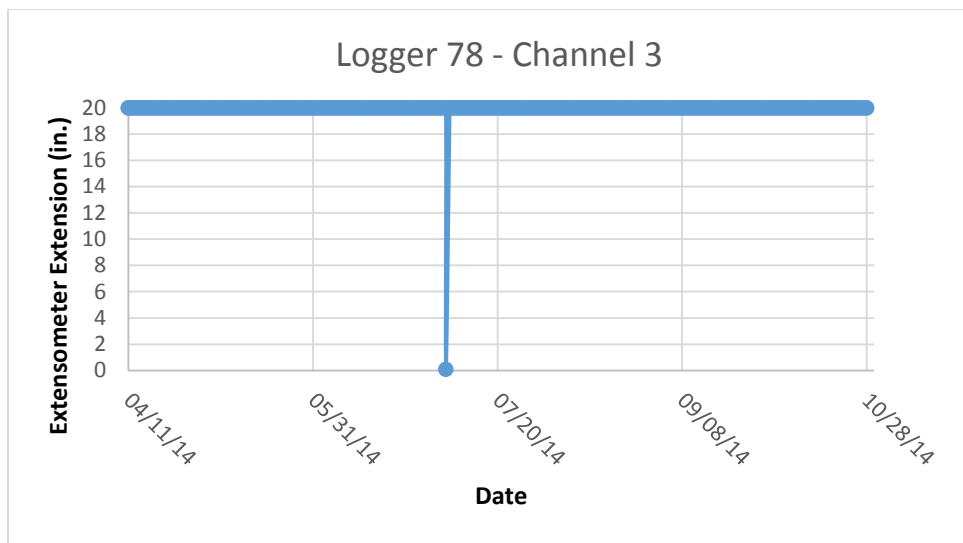


Figure D.34 – Chart of convergence station #078 channel 3 extension monitoring, 20-inch scale

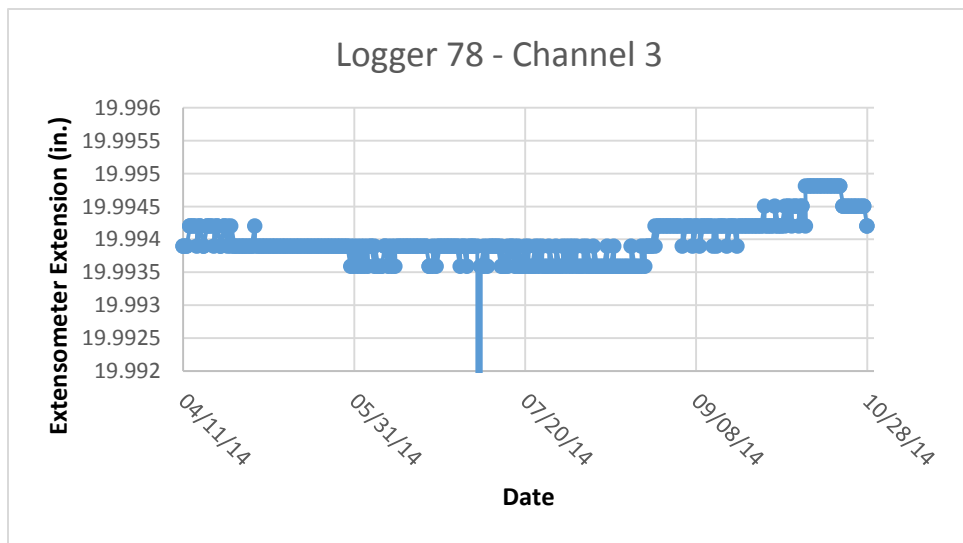


Figure D.35 – Chart of convergence station #078 channel 3 extension monitoring, concentrated scale

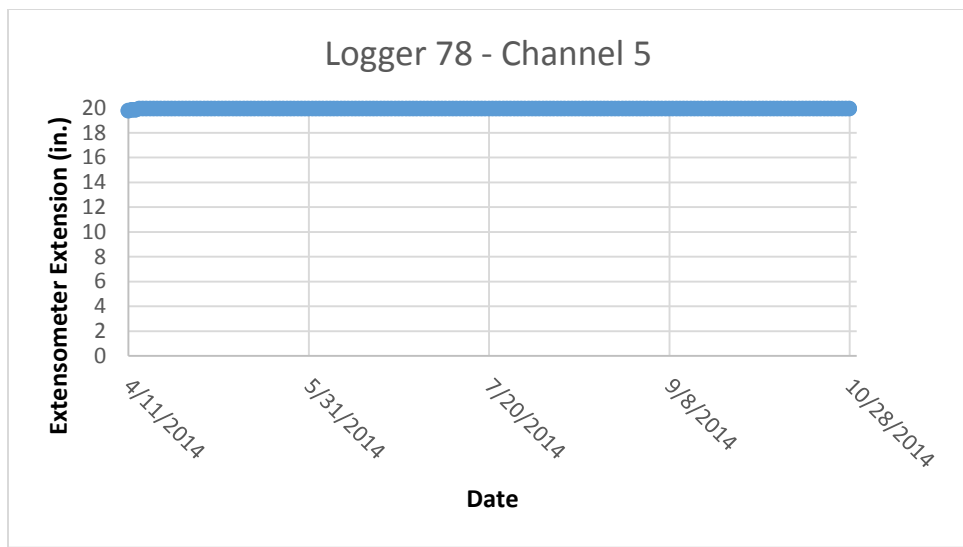


Figure D.36 – Chart of convergence station #078 channel 5 extension monitoring, 20-inch scale

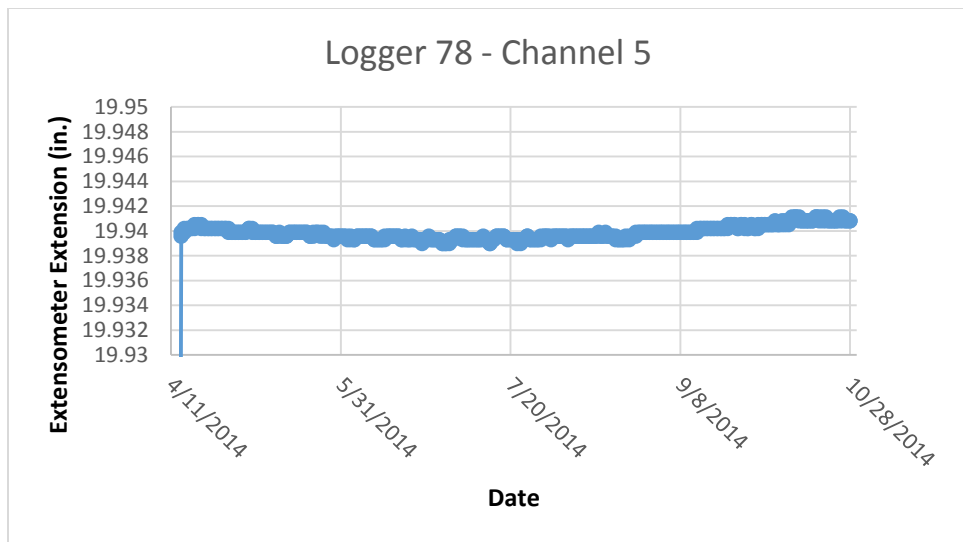


Figure D.37 – Chart of convergence station #078 channel 5 extension monitoring, concentrated scale

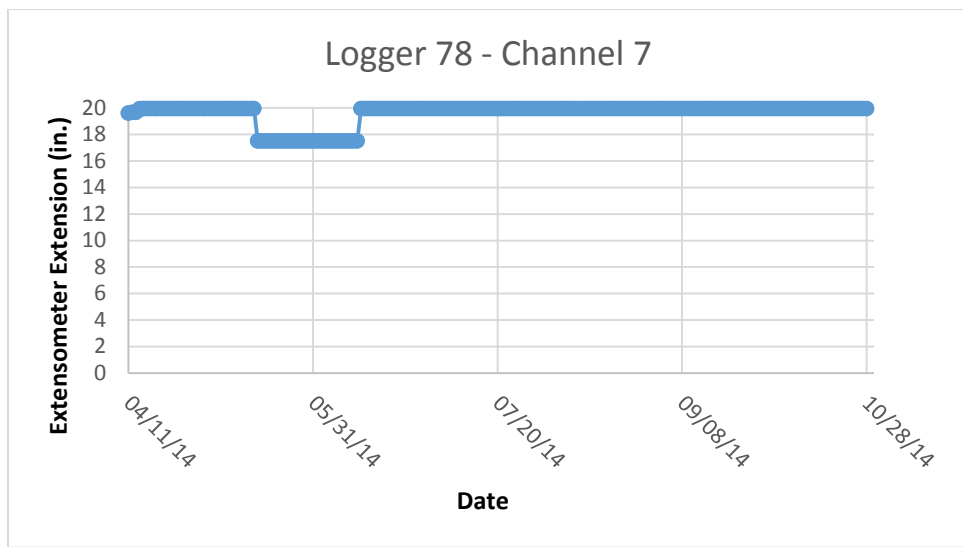


Figure D.38 – Chart of convergence station #078 channel 7 extension monitoring, 20-inch scale

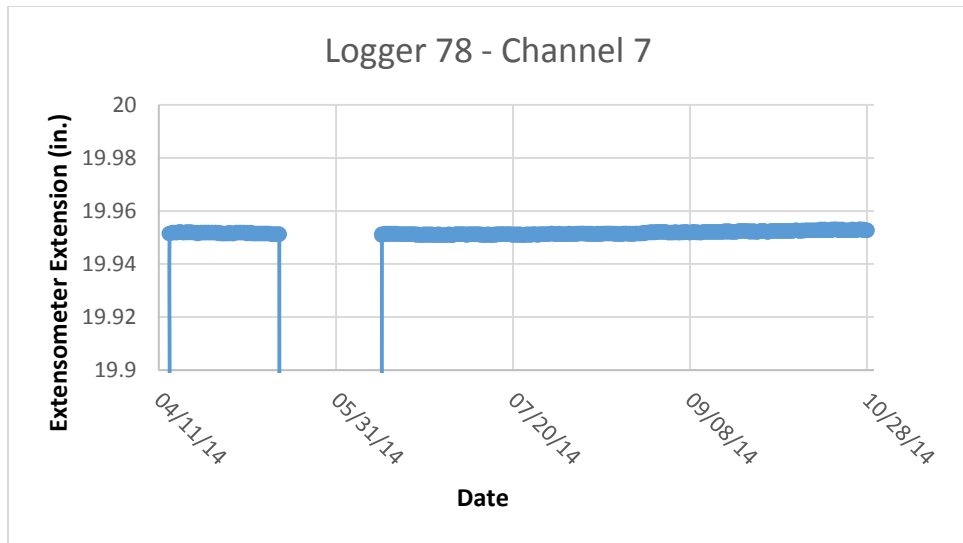
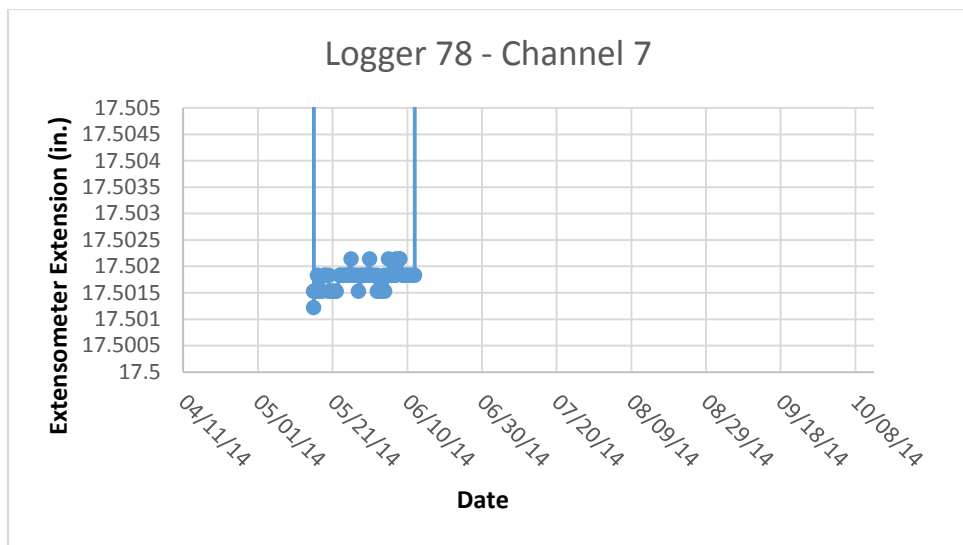


Figure D.39 – Chart of convergence station #078 channel 7 extension monitoring, concentrated scale (high)



**Figure D.40 – Chart of convergence station #078 channel 7 extension monitoring, concentrated scale (low)**

Convergence station #080 was installed and began collecting data on April 11<sup>th</sup>, 2014. This convergence station was mounted in roof supports that were located in the headgate of the first longwall panel in and around crosscut 25. A map of location of the convergence station can be found in Figure D.41. All the extensometers were connected into cement-filled supports. A data point was collected at this site once every 12 hours. The most recent date of data collection was June 12th, 2014. Charts regarding the extension of the #080 extensometers can be found in Figures D.42 through D.49.

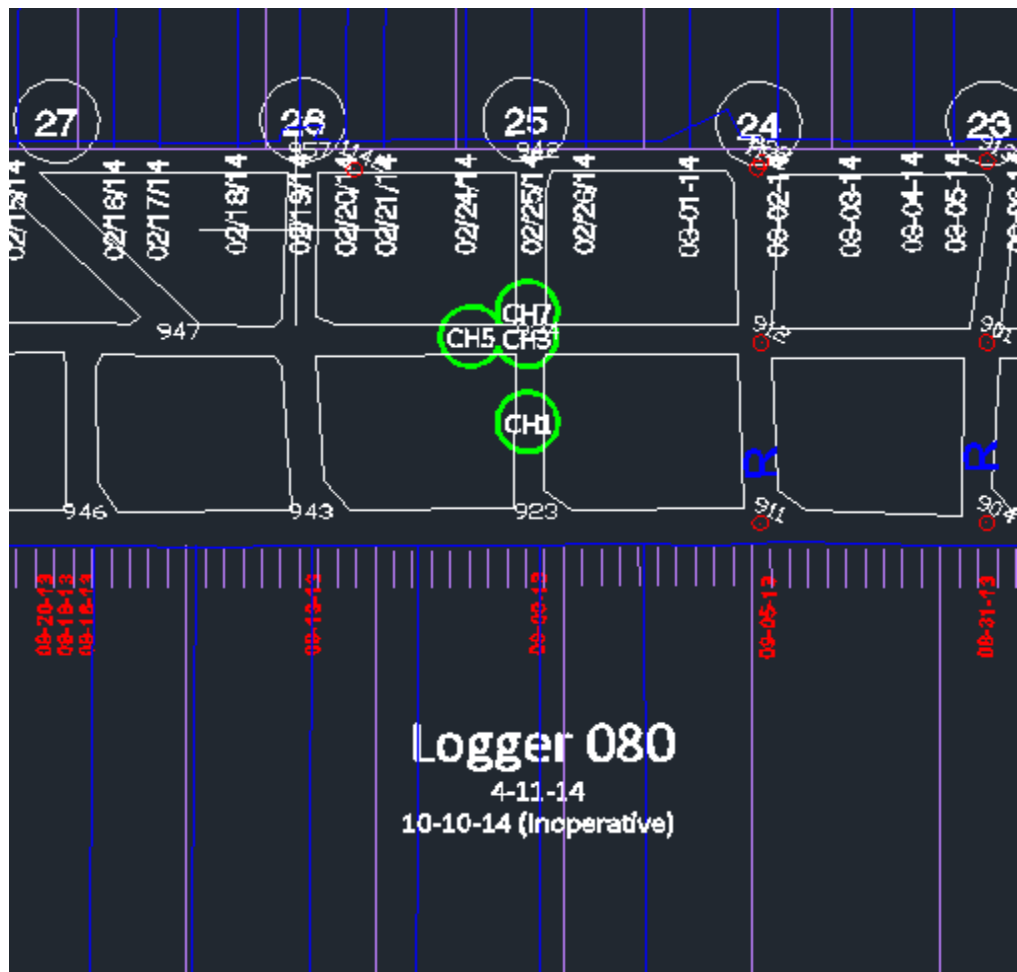
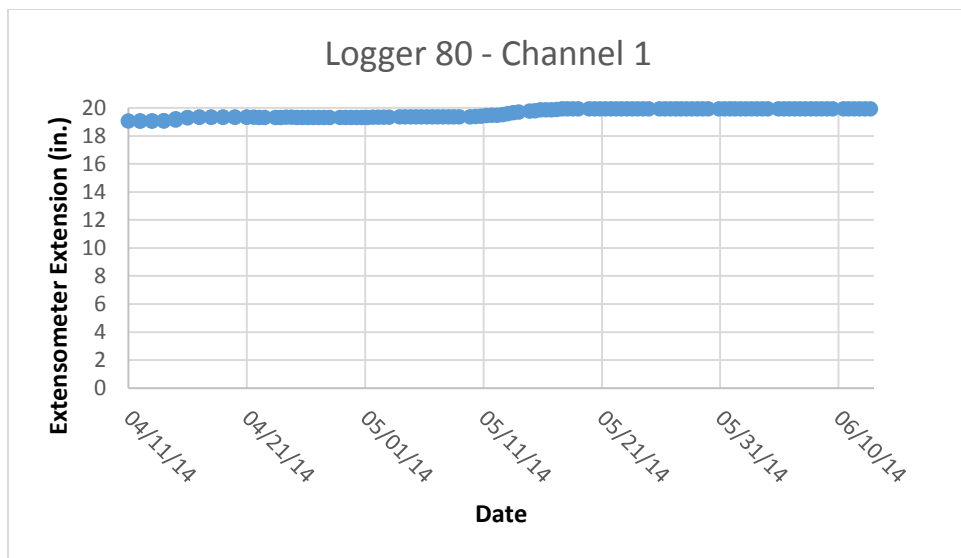
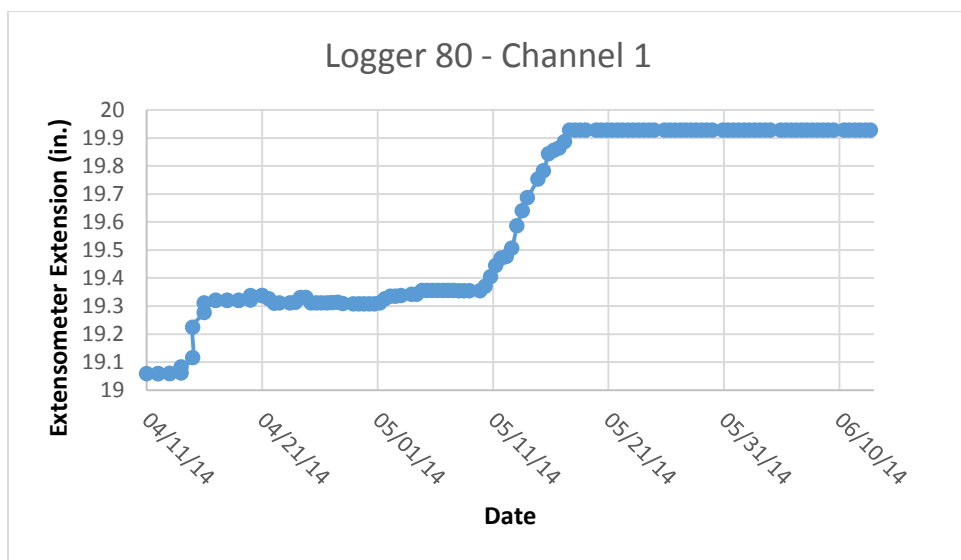


Figure D.41 – Map of convergence station #080's extensometer locations



**Figure D.42 – Chart of convergence station #080 channel 1 extension monitoring, 20-inch scale**



**Figure D.43 – Chart of convergence station #080 channel 1 extension monitoring, concentrated scale**

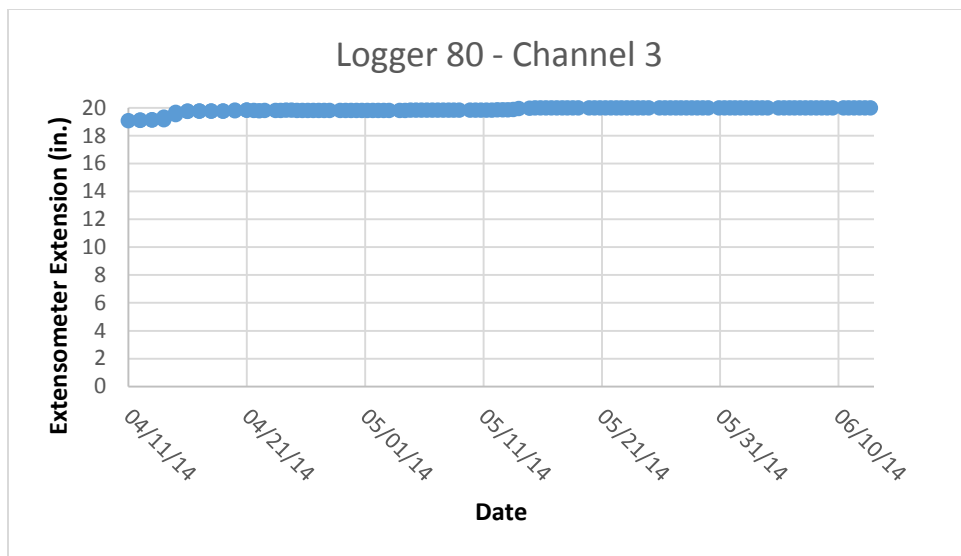


Figure D.44 – Chart of convergence station #080 channel 3 extension monitoring, 20-inch scale

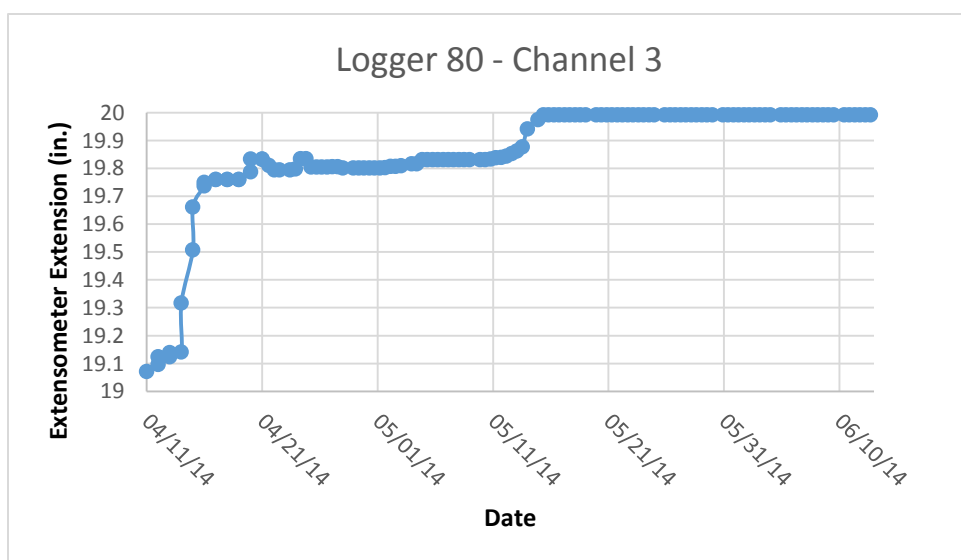


Figure D.45 – Chart of convergence station #080 channel 3 extension monitoring, concentrated scale

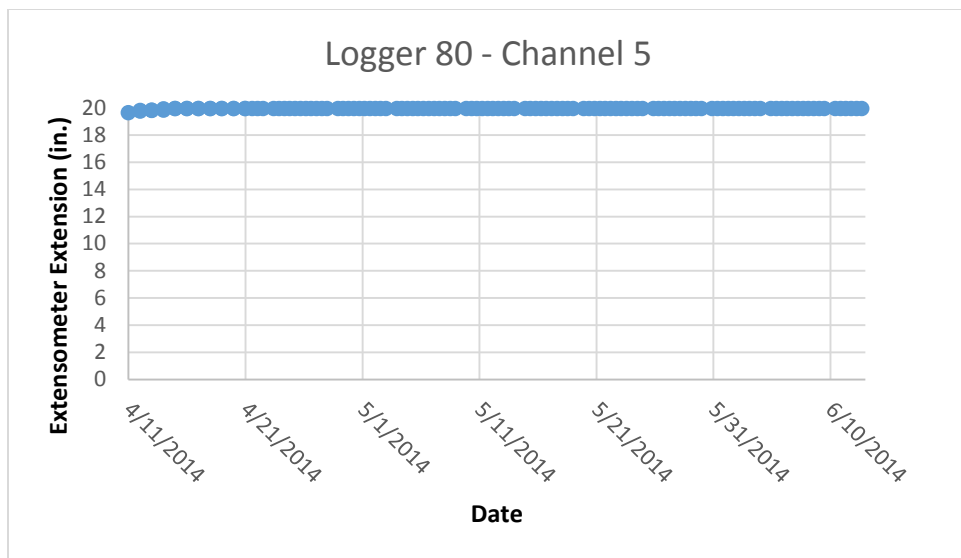


Figure D.46 – Chart of convergence station #080 channel 5 extension monitoring, 20-inch scale

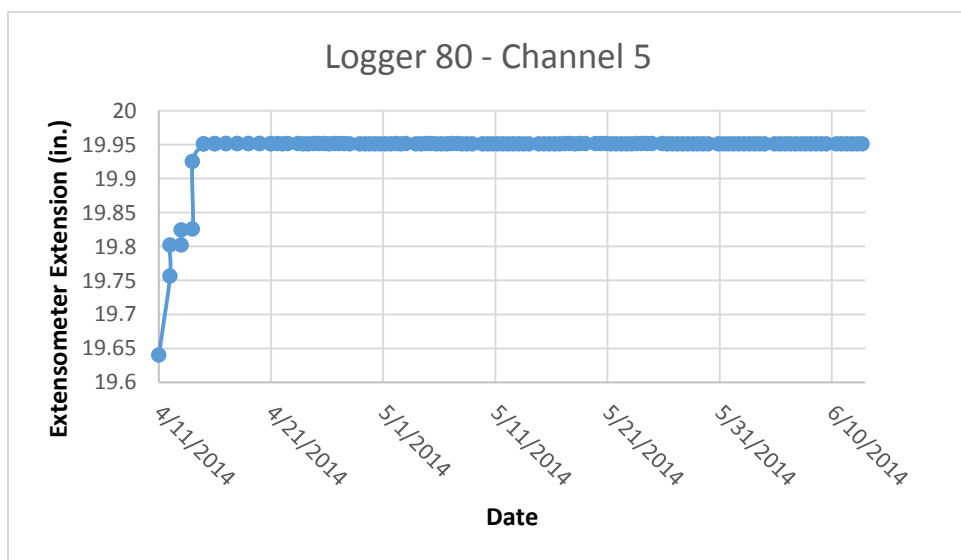
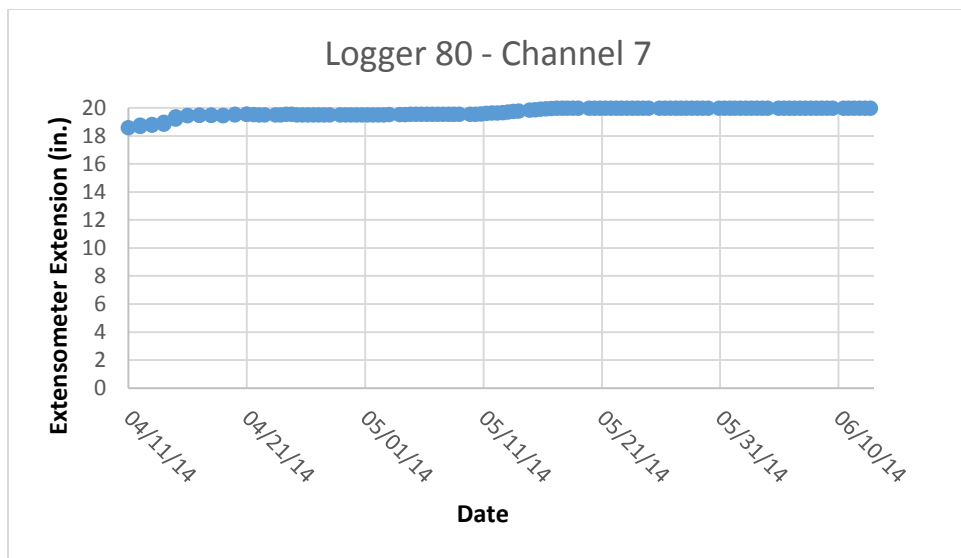
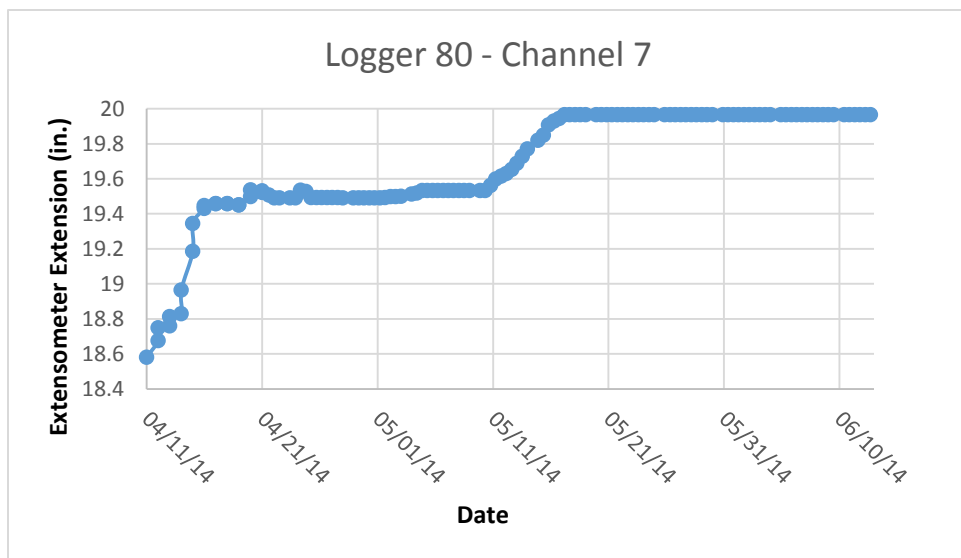


Figure D.47 – Chart of convergence station #080 channel 5 extension monitoring, concentrated scale



**Figure D.48 – Chart of convergence station #080 channel 7 extension monitoring, 20-inch scale**



**Figure D.49 – Chart of convergence station #080 channel 7 extension monitoring, concentrated scale**

Convergence station #074 was installed and began collecting data on June 13th, 2014. This convergence station was mounted in roof supports that were located in the headgate of the first longwall panel in and crosscut 7 and between crosscuts 8 and 7. A map of location of the convergence station can be found in Figure 3.50. All the extensometers were connected into cement-filled supports. A data point was collected at this site once every 12 hours. The most

recent date of data collection was October 30th, 2014. Charts regarding the extension of the #074 extensometers can be found in Figures 3.51 through 3.58.

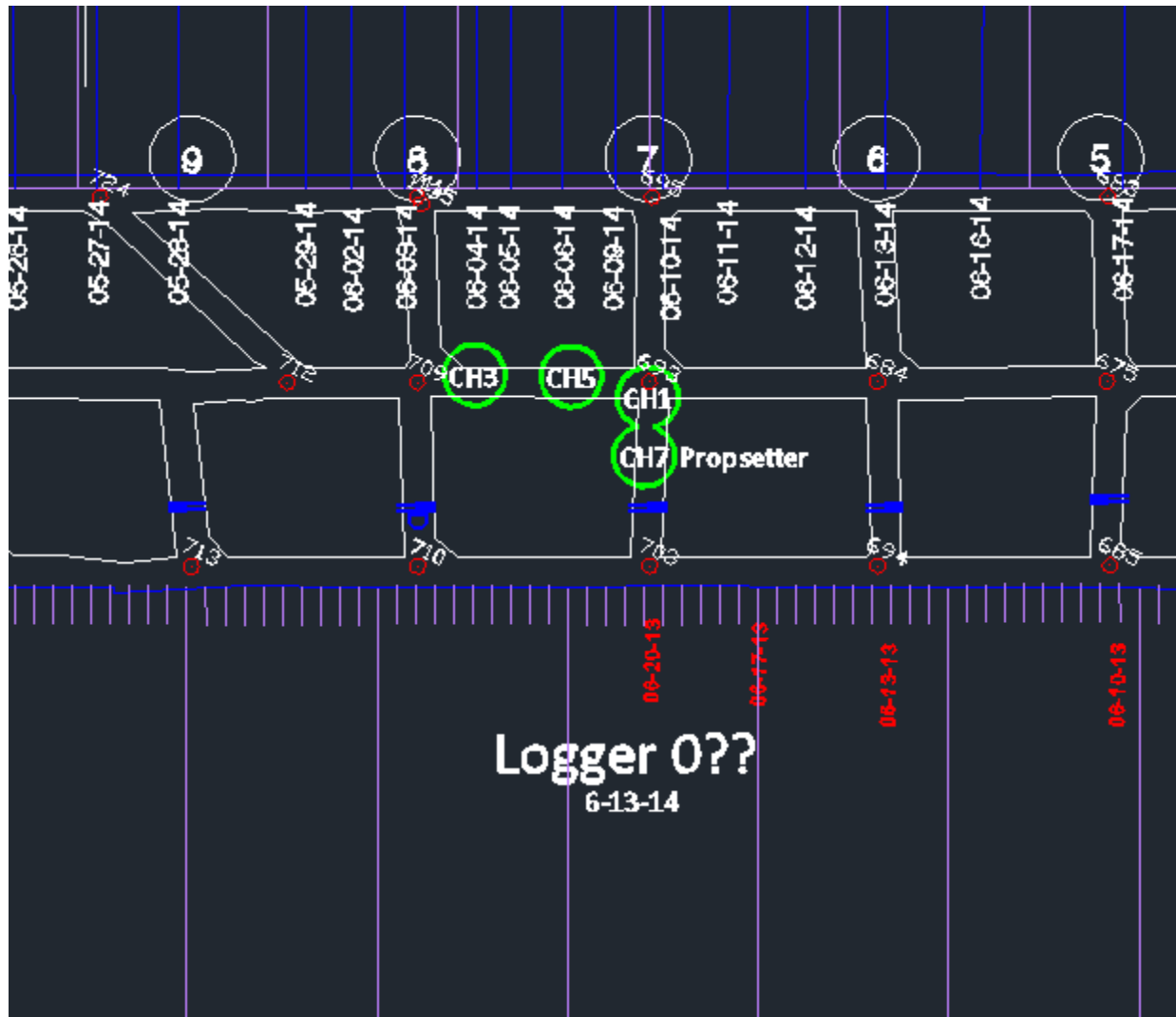


Figure D.50 – Map of convergence station #074's extensometer locations

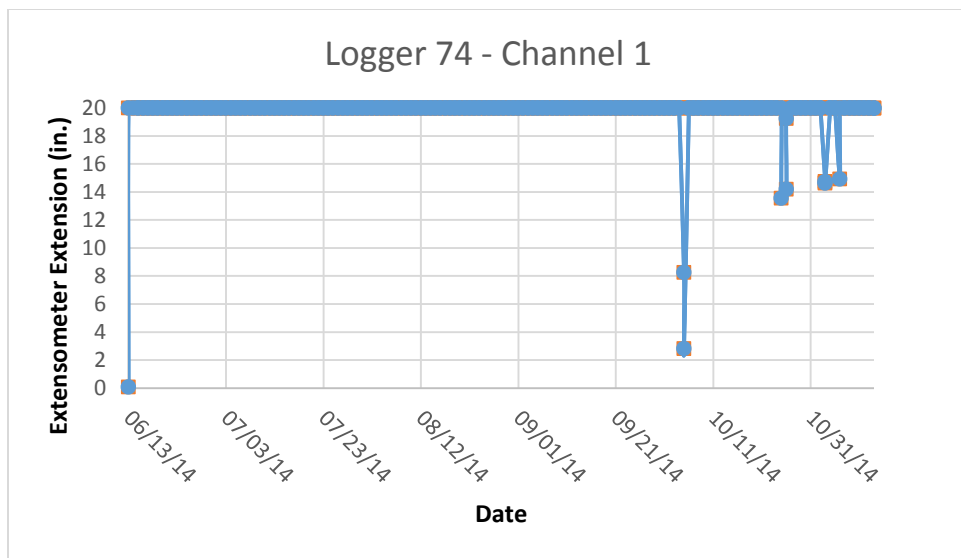


Figure D.51 – Chart of convergence station #074 channel 1 extension monitoring, 20-inch scale

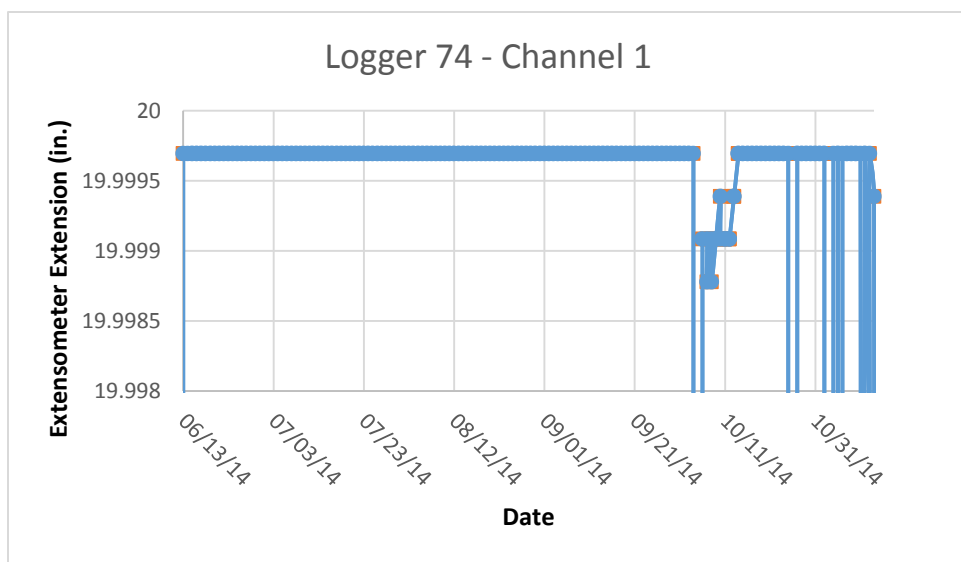


Figure D.52 – Chart of convergence station #074 channel 1 extension monitoring, concentrated scale

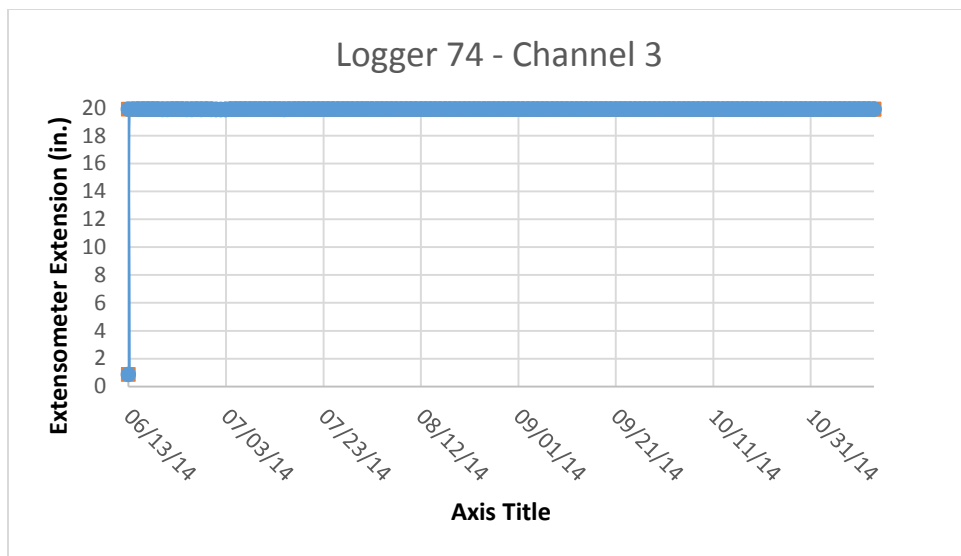


Figure D.53 – Chart of convergence station #074 channel 3 extension monitoring, 20-inch scale

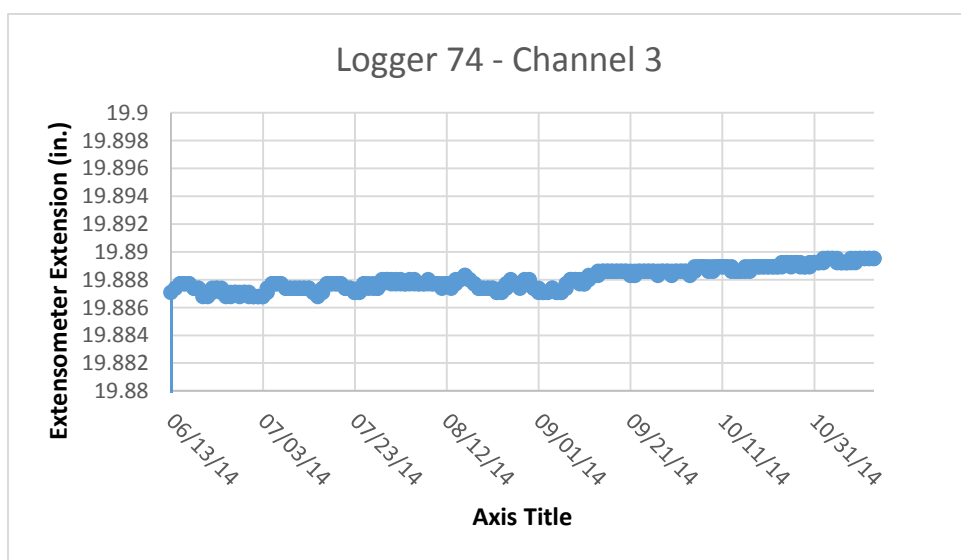


Figure D.54 – Chart of convergence station #074 channel 3 extension monitoring, concentrated scale

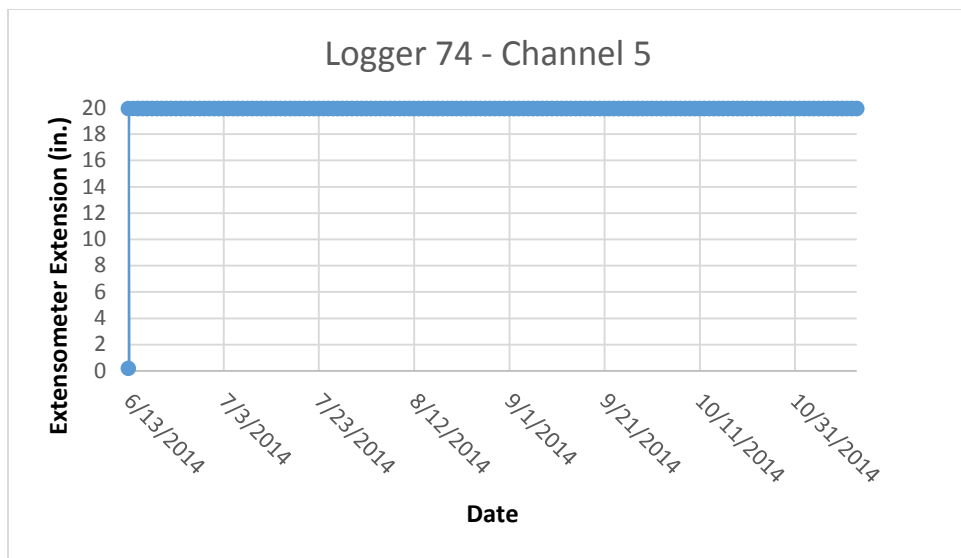


Figure D.55 – Chart of convergence station #074 channel 5 extension monitoring, 20-inch scale

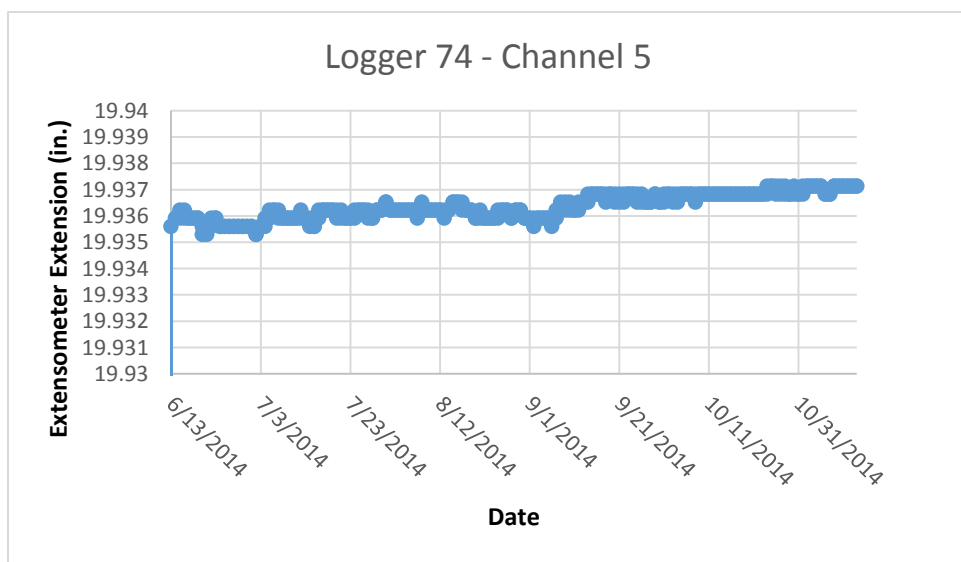
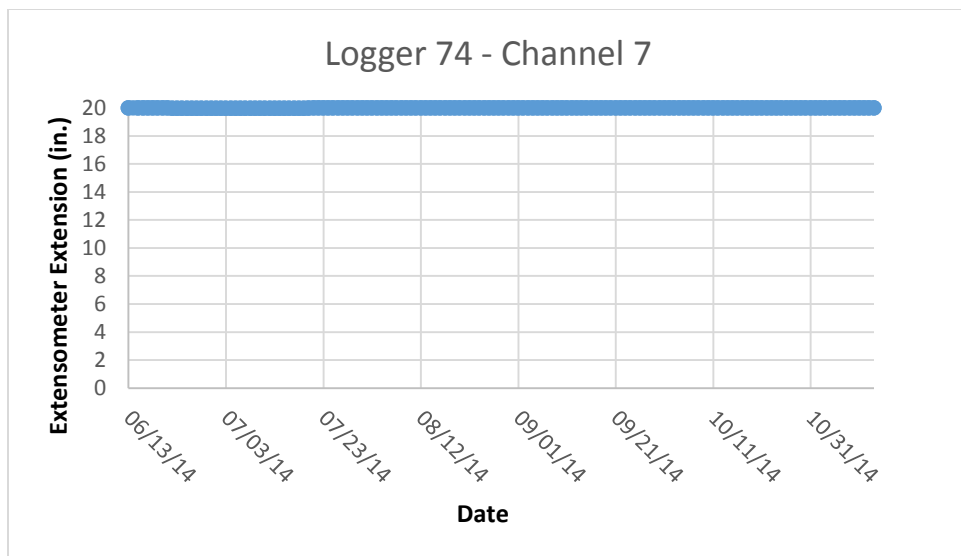
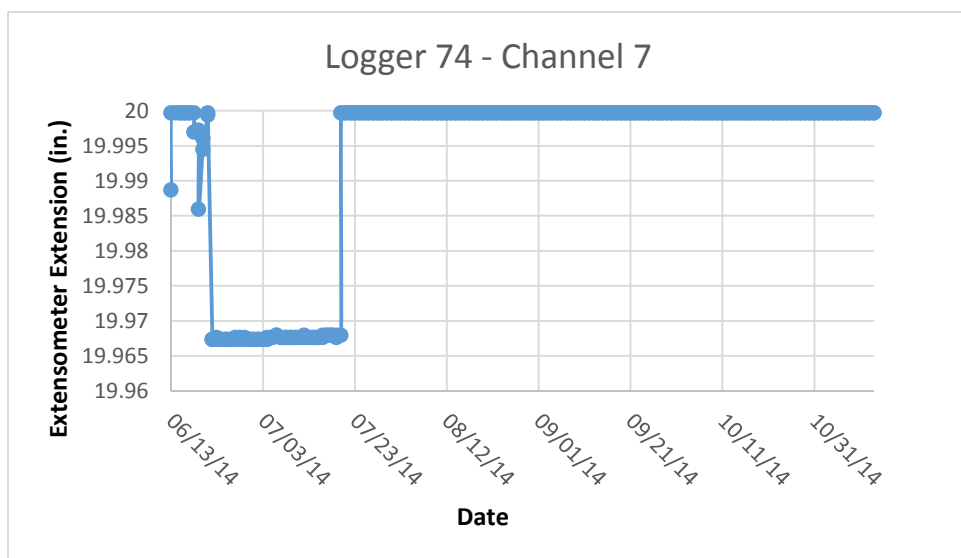


Figure D.56 – Chart of convergence station #074 channel 5 extension monitoring, concentrated scale



**Figure D.57 – Chart of convergence station #074 channel 7 extension monitoring, 20-inch scale**



**Figure D.58 – Chart of convergence station #074 channel 7 extension monitoring, concentrated scale**

## Conclusions

The convergence station design had a varying array of success. It was able to observe steady rates of support deformation when attached to timber supports. However, the cement filled supports resisted convergence to such an extent that the extensometers actually observed some extension in the pillar in some cases. This could be contributed to the fact that the cement-filled standing supports were over-designed for the mine environment. The mine would eventually

abandon this type of support for financial and maintenance-related reasons when it became apparent that the overall strength of the columns was unnecessary.

Installation of the convergence stations also had a wide range of parameters that favored use of timbers over cement-filled supports for convergence monitoring. In the timbers, screws could easily penetrate the wood with no additional effort, simplifying the task and permitting the installation of a second anchor screw for support in many cases. In the cement-filled supports, punching a hole in the exterior shell required a lot more effort and was often met with a great deal of trial-and-error until a suitable penetration point could be established. This often altered the final placement location of the extensometer, making the process less ideal. In cases where the cement-filled supports had wooden boards placed between the column and the roof, the extensometer was connected to the boards rather than the cement column.

The MIDAS datalogger would sometimes misrepresent the amount of deformation in the standing support. This can be attributed to an electrical error within the device. These outliers happened in multiple data loggers and across multiple channels. Although the error would often correct itself, these electrical communication errors contribute to holes within the data set.

Overall, the recommendation for the use of the convergence station is to install in areas where some form of timber supports is used. The timbers flex and deform more easily alongside the mine environment, providing a good representation of convergence in the area.